Research Report 269

FRACTURE OF LAKE AND SEA ICE

W.F. Weeks and A. Assur

September 1969

CORPS OF ENGINEERS, U.S. ARMY
COLD REGIONS RESEARCH AND ENGINEERING LABORATORY
HANOVER, NEW HAMPSHIRE

PREFACE

This report was prepared by Dr. Wilford F. Weeks, Glaciologist, Research Division; and Dr. Andrew Assur, Chief Scientist, U.S. Army Cold Regions Research and Engineering Laboratory. The report was funded by the Arctic Program of the Office of Naval Research.

The authors would like to thank L. Gold, G. Frankenstein, Dr. I. Hawkes, Dr. B. Michel, M. Mellor, R. Ramseier and Dr. V.L. Tsurikov for their advice and critical comments on a number of aspects of this paper. Mr. Gold, Dr. C. Knight and Prof. W. Webb kindly made figures from their papers available.

CONTENTS

ILLUSTRATIONS

CONTENTS (cont'd)

ILLUSTRATIONS (cont'd)

CONTENTS (cont'd)

ILLUSTRATIONS (cont'd)

TABLES

LIST OF SYMBOLS

B	Length of sample (eq 40-41)
C	Charpy impact value
E	Elastic or Young's modulus
F	Average area of brine pockets in a plane parallel to the solid/liquid interface; area of the failure surface
G	Shear modulus
I	Indentation factor for large ice sheets (eq 44)
K	Stress concentration factor associated with the presence of brine pockets in sea ice
K_a	Actual stress concentration factor
K_e	External stress concentration associated with the geometry of the test
K_i	Internal stress concentration associated with internal structural characteristics of the material
K_t	Theoretical stress concentration factor
L	Square root of the area of the failure surface
L_0	Inverse of the slope from a (σ_s/σ_L) vs L plot
P	Parameter related to the geometry of the microstructure (eq 33)
S_i	Salinity of sea ice
V_a	Air porosity
$X_{1...n}$	Parameters affecting the strength of sea ice (eq 37)
a	Empirical constant; height of a failure surface
a_0	Plate spacing, the distance between centers of successive brine layers measured parallel to the c-crystallographic axis
b	Empirical constant (eq 37); width of the indentor (eq 40-42); width of a failure surface
b_0	Center to center spacing of brine pockets as measured in the B direction (see Fig. 22)
c	$= \nu_0^{-k}$ (eq 13); length of a crack (eq 31)
$2c_0$	Original grain length (eq 32)
d	Crystal diameter; length characteristic of the size of the microstructure (eq 33)
d_0	Minimum width of a parallel brine layer before it splits to produce individual brine pockets
g	Length of brine cylinders measured parallel to the growth direction
g_0	Spacing of brine cylinders measured parallel to the growth direction
h	Ice thickness
k	A constant (eq 13); a contact factor (eq 44)

LIST OF SYMBOLS (Cont'd)

l_0	Characteristic length associated with the distance between effective defects (eq 58)
m	Shape factor for the indentor (eq 44)
$2r_a$	Width of brine pockets measured in the c-direction (see Fig. 22)
$2r_b$	Length of brine pockets measured in the B-direction (see Fig. 22)
r_i	Inner radius of sample
r_o	Outer radius of sample
t	Time
v	Growth velocity
$y_{1...n}$	Empirically determined powers of the X's (eq 37)
z	Vertical distance from the upper surface of the ice sheet to any location in the sheet
θ_i	Ice temperature
ψ	Plane porosity
α_0	$= a_0 F^{-1/2}$ (eq 15)
β_0	Relative spacing of brine pockets ($\beta_0 = b_0/a_0$)
γ	Relative spacing of brine cylinders ($\gamma = g/g_0$)
γ'	Total energy required per unit increase in the area of a crack
δ	Dimensions of the intercellular groove (Fig. 8); complicated function of c and c_0 (eq 32)
ϵ	Strain; elliptic ratio of the brine pockets ($\epsilon = r_b/r_a$); ratio of void diameter perpendicular to the stress direction to the diameter parallel to it (eq 47)
$\dot{\epsilon}$	Strain rate ($\dot{\epsilon} = d\epsilon/dt$)
$\epsilon_{\parallel}, \epsilon_{\perp}$	Ratio of the void diameter perpendicular to the stress direction to the diameter parallel to it; the subscripts $\parallel$ and $\perp$ indicate whether the stress direction is parallel or perpendicular to the growth direction (eq 48)
η	Stress concentration index (eq 1); a function of Poisson's ratio (eq 32)
κ	Proportion of the stress exerted on the weak crystal (eq 32)
μ	Poisson's ratio
ν	Total porosity
ν_a	Air porosity
ν_b	Brine volume
ν_0	Volume of brine necessary to cause the ice to have zero strength
ρ	A parameter related to brine pocket geometry, $\rho = 2r_b F^{-1/2}$ (eq 14)
σ	Stress
$\dot{\sigma}$	Stress rate ($\dot{\sigma} = d\sigma/dt$)
σ_L	Failure strength of the larger of two samples that are being compared (eq 57)

LIST OF SYMBOLS (Cont'd)

σ_R	A parameter related to the failure strength, $\sigma_R = \sigma_f/\dot{\sigma}^b$ (eq 38)
σ_s	Failure strength of the smaller of two samples that are being compared (eq 57), in certain cases this sample may be a control with a specified cross section
σ_f	Failure strength
$\sigma_{f(t)}$	Theoretical failure strength assuming that the calculated stress concentration actually occurs
$\sigma_{f(\parallel)}$, $\sigma_{f(\perp)}$	Failure strength determined with the direction of applied stress respectively parallel or perpendicular to the growth direction
σ_i	Failure strength of pure ice
σ_0	Basic strength of sea ice (eq 4); basic crushing reference strength (eq 41)
σ_1	Indentation strength adjusted for the ice thickness and the width of the indentor (eq 41)

FRACTURE OF LAKE AND SEA ICE

by

W.F. Weeks and A. Assur

INTRODUCTION

Because of the pronounced increase in activities during the last 10 years in Arctic and Antarctic regions, a thorough understanding of the fracture of ice has become increasingly desirable. Such knowledge has direct application to a large number of geophysical and engineering problems that occur not only in polar regions but also under winter conditions in temperate zones. Some examples of these problems are: the formation of crevasses, the adhesion of ice to surfaces, the bearing capacity of floating ice sheets and snow surfaces and crusts, the initiation of snow and ice avalanches, the formation of open leads and pressure ridges in sea and lake ice covers, the forces exerted on structures by moving ice floes and jams, the design of a new generation of icebreakers, and the utilization of ice as an indigenous construction material. Unfortunately, the level of understanding required for the effective solution of many of these problems far exceeds the current level of our knowledge. A limited portion of the general problem of ice fracture is discussed in this review: the fracture of lake and sea ice.*

Investigators who have devoted more than passing attention to problems associated with the fracture of sea and lake ice are very few. They are widely separated geographically with limited communication between groups of investigators. A regrettable lack of uniformity both in testing procedures and in the adequate designation of the "state" of the sample at the time of testing has resulted. Thus, direct comparisons of available data are often rather difficult. Because of this, many relations between failure strength and parameters associated with the "state" of the ice sample have not been systematically investigated, although similar relations in metals and ceramics are well established. For example, our knowledge of initial crack formation in lake ice is limited and in sea ice is slightly better than nonexistent. The results of "simple" mechanical determinations of the different failure strengths show a wide scatter and at times reveal very little consistent variation with changes in the physical environment. Our knowledge of the strength of seemingly complex sea ice even appears to be appreciably more advanced than our knowledge of similar phenomena in the purer, and hopefully simpler, lake ice. Inasmuch as unearthing the literature on fracture in sea and lake ice has been a formidable task in itself, we hope that this review will provide the reader with a reasonable survey of the "state of the art" as well as a comprehensive bibliography.

---

* Ice formed essentially by one-dimensional solidification on saline water bodies, mainly oceans, is here discussed as sea ice; while ice formed on quiet fresh water bodies, mainly lakes, is referred to as lake ice.

STRUCTURE OF ICE AND ICE SHEETS

Ice as a mineral

Ordinary ice (ice I) is the only ice polymorph that exists in significant quantities under the conditions encountered at the earth's surface (Shumskii, 1964; Brill, 1962). Considering its chemical simplicity and the fact that ice was one of the first substances studied by X-ray methods, one may be surprised to find that only recently have a number of problems associated with the distribution of the hydrogen atoms in ice crystals been resolved. However, the crystallographic arrangement of the oxygen atoms, which are the principal diffracting centers for X-rays, has been well understood since the early work of Bragg and Barnes (Lonsdale, 1958; Owston, 1958). The oxygen atoms occupy the points of a hexagonal lattice which possesses the wurtzite structure. Each oxygen atom is in turn located at the center of a tetrahedron with four other oxygem atoms located at each of the apices. The 0-0 distance is 2.76 Å at 0C. This produces the low density, open structure diagrammed in Figure 1. The oxygen atoms are concentrated close to planes which are perpendicular to the principal hexagonal axis (*c*-axis). The arrangement is such that, in any unit cell which contains four oxygen atoms, fracture along the (0001) or basal plane involves the rupture of only two bonds. On the other hand, fracture along any plane normal to this plane requires the destruction of at least four bonds. This is, of course, in agreement with the observation that ice glides and cleaves readily on the (0001) plane. When a projection of the oxygen atoms parallel to the [0001] direction is examined, three close-packed rows of atoms can be seen (Fig. 1a). These rows lie in the $\langle 11\bar{2}0 \rangle$ directions parallel to the directions of the three secondary or a-axes.

This crystallographically arranged net of oxygen atoms is bonded together by a series of hydrogen bonds. The positions of the hydrogen atoms in these bonds are disordered and obey the so-called Bernal-Fowler rules: 1) two hydrogens are near each oxygen atom and 2) only one hydrogen

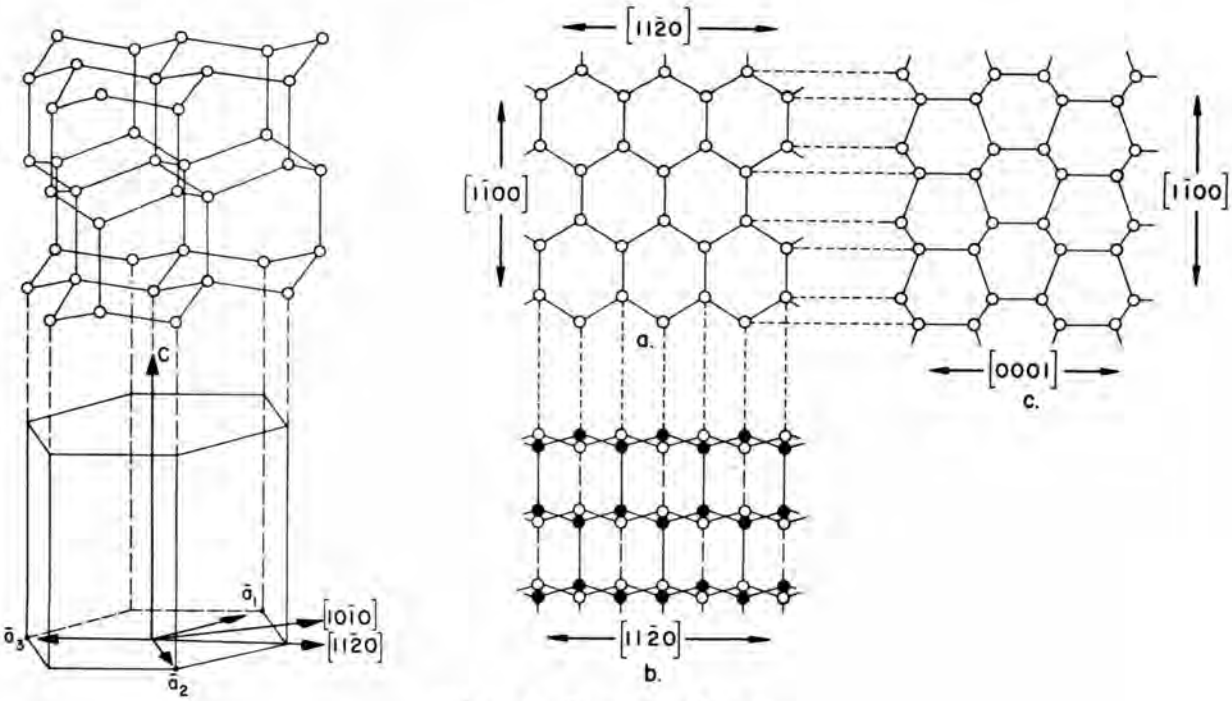

Figure 1. Structure of ice I.

atom can be on or near the line connecting two neighboring oxygen atoms. All configurations compatible with these rules are assumed to be equally probable. The "average" structure that results may be specified by assigning a half-hydrogen to each of the $4N$ sites contained in an array of N oxygen atoms. Each oxygen atom is therefore tetrahedrally surrounded by four "half-hydrogen" atoms. This arrangement of hydrogen atoms has been shown to be in good agreement with both the observed zero point entropy of ice (Pauling, 1935; Nagle, 1966; Suzuki, 1967) and the results of single-crystal neutron diffraction studies (Peterson and Levy, 1957). Any violation of the Bernal-Fowler rules can therefore be considered to produce a defect in the ice structure with a violation of rule 1 giving an ionic defect: an oxygen atom surrounded by three protons produces the positive ion $(H_3O)^+$ while one with only one proton produces the negative ion $(OH)^-$. When rule 2 is violated a Bjerrum defect results: when two protons occur on the bond a so-called D-defect is produced while a bond with no protons produces an L-defect. An understanding of the nature of hydrogen bonding in ice is clearly essential to the study of its electrical, diffusive and thermodynamic properties. It may also be important in understanding certain aspects of its mechanical behavior.

Lake and sea ice

The difference in the initial freezing of lake water and sea water is primarily associated with the fact that in water with a salinity of less than 24.70 ‰ the temperature of maximum density lies above the freezing temperature. In pure water the temperature of maximum density is +3.98C. Therefore, when a homo-haline layer of water with a salinity of less than 24.7 ‰ is cooled, the cooling causes an increase in the density of the water at the surface resulting in free convection. As cooling continues this convection continues until the complete convective column reaches the temperature of maximum density. At this time convection ceases. Without mechanical mixing, further surface cooling results in a stable low density surface layer which will cool until the freezing temperature is reached. If, on the other hand, the initial salinity is greater than 24.7‰, the convective process continues until freezing occurs and the complete convecting layer which may extend to the bottom must be cooled to the freezing point before initial ice formation begins. Therefore, in the fall lake ice will form first, then river ice and finally sea ice. The intermediate position of river ice in this sequence is caused by the complete vertical mixing of heat in the river as the result of turbulence. In the arctic the time lag between the formation of lake ice and of sea ice may be as long as a month.

Once the water starts to freeze, the formation of the initial ice cover proceeds along similar lines regardless of the salinity of the water. The main variable now controlling the "state" of the initial cover is the amount of turbulent mixing of the water in the freezing layer. In lake and sea water this turbulence is usually wind induced. Under calm conditions after the surface water has been supercooled slightly (supercoolings of up to 1C have been measured in the surface layers of lakes; Devik, 1949) initial ice growth will start. Considering the large number of solid impurities in any small volume of naturally existing lake or sea water, it is doubtful if homogeneous nucleation ever occurs. In the polar regions small snow crystals are being deposited nearly continuously in the surface water layer providing nuclei for further growth. The first crystals to form are minute spheres of pure ice: the spherical shape giving a minimum surface to volume ratio. As these spheres grow into the surrounding supercooled water they rapidly change their shape to circular disks (Arakawa, 1955). The disk-like shape is the result of the highly anisotropic surface energy of ice which, although specifying a planar form, does not specify any particular growth direction in this plane. The plane of the disk is, of course, the "close-packed" or (0001) plane (see Fig. 1a). In fresh water the maximum diameter to which these disks grow is on the order of 2 to 3 mm and is undoubtedly some function of the supercooling. Figure 2 shows a large number of such disks developing in the upper centimeter of sea water at Thule, Greenland. Note the characteristic notched edges on several of the tilted plates. At some critical diameter, which in fresh water appears to be on the order of 2 to 3 mm and appears to decrease with increasing salinity, the disk form becomes unstable, changing to a dendritic hexagonal star. As might be expected, the arms of the

Figure 2. Initial disks during the freezing of sea water. Size of disks is approximately 1 mm.

stars are parallel to the a-axis directions $\langle 11\bar{2}0 \rangle$ in the crystal. Although the change to a stellar form causes an increase in the relative amount of surface, this is apparently compensated by the crystal's ability to more readily dispose of heat and solute at the advancing interface. The disk-star transition is, therefore, marked by an appreciable increase in the growth velocity (Kumai and Itagaki, 1953). Because of their tabular nature the star-like crystals float with their basal planes in the plane of the water surface. They grow rapidly across the surface of calm lake and sea water until they overlap and freeze together.

During the initial freezing of fresh water, surface needles are common (Fujino and Suzuki, 1959; Hallett, 1960). The needles form when a disk becomes inclined at an angle to the water surface. Subsequent growth then proceeds rapidly, in the form of long thin needle-like crystals, from the points where the disk intersects the surface. The needles appear to be confined strictly to the thin surface layer of water that is appreciably supercooled. If crystal growth were to continue downward along the basal plane, the crystal would immediately encounter water that is not supercooled and growth would stop. Therefore, during calm conditions the initial lake ice skim is usually composed of an open polygonal network of surface needles that have their *c*-axes inclined at some angle from the vertical. The polygonal areas between these needles are occupied by the star-like crystals with their *c*-axes approximately vertical. The size range of these crystals is quite varied although needles up to roughly 4 m in length and *c*-axes vertical crystals up to 0.7 m in diameter have been observed (Wilson, Zumberge and Marshall, 1954; Ramseier, personal communication). More representative dimensions are in the range of 1 to 10 cm.

The limited observations available on the freezing of sea water indicate that although needles are occasionally encountered, they are apparently much more rare than in fresh water. This observation is readily explained by the fact that prior to the initial nucleation of the sea ice crystals, convective mixing has lowered an appreciable thickness of the water layer to or slightly below the freezing point. This makes it possible for inclined disks to grow both downward as well as along the water surface. A significant downward component causes the disk to develop as a dendritic star instead of as a needle and also produces a moment due to the buoyancy force which tends to rotate the stellar crystal until its (0001) plane is parallel to the water surface. Ideally,

this should produce an ice skim with a completely *c*-axis vertical orientation. However, a number of discoids and stars are usually caught in some intermediate position even under quite calm conditions. Crystal growth process such as described here occur during calm cold periods if there is little or no turbulence in the upper layer of the water body. The resulting ice cover "presents a smooth unbroken surface on which there are no highly evident horizontal changes" in the macroscopic structure of the ice layer and has been termed "sheet ice" by Wilson, Zumberge and Marshall (1954).

In most water bodies there is, however, some turbulence during initial ice formation. This introduces more nuclei into the area of active freezing and provides the energy to overcome the buoyancy forces so that the initial crystals are mixed throughout a depth of up to several meters (Savel'ev, 1958). The effective supercooling is reduced, more crystals form per unit volume and abrasive action between crystals is increased. As a result, extensive discoidal growth is favored. In rivers these discoids and needle-like ice fragments are referred to as frazil ice (Williams, 1959; Michel, 1967a, b, 1968). It has recently been shown (Chalmers and Williamson, 1965) that these disks can multiply rapidly from an existing ice edge removing the necessity of separately nucleating each disk. When turbulence is pronounced, frazil ice may be mixed throughout the complete vertical cross section of a river. If these ice particles were to stick to objects on the river bed so-called anchor ice would be produced.

These frazil crystals freeze together forming irregular crystal aggregates. Similar crystal aggregates can form during calm conditions if snow is falling on the water surface just prior to and during initial freezing. These crystal aggregates are packed together into pancakes and slush balls by wave motion and the general motion of the aggregates against one another. In sea ice visual observation shows that there is some slight tendency for the discoids to be stacked in a vertical position (*c*-axis horizontal) so that a closer lateral packing is permitted. The degree of orientation produced by this packing process is, of course, far from perfect and in many cases the overall orientation is probably close to random. The resulting crystals are equigranular with crystal diameters ranging between 0.5 and 3 mm. The initial ice cover that results when a slush layer congeals is usually several centimeters thick. A series of excellent vertical and horizontal photomicrographs which show both slush ice and the transition to the underlying columnar structure are available for both lake ice (Wilson, Zumberge and Marshall, 1954, Fig. 17) and sea ice (Tabata and Ono, 1957, Fig. 10 and 11 - 1 to 6). If at any time during the initial freeze-over turbulence subsides, sheet ice will form between the pancakes producing a composite ice sheet (Fig. 3). Also, after the initial ice sheet has formed, sheet ice will develop beneath the pancakes and slush ice.

If possible, slush ice should be distinguished from infiltrated snow ice. This latter ice type forms on top of sea, lake, and river ice in subarctic and temperate regions with abundant snowfall. The weight of the snowpack depresses the surface of the ice sheet causing the ice to fracture. Water percolates through these cracks into the overlying snow, producing slush which subsequently freezes. This general process and the resulting ice have been described by Weeks and Lee (1958), Andrews (1962), Ragle (1963), and Butiagin (1966a). At some locations in the Antarctic such a considerable portion of the sea ice cover is composed of infiltrated snow ice, that it is necessary to take this fact into account in bearing capacity calculations (Treshnikov, 1963). Currently, it is not known whether slush ice and infiltrated snow ice have sufficiently similar physical properties to allow them to be considered as one ice type.

Once a continuous skim of ice has formed across the sea surface, crystal growth due to purely "thermal" supercooling is no longer possible. An ice skim now separates the melt from the cold source. The latent heat is therefore extracted entirely through the ice sheet and the growth rate is determined by the temperature gradient in the sheet and its effective thermal conductivity. The "initial" grain sizes and crystal orientations will, however, be those that exist on the bottom of the skim. Therefore, the details of the conditions during freezeover affect, at least to some degree, the structure of the complete ice sheet.

Figure 3. Composite sheet of sea ice, Thule, Greenland.

Macrostructure. When the skim forms, the growing crystals at the lower ice/water interface lose a degree of growth freedom: only if the grain boundaries are exactly perpendicular to the freezing interface can crystal growth proceed without one grain interfering with the growth of another. Any tendency for anisotropic growth will produce geometric selection with the crystals in the favored orientation eliminating the crystals in the unfavored orientation by cutting them off from the melt. As might be expected, this always occurs in natural ice sheets and the ice layer in which the preferred orientation "wins out," producing the characteristic growth fabric, has been termed the *transition layer* by Perey and Pounder (1958). In sea ice the orientation change is usually essentially completed by a distance of 5 to 10 cm below the initial ice/air interface although the base of the transition layer has been found as far as 50 cm below the upper ice surface (Pounder and Little, 1959). These extreme variations are, of course, more apparent than real resulting from local changes in both the snow cover and infiltrated snow ice thickness (Langleben, 1959). The favored sea ice crystals that are still present at the bottom of the transition layer always have a *c*-axis horizontal orientation (Weeks and Assur, 1968).

In lake ice the situation is more complicated with different investigators reporting different orientations ranging from *c*-axes horizontal to *c*-axes vertical. Figure 4 shows an Alaskan lake in which certain areas show *c*-axis vertical orientations while other areas show *c*-axis horizontal orientations (Knight, 1962a). The orientation differences can be seen from the changes in the surface albedo. The reasons for these variations have been recently studied in detail (Ketcham and Hobbs, 1967; Ramseier, 1968) and a series of rules specifying which crystals will be favored has

Figure 4. Candled ice surface of Peters Lake, Alaska. The light-colored ice has vertical c-*axes, whereas the dark-colored ice has horizontal* c-*axes. Note the frozen lead traversing the lake (Knight, 1962a).*

been formulated. Although it is possible for a *c*-axis vertical crystal to encroach upon a *c*-axis horizontal crystal, in general *c*-axis horizontal orientations will be favored. If the orientation on the bottom of the initial skim is random, the change to a *c*-axis horizontal orientation will occur rapidly and there will be a well-defined transition layer in the upper portion of the ice sheet. On the other hand, if the initial skim is composed primarily of crystals with *c*-axis vertical orientation, geometric selection will occur quite gradually and a thick ice sheet will have to develop before the change to a *c*-axis horizontal orientation is completed. Therefore, in many thin lake ice sheets in temperate climates, the change to the preferred growth orientation is never completed and the whole ice sheet can be considered as part of the transition layer.

Below the transition layer in both sea and lake ice, the ice has all the characteristics associated with the so-called "columnar" zone in metal ingots: a strong crystal orientation and a gradual increase in average grain size as the distance from the cold source increases (Walton and Chalmers, 1959). The increase in grain size with depth has only been studied in a few ice sheets. Figure 5 shows a plot of mean grain diameter ($\bar{d}$) vs distance below the upper ice surface (z) for sea ice at Thule, Greenland. A linear increase in $\bar{d}$ with z is indicated. Similar results have been obtained by Weeks and Hamilton (1962) and Tabata and Ono (1962) for sea ice and Ragle (1963) for lake ice. Muguruma and Kikuchi (1963), however, show a linear increase in the average crystal area with an increase in z based on a study of ice on an Alaskan lake. Butiagin (1966a) reports that in lake ice grain sizes in the lower layer increase sharply when ice growth almost ceases as a result of warm air temperatures. This is probably the result of grain boundary migration as described by Knight (1966). Regardless of the exact form of the relation, a systematic and significant grain coarsening is indicated. Only a few observations exist on the maximum crystal sizes that may be encountered at the bottom of thick perennial ice sheets. This lack of data is the result of the difficulty in obtaining large oriented samples. Information on this matter is badly needed in view of Peyton's (1966) designation of "bottom ice" as a separate sea ice type in the columnar

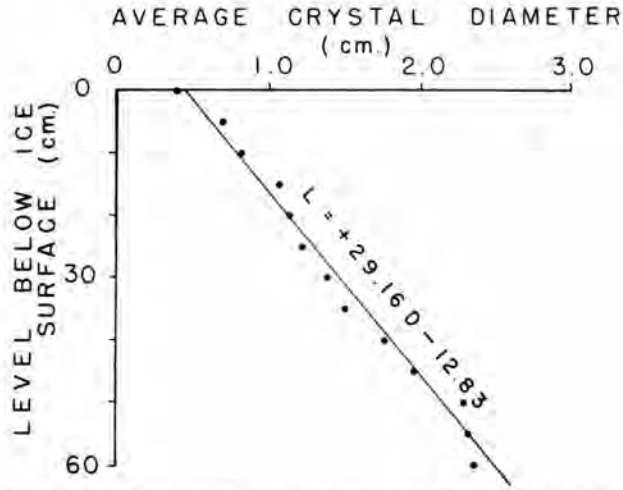

Figure 5. Average grain diameter vs distance below the upper ice surface, sea ice, Thule, Greenland.

zone. This ice is characterized by a *c*-axis horizontal orientation and an extremely large grain size. Peyton (1966) has reported examining a 3 × 3-m block of 1.6-m-thick sea ice and finding that the bottom meter exhibited a constant *c*-axis orientation over the entire 9-m² cross section. Smith (1964) has reported areas as large as 10 m on a side with almost perfect *c*-axis alignment in the old sea ice incorporated in Ice Island Arlis II, and Barnes (1960) has noted the suggestion of lake ice crystals several meters in diameter in the ice of perennially frozen Anguissaq Lake in northern Greenland. Whether or not these large areas are actually single crystals or are composed of a number of crystals with roughly similar orientations is not known.

There are several characteristics of the columnar zone which are most clearly seen in vertical sections. These features commonly appear as sharp, well defined bands or zones which extend for significant lateral distances in the ice. Air bubble layering in lake ice is perhaps the most obvious example of this type of feature. Air bubbles are usually tubular and elongated parallel to the growth direction. They form when the rejection of gas at the interface is fast enough to produce a gas content above the nucleation level in the liquid. Oscillations in both bubble diameters and in alternating layers of clear and bubbly ice are produced by variations in ice growth velocities resulting from weather changes. A pronounced weather event may result in a bubble band that can be traced over one or even several lakes (Ragle, 1963). An example of a lake showing extreme air bubble development (Fig. 6) has recently been described by Swinzow (1966). Because sea ice is opaque, bubble layers are not so obvious. Small scale horizontal banding in sea ice has, however, been noted by a number of investigators (Shumskii, 1955; Tabata and Ono, 1957; Langleben, 1959; Bennington, 1963a). In a number of cases the layering is produced by changes in the amount of impurities (brine + air) trapped in the ice.

Microstructure. In lake ice, a pronounced intracrystalline substructure, which usually forms parallel to the growth direction and has a similar appearance to so-called striation boundaries in metals (Elbaum, 1959), has been described by Knight (1962a, b). These boundaries have been observed to move under stress (Knight, 1962c) indicating that they are dislocation arrays. In *c*-axis vertical crystals the boundaries are present from the onset of growth and are initially rather irregular. As growth proceeds the substructure boundaries arrange themselves in a more orderly pattern while the misorientation between sub-grains increases to as much as 7 to 8° (Fig. 7). In *c*-axis horizontal crystals the boundaries are not present in the initial skim and only appear gradually as ice growth proceeds. When the boundaries initially form they are quite straight but as freezing

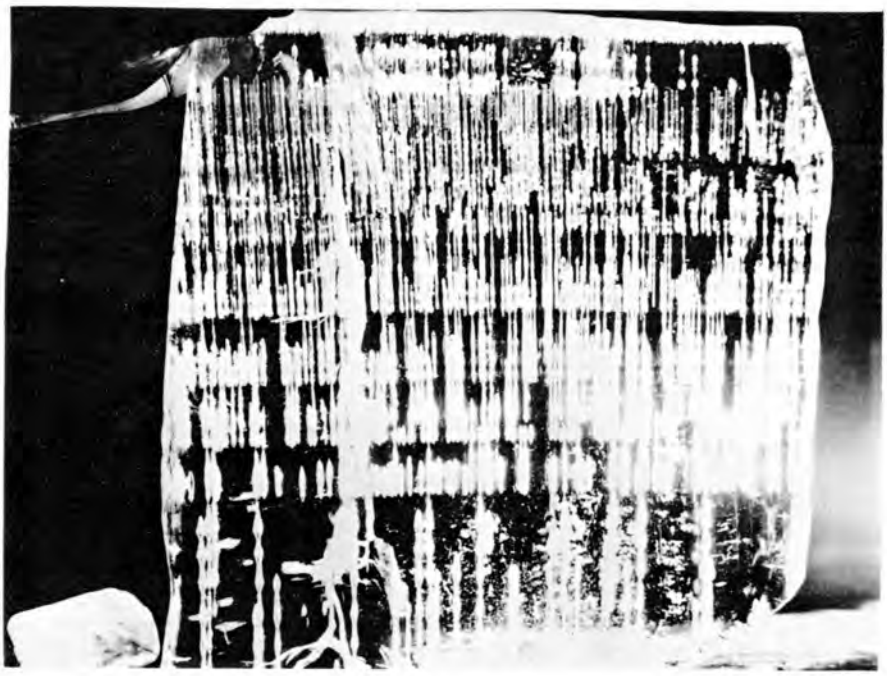

Figure 6. Air bubbles in ice from Lake Tuto, Greenland (Swinzow, 1966). Ice specimen is 48 cm high.

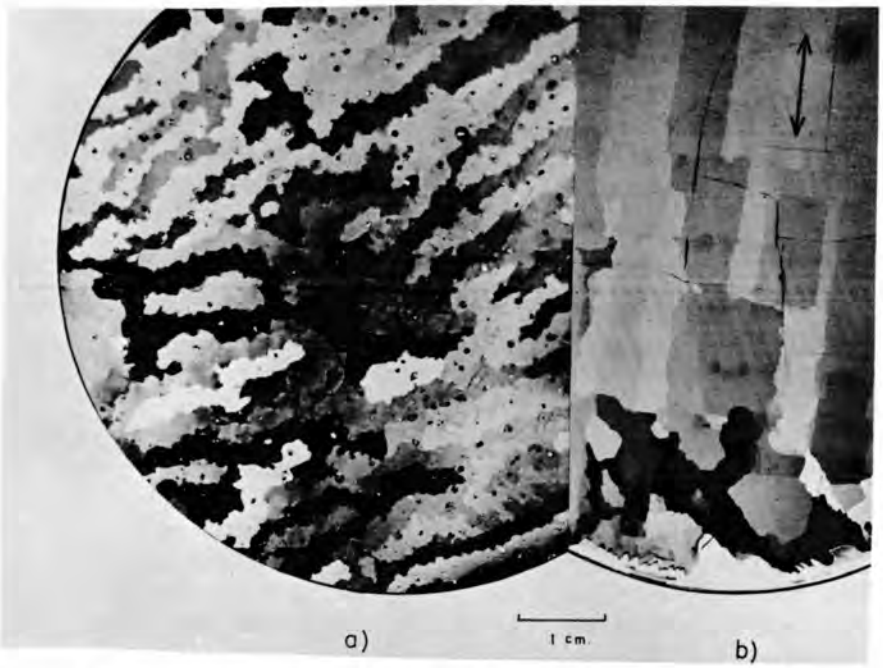

Figure 7. Horizontal thin sections of lake ice: a) c-axis vertical crystals showing sinuous striations; b) c-axis horizontal crystals showing "rectangular" striation pattern (Knight, 1962a).

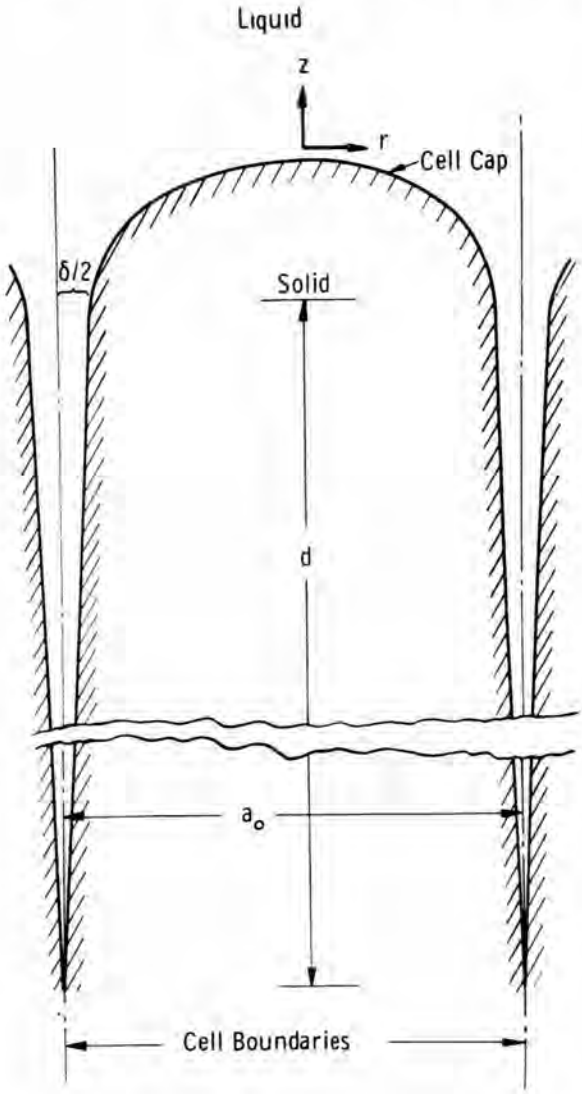

Figure 8. Schematic representation of a cut through a two-dimensional cell illustrating the relative dimensions of the cell groove δ to the cell or plate spacing a_0 (Tiller, 1963).

progresses they become irregular as well as more numerous. The final substructure that develops appears in horizontal thin sections as a roughly rectangular pattern with boundaries oriented both parallel and perpendicular to the c-axis. Misorientations of 2 to 3° are most common.

The substructure that develops in sea ice is even more pronounced because it is marked by the presence of numerous liquid inclusions, the so-called brine pockets of sea ice. The general reasons for the formation of this substructure are quite clear. When seawater freezes the rejection of solute by the solid causes a solute concentration maximum in the liquid next to the advancing solid/liquid interface. This solute profile, via the phase relations, specifies an equilibrium freezing temperature profile in the liquid. If certain temperature profiles occur in the liquid, a zone of constitutionally supercooled liquid is produced ahead of the interface. Because of the formation of this zone, a planar interface ceases to be stable and a cellular or dendritic interface forms. This phenomenon is called constitutional supercooling and is described in detail by Rutter and Chalmers (1953), Tiller, Jackson, Rutter and Chalmers (1953) and Harrison and Tiller (1963). Once a non-planar interface becomes stable, its exact geometry is specified by the details of the growth conditions. Although there are no detailed observations of sea ice interfaces during natural growth, examination of the resulting substructure suggests that typical morphologies are similar to the elongated cell shown in Figure 8. For a distance of about 2.5 cm above the macroscopic ice/water interface, these ice plates are not connected. This strengthless layer has been termed the skeleton layer since it can be considered to be the result of "skeletal" growth. The rather sharp transition to the typical sea ice of the columnar zone occurs at the bridging layer where ice-ice bonds form between adjacent ice plates. It is easy to visualize how brine becomes trapped in the intercellular grooves above the bridging layer producing the characteristic platy sea ice substructure shown in Figures 9 and 10. Slight orientation differences also exist between neighboring plates producing small angle grain boundaries. Knight (1962c) has also shown how old sea ice sub-boundary arrays are caused by stresses produced by volume changes in the brine inclusions. As seen in Figure 9, single crystals of sea ice are readily distinguished under crossed polaroids because they behave as common extinction units. Each single crystal is composed of a "packet" of plates and each plate is separated by an array of brine pockets.

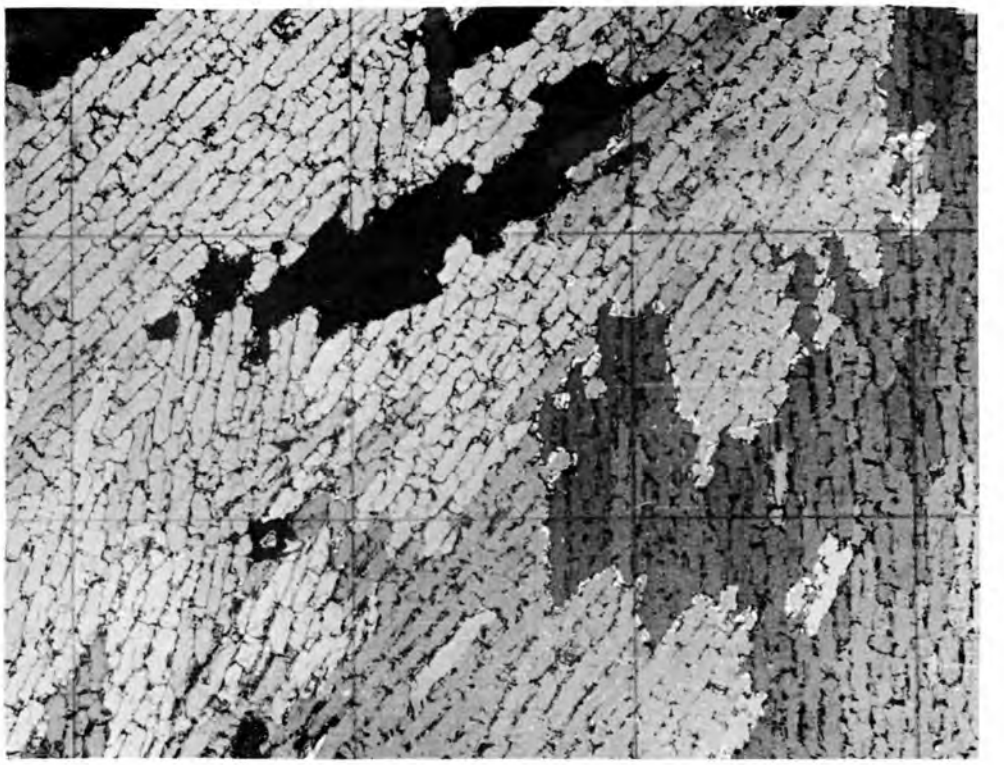

Figure 9. Horizontal thin section of sea ice from 27.9 cm below the upper ice surface, Point Barrow, Alaska (Weeks and Hamilton, 1962). Grid is 1 cm on a side.

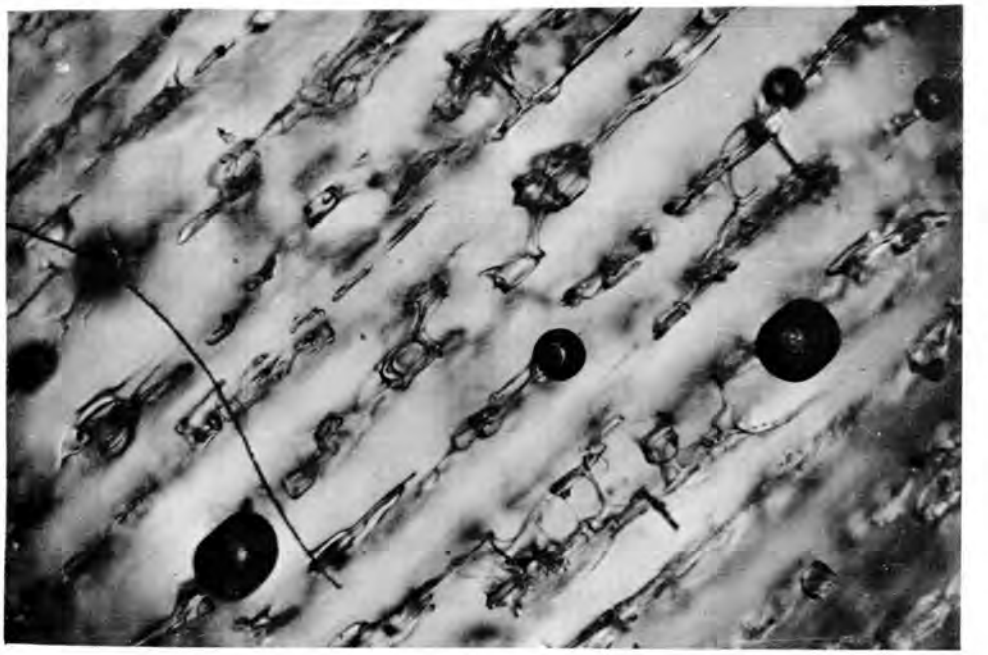

Figure 10. Thin section of sea ice illustrating complex brine pocket shapes (Hopedale, Labrador).

The distance between adjacent brine layers in the same crystal measured parallel to the c-axis has been termed the plate spacing a_0. This distance is a function of the growth velocity v of the sea ice and increases as v decreases (Rohatgi and Adams, 1967a, b, c; Lofgren and Weeks, 1969). Therefore, in general the spacing between the brine layers increases as the distance below the ice/air interface increases. At the present time plate spacing is the only aspect of the sea ice substructure that has definitely been related to the growth conditions when a given increment of ice forms. It is, however, reasonable tu suppose that other structural features such as the spacing between brine pockets measured in a horizontal plane are also some function of growth conditions. As will be seen later a knowledge of such interrelations, if they exist, is important in developing an adequate sea ice strength theory.

CHEMISTRY AND PHASE RELATIONS

After the initial ice skim is formed, lake and river ice usually grows with a planar solid/liquid interface. Therefore, the effective distribution coefficient k ($k = S_i/S_w$ where S_i and S_w are the salinity of the ice and the solution) would be expected to have a value similar to k_0, the equilibrium distribution coefficient. Unfortunately, exact values of k_0 for the more important solutes that are partitioned between water and ice in naturally occurring systems are unknown. NH_4^+ and F^- which show a measurable amount of solid solution in ice are, of course, of negligible importance in river and lake water. It is possible to calculate k_0 for different impurities by studying the breakdown of a macroscopically smooth solid/liquid interface to a cellular interface or by extrapolating a plot of effective k versus growth velocity to a condition of zero velocity. When this is done the estimated values of k_0 are usually 10^{-4} or less (Harrison and Tiller, 1963; Anantha and Chalmers, 1967; Weeks and Lofgren, 1967) indicating that when lake or river ice forms, effectively all the impurities are rejected back into the melt. Therefore, the variations in the properties of lake and river ice with changes in temperature should be caused primarily by variations in the properties of pure ice and not by changes in the relative amounts of solid, liquid, or gas in the sample.

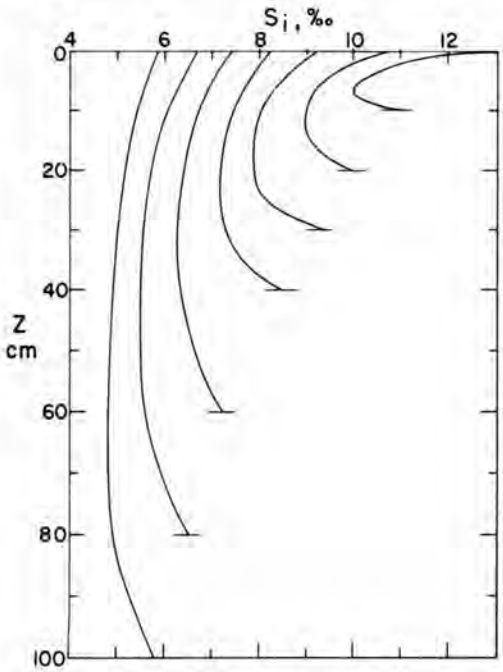

Figure 11. Schematic salinity profiles for sea ice with a thickness of 100 cm or less.

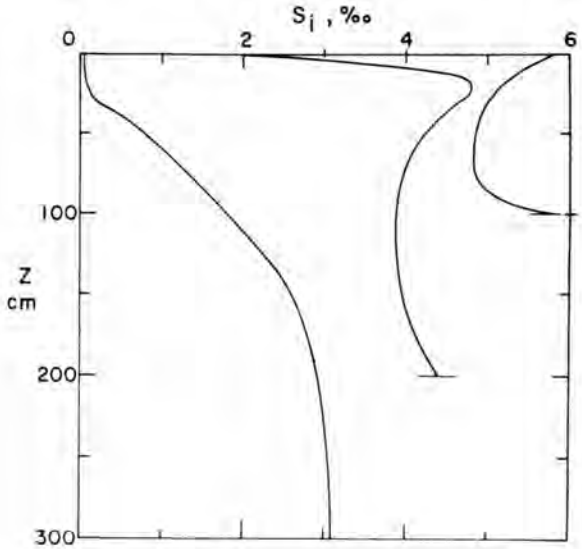

Figure 12. Schematic salinity profiles for sea ice 100, 200 and 300 cm thick. The low salinity values at the top of the 200-cm profile indicate that this ice has been through a period of summer melt.

Sea ice, on the other hand, because of the presence of a stable non-planar interface traps significant amounts of brine within the ice. The initial amount entrapped changes systematically with variations in growth parameters (Tsurikov, 1965; Weeks and Lofgren, 1967). Simultaneously brine drainage modifies the initial profile (Untersteiner, 1967). A schematic series of salinity profiles for ice of different thicknesses is shown in Figures 11 and 12. If the ice salinity and temperature are known, they specify via the phase diagram the relative volumes of ice, brine and solid salts that coexist at equilibrium in sea ice. The use of such a diagram assumes that the ratios of the ions in the system that is frozen are the same as in standard sea water. Figure 13 shows the phase diagram that is currently in general use (Assur, 1958; Anderson, 1958a; 1960). This diagram also indicates the temperatures of crystallization of the solid salts $CaCO_3 \cdot 6H_2O$, $Na_2SO_4 \cdot 10H_2O$, $NaCl \cdot 2H_2O$, etc. Although there is a considerable amount of checking that is required to clarify some of the details of this diagram, current information indicates that it will prove to be reasonably accurate at least at temperatures above the $NaCl \cdot 2H_2O$ precipitation temperature. For calculating the brine volume as a function of ice temperature and salinity, the linear expression determined by Frankenstein and Garner (1967) can be used.

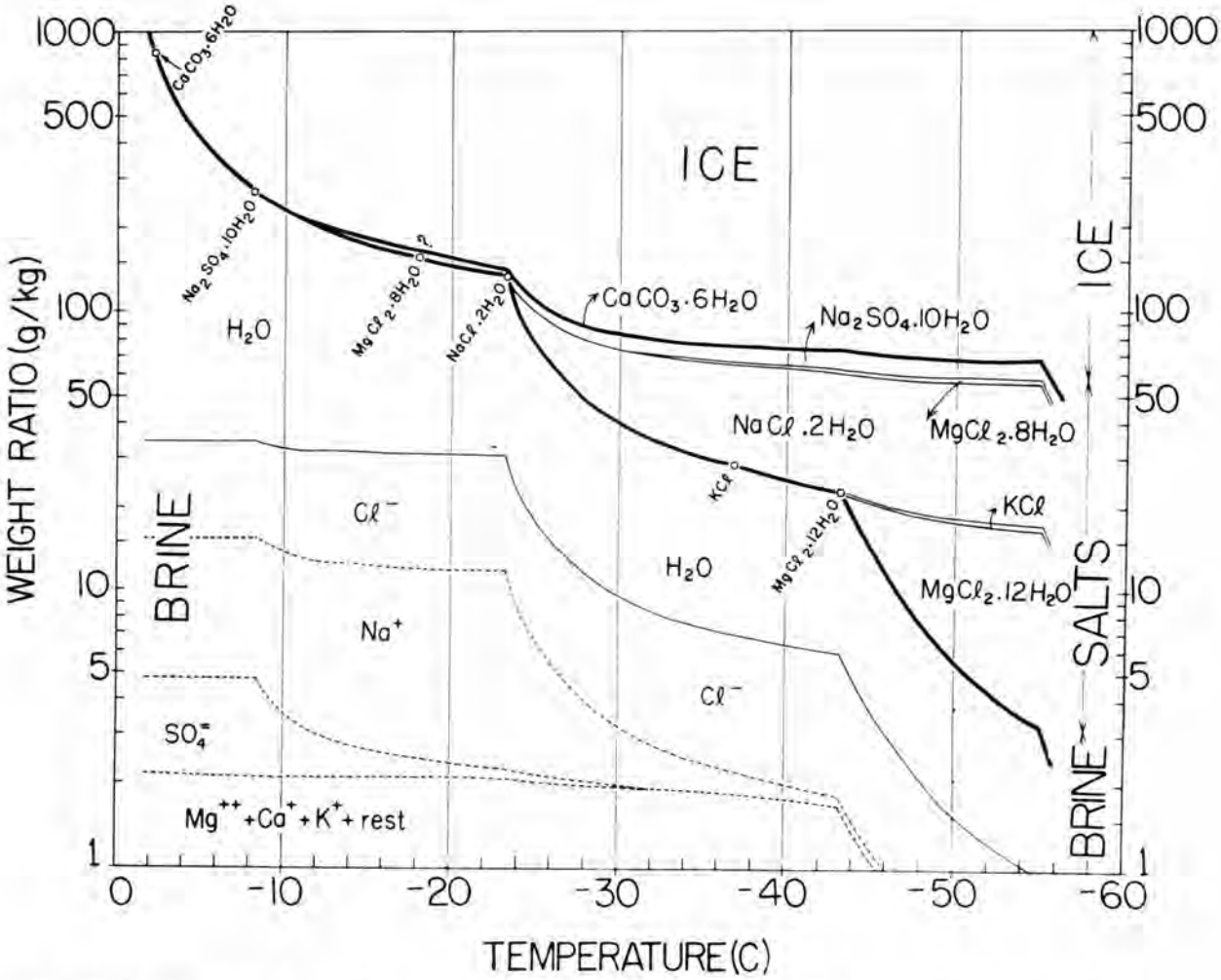

Figure 13. Phase relations for "standard" sea ice. Circles on the brine-salt line indicate temperatures at which solid salts precipitate (Assur, 1958).

The other component of the void volume in sea ice is the volume of air* in the sample. Fortunately it is fairly easy to determine the volume of air in a sea ice specimen (Arnol'd-Aliab'ev, 1925, 1934; Kusunoki, 1958) and some investigators have been able to show excellent correlations between physical properties and void volume (Tabata, 1958). At least in some of these cases, however, it appears that the initial brine had drained from the sample during the appreciable storage period between collection and testing. Canadian and American investigators have preferred to use the brine volume computed from the phase diagram and have commonly ignored the volume of air present in the ice. Ideally both brine and air volumes should be determined independently.

It is hoped that the preceding discussion of the structure and chemistry of natural ice sheets will convince the reader of the importance of combining tests of the physical properties of ice with an adequate specification of the "state" of the ice prior to the tests. Otherwise, an adequate analysis of the test results will be extremely difficult, if not impossible.

DISLOCATIONS, CRACKS, AND STRESS CONCENTRATORS

The development of the basic background information that is necessary for a thorough understanding of fracture in ice has lagged behind the accumulation of both laboratory and field information on the "ultimate" strength of ice as determined using different modes of testing. This lag has been caused by the limited number of investigators, the difficulties encountered in adapting certain metallurgical techniques to the study of ice, and the more obvious immediate applicability of test results to a given applied problem. Fortunately, limited information on subjects such as dislocation configurations, crack nucleation and crack propagation is now becoming available. We expect that there will be marked increase in activity in this general area in the near future.

Direct observation of dislocations

Until quite recently studies regarding the dislocation structure of ice crystals were based on the use of etch techniques to reveal the intersections of the dislocations with the surfaces of the crystals (Bryant and Mason, 1960; Kuroiwa and Hamilton, 1963; Wakahama, 1964; Higashi, Koinuma, and Mae, 1964). Although these studies strongly suggested that dislocation motion and pile-ups do occur in ice, the conclusions were speculative because of uncertainties in interpreting etch pit observations. Fortunately, dislocation configurations in ice can now be observed directly by using X-ray diffraction topography (Lang, 1958, 1959). The following discussion is based on the work of Webb and Hayes (1967) who have studied artificially prepared small dendrites of distilled water ice (Fig. 14).

They found evidence only for dislocation lines that lie nearly in (0001) planes and appear to have been generated by slip in these planes. This is in agreement with the fact that the lowest energy perfect dislocations should have (a/3) $\langle 11\bar{2}0 \rangle$ Burgers vectors since these are the shortest primitive lattice vectors. No evidence was found for partial dislocations or stacking faults although Yoshida and Wakahama (1962) have shown that certain partial dislocations and stacking faults can occur with minimal local lattice distortion. There was also no evidence for pure screw dislocations with Burgers vectors parallel to the *c*-axis. In a number of the X-ray topographs, incipient dislocation network formation was noted. This results from any two of the three prime Burgers vectors in the basal plane (a/3) $\langle 11\bar{2}0 \rangle$ reacting at intersection points to produce a third type Burgers vector. For example, when two $\langle 11\bar{2}0 \rangle$ type dislocations with Burgers vectors at 120° angles intersect, a new dislocation with a third Burgers vector at 60° to both of these may form.

---

* More precisely gas because the composition may be different from normal air.

***Figure 14. X-ray diffraction topograph of a portion of a tabular ice dendrite** after gentle straining. Dislocations are visible as dark thin lines extending from sources at interdendritic inclusions. Regions of the crystal that are smoothly shaded are virtually perfect. Optically magnified 10X (Webb and Hayes, 1967).*

Because some of the crystals that had not been deformed showed dislocation-free areas as large as 0.5 cm^2, Webb and Hayes (1967) suggest that most of the dislocations in their samples were generated by plastic deformation after the initial growth. Many times the dislocations appear to nucleate at interdendritic inclusions (Fig. 14): dislocation loops on $\{0001\}$ planes expanding from localized inclusion sites were specifically noted. They also found cross slip of the screw segments of $\langle 11\bar{2}0 \rangle$ type dislocations on $\{1\bar{1}0n\}$ planes. The most probably cross slip plane appears to be $\{10\bar{1}1\}$. Although large stresses would be required to initiate such a process, once it occurs the resulting edge segments should be highly mobile. Webb and Hayes suggest that this process is sufficient to explain the complex etch pit structures and etch channel behavior that has been observed in ice by Muguruma and Higashi (1963) and by Levi, de Achaval, and Suraski (1965). These authors had explained their observations by postulating the existence of dislocations with non-basal plane Burgers vectors.

As Webb and Hayes point out, even though their work has only revealed dislocations with Burgers vectors in the basal plane, it is not at the present possible to rule out the possible existence of dislocations with non-basal plane Burgers vectors. The current results are, however, in agreement with the expectation that dislocations with non-basal plane Burgers vectors will have much higher energies and be more difficult to form. As will be discussed later, Gold (1963a, 1966) has shown that when attempts are made to produce slip in non-basal plane directions, the ice commonly fractures before slip occurs. Other dislocations may, however, be formed when ice is subjected to a hydrostatic pressure so that fracture is prevented and then strongly deformed. The samples examined by Webb and Hayes were only subjected to small stresses. In conclusion, our knowledge of the dislocation configurations in ice as shown in the studies of Webb and Hayes indicatesthat ice behaves similarly to other plastically deformable materials. Specifically it shows

the characteristic dislocation symmetries and anisotropies found in other refractory hexagonal materials that have tetrahedral bonding.

When a dislocation moves along a basal slip plane in ice, it translates the material above the plane relative to the material below by an amount equal to the Burgers vector. Because in ice the Burgers vector is a translation vector of the crystal symmetry as specified by the oxygen atoms, the passing of the dislocation will not alter the general arrangement of the crystal. The hydrogen atoms are, however, arranged randomly in accordance with the Bernal-Fowler rules. Therefore, when a dislocation passes, it causes breaches in the Bernal-Fowler rules producing ionic defects. This process and its implications regarding the plasticity of ice have been discussed by Glen (1968) who shows that the stress required to move the dislocation and produce the resulting ionic defects is very high. At the near melting temperatures at which ice is usually found, the continuous movement of defects through the crystal causes each bond to change its orientation from time to time. When a "wrongly" oriented bond that is holding up the movement of a dislocation changes its orientation, the dislocation is free to move on. The true situation is undoubtedly quite complex because each dislocation is in fact a line defect. Presumably kinks will develop in this line when favorably oriented bonds are encountered allowing that portion of the dislocation line to move on until an incorrectly oriented bond is encountered. The overall velocity of a dislocation in ice will, therefore, be greatly reduced because the dislocation is continuously having to wait for the reorientation of bonds. Glen (1968) discusses the possible application of this model in explaining why ice does not show decelerating creep or work hardening in the case of constant strain rate tests and why fluoride doping of ice produces a large increase in the creep rate at a given stress. These ideas may also have considerable bearing on understanding the plastic relief of locally high stresses in the vicinity of stress concentrators.

Crack formation

Virtually all the work on crack formation and propagation in fresh water ice has been by Gold (1960a, 1963a, 1963b, 1965, 1966, 1967). His tests were on rectangular specimens of tap water ice that had been formed by unidirectional freezing and contained no air bubbles. The specimen size was usually 5 × 10 × 25 cm and the freezing direction as well as the long axes of the crystals were normal to the 10 × 25-cm face. The crystallographic *c*-axes were normal to the long axes of the crystals and were, therefore, randomly oriented in the plane of the 10 × 25-cm face. A compressive stress was then applied normal to the 5 × 10-cm face. The formation of cracks was noted either visually or by recording the output of a piezoelectric crystal frozen to the test specimen. Linear relations were observed between the log (total cracking activity) and the applied stress (Gold, 1960a) and between log (time to formation of the first large crack) and the applied stress (Gold, 1967). This latter relation gives added support to the results of Kingery and French (1963) who found a linear relation between log (time to failure) and applied stress. At a given stress level both log (time to formation of first large crack) and log (creep strain to formation of first large crack) appear to be normally distributed. The cracks that formed were usually long and narrow with the long direction of the crack in the long direction of the grain. The average orientation of the crack planes was parallel to the direction of the applied stress and the crack angles were normally distributed around this value. Most cracks involved only one or two grains. When a crack involved only one grain, one edge of the crack was usually located at a grain boundary. Of the cracks studied, roughly 30% were intercrystalline and 70% transcrystalline. The majority of cracks tended to have traces either parallel or perpendicular to the surface traces of the basal planes in the crystals in which they formed (Fig. 15). If a crack involved more than one grain, it usually changed direction at the grain boundary so that it would remain either parallel or perpendicular to (0001) (Fig. 16). If the crack was in neither of these orientations, it sometimes curved into the basal plane or tended to be irregular and die out.

Gold (1963b) also produced cracks by thermal shock using a brass plate cooled by dry ice in contact with the upper surface of the ice specimen. Etch pits were then used to obtain information on the crystallographic orientation of the cracks. In coarse grained ice with an average grain

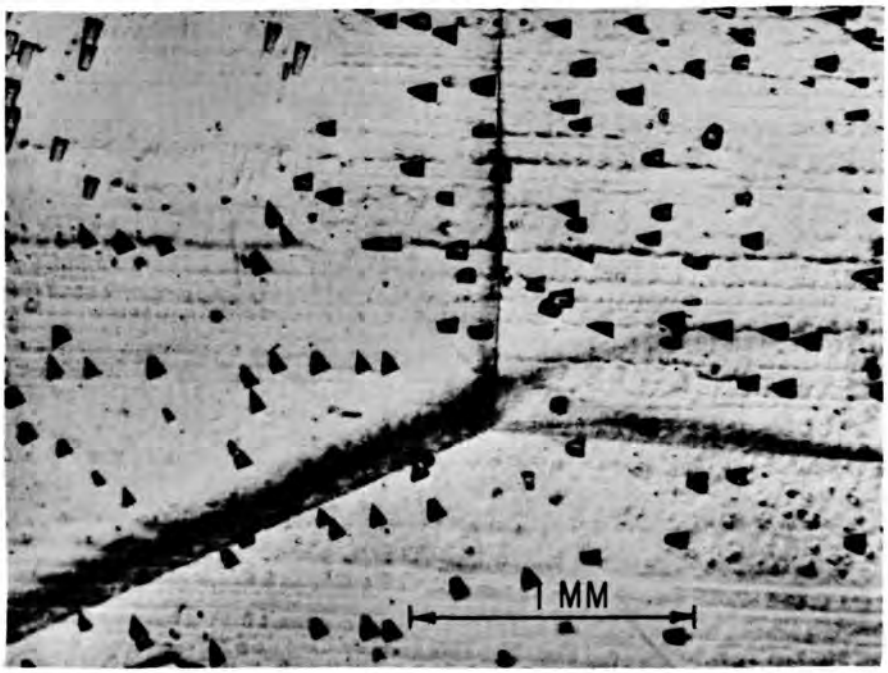

Figure 15. Crack formation in polycrystalline ice: when the crack parallel to the basal plane in the lower left grain strikes a grain boundary, it branches into two cracks, one parallel and one perpendicular to the basal plane (Gold, 1963b).

Figure 16. Crack parallel to basal plane in left grain and perpendicular to it in right as shown by etch pits. The darkened edge of the pits is due to reflection from one of the prism planes perpendicular to the basal plane (Gold, 1966).

Figure 17. Crack pattern in a plate of coarse-grained ice viewed with normal and polarized light. C-axis *of grains with rectangular pattern is almost parallel to the surface, with triangular pattern almost perpendicular (Gold, 1963b).*

diameter of 2 cm or more, the crystallographic control of the cracks was quite obvious (Fig. 17). When the *c*-axis was normal to the surface, a triangular crack pattern was observed with the cracks paralleling the prism planes; when the *c*-axis was parallel to the surface, a rectangular crack pattern formed with the cracks paralleling the basal and the prism planes. The cracks that paralleled the basal or prism faces were very straight and smooth and often showed the striated features commonly associated with cleavage cracks. Cracks in other orientations were usually curved. This strong crystallographic dependence was also found in fine grained ice; of 487 cracks observed, 67% were either parallel or perpendicular to the basal plane. In the thermal shock experiments a stress distribution was established in the ice in which the principal stresses are parallel to the shocked surface and were equal over the central area of the surface. The third principal stress was zero. Because of the orientation of the columnar grains relative to the shocked surface, there was little or no shear stress developed in the basal plane prior to crack formation. Therefore, Gold (1963b) suggests that in these experiments, little, if any, creep and stress relaxation occurred. Gold also shows that in these experiments the strain energy release rate at crack arrest is approximately equal to the rate of increase of the surface times the surface energy. This also implies that very little plastic deformation occurred at the crack edge.

Gold (1963a, 1965) has also noted the formation of small angle grain boundaries, cavities, and kink bands during deformation. The small angle grain boundaries do not usually form until the strain is greater than roughly 0.1% and the degree of their development increases with increasing strain. Two types of these boundaries were observed: one etches as a sharp line and appears in grains in which the *c*-axis is not parallel to the surface being examined; the other etches as a broad band and occurs in grains with their prism faces parallel to the surface. The boundaries usually appear to be parallel or very nearly parallel to the plane that contains the *c*-axis. Therefore, when small angle grain boundaries are associated with cracks, they are usually perpendicular to the crack. When the crack terminates within a grain, Gold (1965) observed that the crack tip was associated with a small angle grain boundary on only one side of the crack.

Before creep strain had exceeded 3%, the cavities that had formed in some specimens during deformation were clearly visible with 10× magnification. These cavities developed near grain boundaries, at grain boundary triple points, and at the intersections of slip planes and sub-boundaries. Their formation presumably occurs in planes that are oriented transverse to the local tensile stresses that result from the compressive load and should cause the reduction of these stresses. The cavities presumably nucleate heterogeneously at impurity particles present in the grain boundary regions (Low, 1963). The kink bands observed by Gold are similar to those noted in other hexagonal crystals with only one or two possible slip directions. Their formation relieves a bending moment transverse to the slip direction. The small angle grain boundaries that separate the

Figure 18. Example of the deformation of columnar ice grains due to imposed strain. Note the highly deformed region at the grain boundaries (Gold, 1966).

kink bands absorb the dislocations generated by the deformation. During the experiments no evidence for twinning was observed.

Several authors have concluded that five independent slip systems are required for a grain in a polycrystalline solid to undergo an arbitrary shape change while still conforming to the shape of the neighboring grains. In Gold's experiments, however, because of the orientation of both the crystals and the stresses, the deformation was essentially two-dimensional. For two-dimensional deformation the number of required independent slip planes reduces to two, each being in the plane of the deformation. Ice, however, has only one effective slip plane and slip in this plane is apparently independent of direction (Kamb, 1961). Therefore, for the imposed stress conditions each columnar crystal has only one slip direction available and non-uniform internal stresses develop as the result of both the constraints placed on a grain by its neighbors and the pile-up of dislocations at incompatible grain boundaries. These stresses cause highly deformed regions to develop in the vicinity of incompatible grain boundaries (Fig. 18) and in some materials may produce stress concentrations high enough to activate secondary slip systems. In ice, however, Gold's experiments indicate that even for creep strains of up to 3%, non-basal plane slip did not participate in the change of shape of the grains to nearly the same extent as did basal plane slip, if it participated at all. When evidence suggestive of non-basal plane slip occurred, it was invariably in the highly deformed grain boundary regions. Because the slip in each grain is in only one set of planes, ice is able to conform to the imposed deformation by violating one of the conditions that was assumed in determining the number of independent slip systems required: the condition of constant volume. This is possible because the stress required to initiate cracks is small enough so that cracks form and relieve the internal stresses before other slip planes are activated or other modes of deformation occur. Gold (1967) notes that many of the observations of crack formation in ice coincide quite well with the model for crack nucleation by pure edge dislocation pile-up developed by Stroh (1954, 1957) and Bullough (1964).

Detailed studies comparable to Gold's work are not available for sea ice. The only information available is from rubbings and photographs of fracture surfaces after a specimen has failed. Figure 19 is a rubbing of the horizontal undersurface of a sea ice beam that failed in tension (Anderson and Weeks, 1958). Similar rubbings and photographs have been published by Tabata

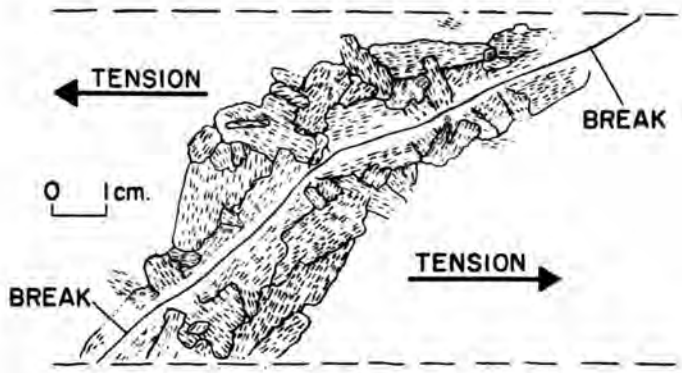

Figure 19. Rubbing of a broken segment of sea ice (Anderson and Weeks, 1958).

(1960) and by Paige and Kennedy (1967). The parallel lines in Figure 19 are, of course, traces of the edges of the individual ice plates that compose a crystal of sea ice. The *c*-axis is perpendicular to these platelets. Note how the break only transects the platelets in a few unfavorably located grains and in general follows the planes where the brine pockets are located. The current theoretical analysis of the structural control of the strength of sea ice is based on this type of observation.

Stress concentration

The bulk stress in a general form is defined by the force applied divided by the area. It is, however, known that real samples invariably fail because of the existence of higher localized stress levels. The resulting stress concentration can be either internal, within the material because of voids such as air bubbles or brine pockets or grain boundaries as shown in Figure 18; or external, caused by the shape of the sample. An example of the latter is the stress concentration caused by the sharp transition in cross section at the butt of a cantilever beam. When the strength of an ideally brittle material is exceeded as a result of a local stress concentration, failure results. This is not necessarily true in a plastic material where stress relief occurs in the region of the stress concentration. This stress relief will depend upon such factors as temperature and strain rate. If time is considered as a factor, we will speak about viscosity. At low temperatures ice is more brittle, while near the melting point it becomes highly viscous. This is especially true for sea ice at temperatures warmer than -8C where the salt content produces large increases in the brine volume and as a result decreases in the viscosity.

The effect of viscosity on stress concentration can be marked and may produce significant distortions in calculated strength values. Introducing the theoretical stress concentration factor K_t as the ratio of the computed local stress to the mean stress and the reduced actual stress concentration factor K_a, one may (Sala, 1961) use a stress concentration index η,

$$\eta = \frac{K_a - 1}{K_t - 1} \tag{1}$$

which is a characteristic of a material and its state (temperature, strain rate, impurity levels, etc.). The parameter η characterizes the degree of plasticity and is 1 for an ideally brittle substance and 0 for an ideally plastic substance.

Stress concentration can conveniently be discussed by using the model of a perforated plate in tension. Anderson and Weeks (1958) discussed the differences in the strengths of fresh and sea ice in terms of such a model and suggested that

$$\sigma_f = \frac{\sigma_i}{K}(1 - \psi) \tag{2}$$

where σ_f is the strength of sea ice, σ_i is the strength of air-free fresh ice without stress concentration, ψ is the "plane porosity" or relative reduction in the area of the failure plane due to the presence of brine and air inclusions, and K is a stress concentration caused by the presence of the brine pockets in sea ice. As long as the circular holes are sufficiently separated the theory gives $K_t = 3$ for pure tension. Now suppose $\eta = ½$, then

$$K = K_a = 1 + \eta(K_t - 1) = 2 \tag{3}$$

and the actual strength is 50% higher than eq 2 would predict.

An interesting case occurs when a ring tensile test rather than a pure tension test is used. For an infinitesimally small coaxial hole in the ring $K_t = 6$ (Assur, 1958). If we again suppose that $\eta = ½$, then $K = K_a = 1 + ½(6 - 1) = 3.5$ and the actual strength is $^6/_{3.5}$ or 71% higher than eq 2 would predict. The ring tensile test would give a nominal value of $^{3.5}/_2$ or 75% higher than a pure tensile test. In the case of an ideally brittle material ($\eta = 1$), the ratio would be $^6/_3 = 2$. Furthermore, the stress concentration index η itself must be a function of ψ since ψ depends upon the brine volume which is, in turn, a function of salinity and of temperature which effects viscosity. Therefore, eq 2 itself depends upon viscosity and will be very dependent upon the type of test. All this illustrates the conceptual difficulties in designing adequate testing procedures and analyzing the results of such tests.

Equation 2 also implies that the basic strength of sea ice σ_0 is one-third the strength of fresh ice σ_i/K, and that this difference is produced by the presence of brine pockets ($K = 3$) in sea ice. Here σ_0 is the extrapolated intercept value of σ_f at $\nu_b = 0$ as determined from a plot of σ_f vs ν_b or $\sqrt{\nu_b}$. It can be thought of as the strength of a conceptual material that contains no brine or air, but still possesses the sea ice substructure and fails as a result of the same mechanism that causes sea ice to fail. Assur, on the other hand, argued that the presence of brine inclusions does not explain the difference between fresh and sea ice, because fresh ice invariably contains small bubbles or flows that act as stress concentrators. Indeed, when one performs solid cylinder tests (without a coaxial hole) with a theoretical $K_t = 1$ as well as ring tensile tests on fresh ice, one finds that the results can be reconciled only by assuming that $K \approx 6$ for the solid cylinder test (Butkovich, 1959b; Weeks, 1962). This is the theoretical K_t value for an infinitesimally small hole. Further experimental data bearing on this general problem have been provided by Weeks (1962) and Graystone and Langleben (1963) who demonstrated that for both NaCl ice and sea ice σ_0 was roughly equal to the bulk strength of fresh ice. However, the formal equating of σ_0 with σ_i is still a rather suspect procedure (Goetz, 1965), inasmuch as the aspect of the microstructure of fresh water ice that causes the failure is unspecified. Furthermore, because fresh water ice contains no brine pockets, it may fail by quite a different mechanism than does sea ice. The initial suggestion of a pronounced strength difference of roughly three between fresh and sea ice was based on comparing the results of *in situ* cantilever tests on sea ice with the results of small beams and pure tension tests on fresh ice. The difference of a factor of three was, therefore, the result of differences in testing procedures as well as the result of a scale effect.

THEORETICAL CONSIDERATIONS

Up to the present time there has been almost no theoretical analysis of fracture in lake and river ice. It has simply been assumed that lake and river ice were pure ice. The fact that most freshwater ice contains an appreciable amount of air and has a structure that may vary widely from

one location to another has been largely ignored. This oversimplification was possible because the differences in failure strengths determined by different testing techniques were much more pronounced than differences that could readily be associated with changes in the nature of the ice. In sea ice, however, large variations in strength values as determined by a given testing technique made the development of formal strength models highly desirable in the hope that they would suggest compact forms for correlating and extrapolating available data.

The treatment of the mechanical properties of sea ice on the basis of structural models was pioneered by Tsurikov (1940, 1947a). He initially considered porosity only in terms of air content although he later (Tsurikov, 1947b) introduced brine volume based on Malmgren's (1927) calculations. His imaginative approach was limited by the fact that he did not have available an adequate description of the sea ice microstructure. He therefore assumed that the voids in sea ice were uniformly distributed and were either spherical or cylindrical in shape. A brief review of Tsurikov's papers can be found in Weeks and Assur (1968). Other Russian investigators appear to have paid little attention to Tsurikov's work although it clearly demonstrated the possibility of developing a structurally based theory of sea ice strength.

Even a casual examination of a fractured piece of sea ice indicates that the fracture surface is controlled by the sea ice substructure: the breaks follow the planes where the brine pockets are concentrated and only transect the platelets in a few unfavorably oriented grains (Fig. 19, Anderson and Weeks, 1958; Tabata, 1960). If a potential failure plane between two ice platelets is considered, one sees that in cold sea ice (Fig. 20) with a small brine volume, the brine pockets are small and widely separated. An appreciable portion of the "failure" plane is, therefore, ice and the sample would be expected to have a strength only slightly less than the strength of pure ice. Warm sea ice, on the other hand, may contain a large volume of brine. For example, in Figure 21 a plane can be passed "horizontally" through the sample without encountering more than a few ice-ice bonds. Therefore, this specimen would be expected to have a tensile strength close to zero even though it contains an appreciable amount of ice. Tests verify this expected behavior in that failure strength σ_f decreases from a maximum at zero brine volume ($\nu_b = 0$) to a strength of zero at brine volume ν_0. Therefore, it should be possible to express sea ice strength in the general form

$$\frac{\sigma_f}{\sigma_0} = 1 - \psi \tag{4}$$

where σ_0 can be considered the basic strength of sea ice (i.e., the strength of an imaginary material that contains no brine, but still possesses the sea ice substructure and fails as a result of the same mechanism that causes failure in natural sea ice) and ψ is the "plane porosity" or relative reduction in area of the failure plane as the result of the presence of brine and air inclusions. The critical value of ψ in the failure plane is

$$\psi = f(\nu) = f(\nu_a + \nu_b) \tag{5}$$

where ν is the void volume or porosity and ν_a and ν_b are the volume of air and brine respectively in the ice. We will now for simplicity consider a sea ice specimen in which $\nu_b >> \nu_a$. To express ψ in terms of ν_b, a simplified model of the brine geometry of real sea ice must be given. This has been done by Assur (1958), Anderson and Weeks (1958), and Anderson (1958a, 1960), who fortunately had available a considerable amount of information on the structure of sea ice. If the brine is assumed to be distributed as shown in Figure 22 (Assur, 1958), the relative brine volume is

$$\nu_b = \frac{F g}{a_0 b_0 g_0} . \tag{6}$$

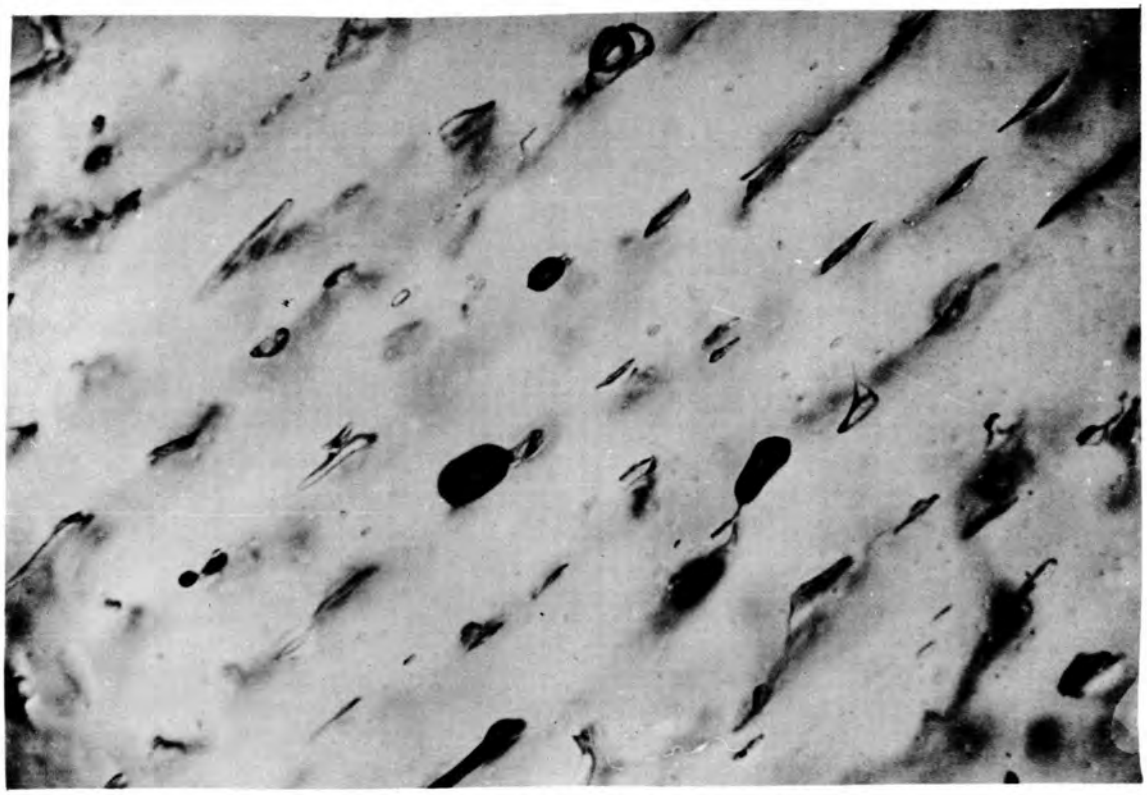

Figure 20. Cold sea ice (Thule, Greenland).

Figure 21. Sea ice at a temperature of -3C (Thule, Greenland). Essentially all the brine had drained from the sample.

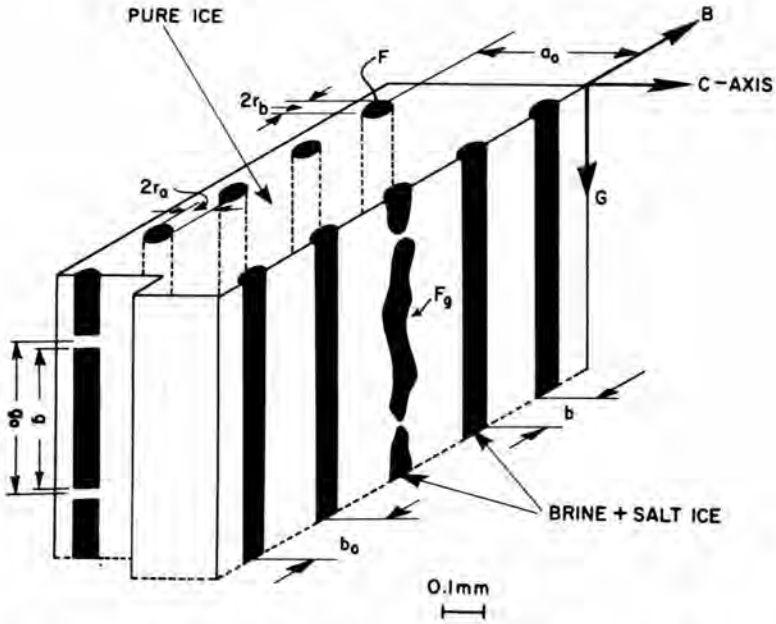

Figure 22. Idealized diagram of the shape of the brine inclusions in sea ice (Assur, 1958).

If we define

$$\beta_0 \equiv \frac{b_0}{a_0} \tag{7}$$

and

$$\gamma = \frac{g}{g_0} \tag{8}$$

we find that the reduction in cross-sectional area as the result of the presence of the brine pockets is

$$\psi = \frac{2\, r_b\, g}{b_0\, g_0} = \frac{2\, r_b\, \gamma}{\beta_0\, a_0} \,. \tag{10}$$

The question now is how the geometric parameters r_b and γ vary with ν_b. Although a number of different assumptions can be made here, only two are commonly used. The simplest is to assume that geometric similarity is preserved only along the B-axis (see Fig. 22), and that the width as well as the relative length (γ) of the brine inclusions remains constant. In this case r_b must change proportionally to ν_b and an equation of the form

$$\frac{\sigma_f}{\sigma_0} = 1 - c\, \nu_b \tag{11}$$

results. If, on the other hand, the average length and spacing of the brine cylinders remain constant, changes in ν_b will be reflected only in the *BC* cross section. If geometric similarity is preserved in this cross section, then our equation is of the form

$$\frac{\sigma_f}{\sigma_0} = 1 - c\,\nu_b^{1/2} \tag{12}$$

These two models can be represented as straight lines in σ_f, ν^k coordinates where k is 1 and ½ respectively. The σ_f axis intercept is σ_0 and

$$c = \nu_0^{-k} \tag{13}$$

where ν_0 is the volume of brine necessary to cause the ice to have zero strength. Defining

$$\rho \equiv \frac{2\,r_b}{\sqrt{F}} \tag{14}$$

and

$$\alpha_0 \equiv \frac{a_0}{\sqrt{F}} \tag{15}$$

ν_0 for these models may be written as

$$k = 1:\ \nu_0 = \frac{1}{\rho\,\alpha_0} = \frac{F}{2\,r_b\,a_0} \tag{16}$$

and

$$k = 1/2:\ \nu_0 = \frac{\beta_0}{\rho^2\,\gamma} = \frac{b_0\,g_0\,F}{4\,r_b^2\,g\,a_0} \tag{17}$$

The two specific models that have been utilized in discussing strength results are the constant width and elliptical cylinder models.

In the constant width model

$$F = 4\,r_a\,r_b \tag{18}$$

and

$$\nu_0 = \frac{2\,r_a}{a_0} = \frac{d_0}{a_0} \tag{19}$$

where d_0 is the minimum width of a parallel brine layer before it splits as the result of interfacial tension to produce individual brine pockets. It is usually assumed (Weeks and Assur, 1963) that d_0 = constant because the ice/brine interfacial tension would not be expected to be particularly

temperature sensitive in the temperature interval where sea ice observations are made. A value of d_0 of 7×10^{-3} cm has been measured in natural sea ice (Anderson and Weeks, 1958) by direct petrographic methods and a value of 11×10^{-3} cm in NaCl ice by an indirect calculation (Weeks and Assur, 1963). When a brine layer becomes thinner than this value it necks, causing ice-ice bonds to form. When the first of these bonds forms between the growing plates at the bottom of an ice sheet, it establishes the location of the "bridging" layer. The ice platelets below this location are not laterally connected and, therefore, have zero tensile strength. The thickness of this strengthless skeleton layer should be neglected in strength calculations.

In the elliptical cylinder model let

$$\epsilon = \frac{r_b}{r_a} \tag{20}$$

and

$$F = \pi r_b r_a = \frac{\pi r_b^2}{\epsilon} \tag{21}$$

and eq 12 becomes

$$\frac{\sigma_f}{\sigma_0} = 1 - 2\sqrt{\frac{\epsilon \gamma}{\pi \beta_0}} \sqrt{\nu_b} \tag{22}$$

If we wish to consider circular cylinders ($\epsilon = 1$) and neglecting any interruption of brine pockets in the vertical direction ($\gamma = 1$), eq 22 becomes

$$\frac{\sigma_f}{\sigma_0} = 1 - \frac{2}{\sqrt{\pi \beta_0}} \sqrt{\nu_b} \tag{23}$$

As will be discussed in detail later, recent experimental results (Frankenstein, 1968a) have verified the tentative suggestion of Assur (1958) that the strength of warm sea ice does not approach zero as a linear function of ν_b^k as suggested by these previous models. Instead, if σ_f is plotted versus $\sqrt{\nu_b}$, the resulting curves are convex toward the origin of the coordinate system in the high brine part of the diagram (Fig. 35). It is possible (Weeks and Assur, 1968) to modify eq 22 in such a way that it more properly describes this observed strength variation by writing it as

$$\frac{\sigma_f}{\sigma_0} = \left[1 - \sqrt{\frac{\nu_b}{\nu_0}}\right]^n \tag{24}$$

If we make the simple assumption that $n = 2$

$$\frac{\sigma_f}{\sigma_0} = 1 - 2\sqrt{\frac{\nu_b}{\nu_0}} + \frac{\nu_b}{\nu_0} \tag{25}$$

which is a second order polynomial in $\sqrt{\nu_b}$ and is a combination of the two main models discussed above; one linear in $\sqrt{\nu_b}$, the other in ν_b. Furthermore, if we assume that $\nu_0 = 1$ so that only one parameter σ_0 needs to be determined then

$$\frac{\sigma_f}{\sigma_0} = 1 - \sqrt{\nu_b}\,(2 - \sqrt{\nu_b}) \tag{26}$$

which for small $\sqrt{\nu_b}$ gives the same slope as observed from tests using eq 22 (Assur, 1958; Weeks, 1962; Frankenstein, 1968a). This relation may be an oversimplification and prove difficult to fit to some data.

To provide more flexibility in data analysis, we can start with the general relation given in eq 22 with

$$\nu_0 = \frac{\pi \beta_0}{4 \epsilon \gamma} \tag{27}$$

as in eq 24. Expanding eq 24 in terms of a power series gives

$$\frac{\sigma_f}{\sigma_0} = 1 - n\sqrt{\frac{\nu_b}{\nu_0}} + \frac{n(n-1)\nu_b}{2!\ \nu_0} - \cdots \tag{28}$$

if the higher order terms are omitted. To reduce the number of parameters which must be specified from three to two, we assume the same ratio 1:2 between the coefficients of the third and second terms of the polynomial eq 28 as in the simplified eq 26. This leads to the condition

$$\frac{n-1}{\sqrt{\nu_0}} = 1 \tag{29}$$

In other words, if ν_0 happens to be less than 1 we assume that n in eq 28 is also slightly less so that the condition given in eq 29 is still valid. We can then rewrite eq 28 as

$$\frac{\sigma_f}{\sigma_0} = 1 - \sqrt{\frac{\nu_b}{\nu_0}}\ (2 - \sqrt{\nu_b}) \tag{30}$$

and eq 29 will always be satisfied. Equation 30 has the advantage over eq 26 in that it leaves the choice of ν_0 open. It is also linear when plotted as σ_f vs $[\sqrt{\nu_b}\,(2 - \sqrt{\nu_b})]$.

It should be noted that additional petrographic observations are needed on the distribution of air pockets in sea ice. If, as seems reasonable, air bubbles are localized along the same substructure as the brine pockets, then we may simply treat ν_a as an additional contribution to ν_b and deal with the total void volume ν where $\nu = \nu_a + \nu_b$. If, on the other hand, the geometrical considerations governing the distribution of the air bubbles are quite different from those controlling the brine distribution, ν_a will have to be considered separately.

There has been some discussion in the recent sea ice literature regarding the possible effects of $Na_2SO_4 \cdot 10H_2O$ in increasing the values of σ_f beyond the normal increase that would be associated with the decrease in the size of the brine pockets as the solid salt precipitates. Possible hypotheses for this so-called solid salt reinforcement of the brine pockets have been advanced by Assur (1958) and Peyton (1966). Because the experimental verification for this effect is still in doubt, we will not discuss these theories here. It should, however, be noted that both hypotheses depend upon how the solid salts are distributed in the brine pockets during precipitation. The salts may precipitate in a solid mixture with the ice in which case reinforcement is

possible. Or the solid salt crystals may remain in the liquid brine in which case no reinforcement is possible. If the solid salts enter into a solid mixture with ice, they will not participate in further brine drainage and a change in the ion ratios with time should be observed. If the solid salts drain together with the brine, the ion ratios should remain constant in sea ice. Sporadic evidence to support either of these views is available (Savel'ev, 1963; Bennington, 1963b).

Goetz (1965) has also pointed out that it is possible to approach the sea ice strength problem as a problem in elastic instability in a brittle material. The well known Griffith crack problem is of this type. In the Griffith crack analysis, it has been shown that two conditions must be satisfied for spontaneous crack growth:

1. A stress concentration must exist that is sufficient to overcome the intrinsic strength of the material.

2. Elastic readjustment as the crack develops must provide a decreasing energy path for the specimen as a whole.

Griffith's criterion for a failure stress is

$$\sigma_f \geq \sqrt{\frac{2\,E\,\gamma'}{\pi\,c}} \tag{31}$$

where σ_f is the failure stress, E is Young's modulus, γ' is the total energy required per unit increase in the area of the crack (composed of the true surface energy and the plastic work done by the stress concentration at the tip of the moving crack), and c is the crack length. Goetz (1965) has extended this treatment by considering the failure criterion for a polycrystalline, elastic material which contains a "microstructure" capable of generating a stress concentration. This is done by considering a grain that has for some reason, perhaps orientation differences, an apparent E lower than its surroundings. The result is

$$\sigma_f \geq \sqrt{\frac{8\,\gamma'\,G}{\pi(\eta+1)(1-\frac{\kappa\delta}{\pi})\,c_0}} \tag{32}$$

where G is the shear modulus, $\eta = \frac{3-\mu}{1+\mu}$ where μ is Poisson's ratio, κ is the proportion of the stress σ that is exerted on the weak crystal ($0 \leq \kappa \leq 1$), and δ is a complicated function of c_0 and c where $2c_0$ is the original grain length and $(c - c_0)$ is the length of the crack (prior to cracking $c = c_0$ and $\delta = \pi$). If $(1-\kappa) > 0$, failure can clearly occur for sufficiently large σ without the presence of a crack prior to failure. This is not true in a homogeneous material. Goetze then shows by a dimensionless argument that elastic instability can occur during plane stress when

$$\sigma \geq \sqrt{\frac{2\,E\,\gamma'}{\pi\,P\,d}} \tag{33}$$

where P has a value close to 1 and when a class of materials is considered in which the microstructure varies only in size, P remains constant. The length d is taken to be a characteristic of the size of the microstructure. Therefore, when dealing with failure stresses

$$\sigma_f^2\,d = \frac{2\,E\,\gamma'}{\pi\,P} \approx \text{const.} \tag{34}$$

Considering ring tensile results on sea ice, we find that $\sigma_f \approx 15$ kg/cm^2 and that $E \approx 5 - 10 \times 10^{10}$ dynes/cm^2, $\gamma' \approx 76$ ergs/cm^2 and, assuming that $P \approx 1$, eq 34 implies that the fracture originates

in a microstructure with a size of 0.1 to 1.0 mm. This is clearly of the same scale as the brine pockets in sea ice.

To treat sea ice as an instability problem it is necessary to assume that only the brine pockets within a given plane interact elastically. This, of course, is quite reasonable considering the structure of sea ice. We then must obtain the elastic solution for a periodic array of cracks. This apparently is not known. Therefore, Goetz (1965) makes a number of approximations to get some idea of the general solution. If b_0 and r_b are defined in Figure 22, his approximate fracture relation is

$$\sigma_f \geq \text{const}\left(\frac{b_0}{2\,r_b} - 1\right). \tag{35}$$

He then assumes that $2r_b$ can be identified with $\sqrt{\nu_b}$ where ν_b is the brine volume and shows that a σ_f vs $1/\sqrt{\nu_b}$ plot of Assur's (1958) ring tensile data is, to a good approximation, linear. There are some obvious difficulties with eq 35; note that when $r_b \to 0$, $\sigma_f \to \infty$. Yet it is cold sea ice with its correspondingly low brine volumes that most closely approximates the brittle behavior postulated by an elastic instability analysis. Nevertheless, this is an interesting and promising approach, if not for sea ice which is always quite close to its melting temperature, then for other porous materials which show brittle fracture characteristics.

Inasmuch as structural models based on a random distribution of voids have been quite successful in analyzing variations in the failure strength of snow (Ballard and McGaw, 1966; Ballard and Feldt, 1966), it is reasonable that a similar approach would prove useful in the study of lake and river ice. To develop such models quantitative information is needed on the size and spacing of air bubbles in fresh ice. Hopefully it may eventually prove possible to calculate this from the dissolved air content of the water and the growth velocity of the ice. If the air bubbles prove to be randomly distributed, the equations developed by Tsurikov (1940, 1947a) will be applicable (see Weeks and Assur, 1968, eq 3.3, 3.4, 3.9 and 3.10).

Several attempts have been made to show how structural changes in ice resulting from changes in the meteorological conditions during growth can affect the overall properties of the ice sheet. Assur and Weeks (1963, 1964) have shown how growth induced changes in the geometry of the sea ice microstructure influence the failure strength. To do this they assumed that the relation between the plate spacing a_0 and the growth velocity v could be expressed as

$$a_0\sqrt{v} = \text{const}. \tag{36}$$

Then using the fresh ice growth equation and the results of the formal strength models which indicate that σ_f is a function of a_0, they offer a scientific justification for the intuitive conclusions of early Russian observers who felt that the strength of young sea ice was in some way influenced by its growth conditions. Assur and Weeks also consider the effect of a snow cover and ways of incorporating the change in the salinity of the ice sheet with time. Changes in the initial salinity and brine volume profiles as a function of growth conditions have been studied by Weeks and Lofgren (1967). Peschanskii (1967) has introduced a special coefficient of ice formation in an attempt to account for this. Field observation shows that lake ice that forms rapidly under very low air temperatures has a 15% lower strength than ice that grew more slowly. Based on experience with other materials, the decreased grain size associated with rapid freezing (Lavrov, 1962) would cause an increase in strength (Tegart, 1966). The observed strength decrease is probably related to an increase in the amount of air trapped in the ice or to the formation of thermal cracks.

EXPERIMENTAL RESULTS

As mentioned earlier, the quality of experimental studies on the failure strength of lake and sea ice as determined by rapid testing procedures is quite varied. Many investigators have not adadequately specified the state of the ice at the time of testing . Ideally, every measure of a failure strength or a mechanical property should be coupled with a measure of the ice temperature, the volume of included air, the history of both the ice sheet and the sample after it was removed from the ice sheet, the location of the sample in the ice sheet, the sample orientation, a designation of the structural aspects of the sample such as grain size and crystal orientation, and if applicable, a determination of the salinity. The available sets of tests that are accompanied with all this subsidiary data are few and for a good reason: the collection of this type of information is time consuming. However, when it is not available there is usually no way to account for discrepancies between the results of different investigators who have studied what is presumably identical ice.

There are also a number of differences in the testing procedures that have been used to determine a single parameter such as the tensile strength of ice. Even the test procedures and equipment recommended by the different groups studying ice vary somewhat although the overall approach is similar. General descriptions of these procedures and equipment as used in Russia and in the United States and Canada are given in Kudriavtsev (1957), Butiagin (1966a), and Peschanskii (1967), and Butkovich (1958) respectively. The main types of tests considered are *compressive, tensile* (ring and "dog-bone"), *flexural* (small beam and *in-situ*) and *shear*. Kudriavtsev (1957) and Korzhavin (1962) also discuss a *ball impression* test and *indentation* tests. All these authors stress the importance of determining at least the temperature of the sample and when applicable its salinity. It is also commonly recommended that in tests concerned with the elastic behavior of ice, the rate of stress application $\dot{\sigma}$ should be greater than some critical value. A critical value of $\dot{\sigma}$ that has commonly been used is 0.5 kg/cm^2 sec (Butkovich, 1958). This suggestion is based on the data of Jellinek (1958) who studied the variation of the tensile strength of snow ice cylinders as a function of $\dot{\sigma}$. As will be discussed later, recent data suggest that for certain types of tests this value may be far too low.

In this review we will only discuss those papers which have provided a reasonable amount of supplementary data with their test results. In a few cases exceptions will have to be made when there are almost no data available regardless of quality.

Compressive strength

As has been noted by several authors, the values obtained by crushing tests vary significantly with the conditions of deformation: i.e. the dimensions of the sample and the stress rate $\dot{\sigma}$ (Butkovich, 1958; Voitkovskii, 1960; Peyton, 1966). Unfortunately, there have been consistent differences between the sample geometry used by American and Canadian as compared with Russian investigators. The North Americans have commonly used ice cylinders or prisms with a 2 or 3 to 1 ratio of length to width, while the Russians have used cubic specimens. In freshwater ice as the length to width ratio increases, the strength decreases. This is strikingly shown in Figure 23 which plots the results of Butkovich (1955) determined from prismatic samples at -7C with length/width ratios of 2/1 and 3/1 and the results of Butiagin (1966a) determined on cubic specimens at 0C (the lower curve). To compare Butiagin's results with Butkovich's, two corrections must be made. The first is caused by the samples being at different temperatures. The second is necessary because in Butiagin's tests the axis of compression was normal to the long axes of the ice crystals, while in Butkovich's tests they were parallel. When these tentative corrections are made Butiagin's results plot as the dashed upper curve and when compared with Butkovich's results show the expected systematic decrease in compressive strength as the ratio l/w increases. This is also a good example of two sets of data that, while actually in very good

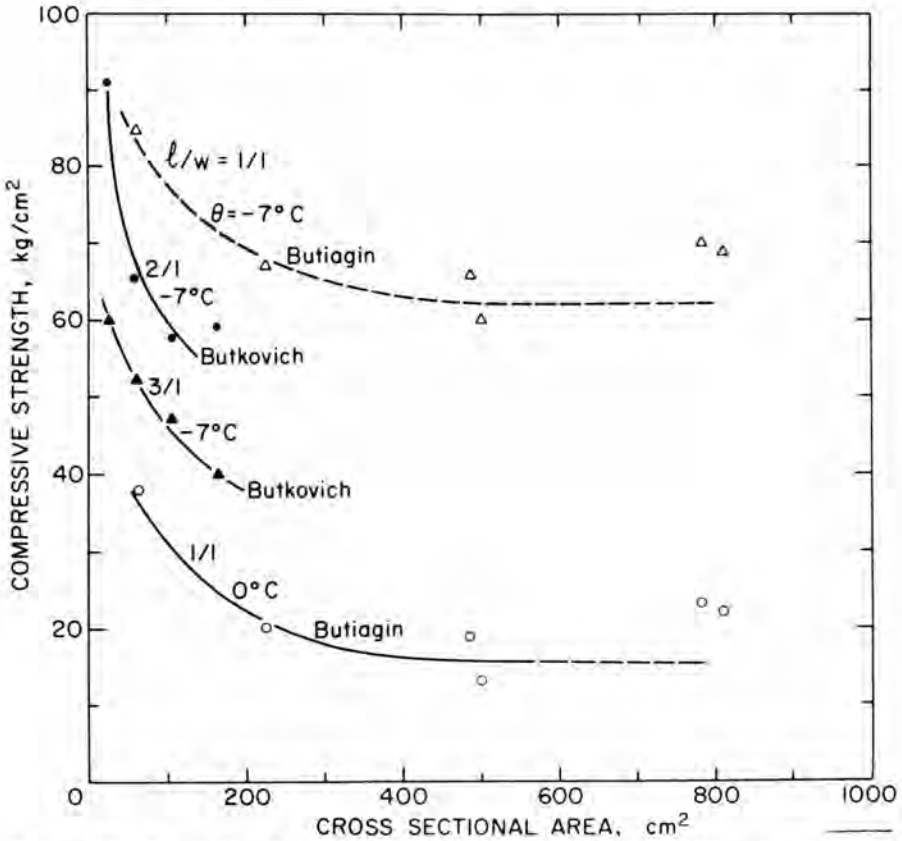

Figure 23. Unconfined compressive strength of several different sizes of lake ice samples vs cross-sectional area of the specimen (Butkovich, 1955; Butiagin, 1966a).

agreement, would appear to be "unrelated" if detailed supplementary data on the state of the ice and the test procedure were not available.

Figure 24 shows the pronounced effect of temperature on the fresh ice compressive results of Butkovich (1954) and Vitman and Shandrikov (1938). In Butkovich's tests the circles indicate that the load was applied parallel to the long axes of the crystals and the triangles that it was applied normal to the axes. The fact that for cold fresh ice the strength as determined with the force exerted parallel to the crystal axes is roughly 25% higher than when exerted normal has also been noted by Korzhavin (1962) and Voitkovskii (1960). Butkovich (1956, 1959a) also obtained a similar but more pronounced increase in the compressive strength of vertical cores of sea ice as compared with the strength of horizontal cores. For vertical sea ice specimens, Butkovich found median strength values ranging from 78 kg/cm² at -5C to roughly 120 kg/cm² at -16C. Average values on horizontal cores in the same temperature range vary from 21 to 43 kg/cm². Considering the structure of the ice tested this is to be expected. In Butkovich's fresh ice tests the *c*-axes were known to be normal to the long axes of the crystals while in sea ice this same orientation invariably occurs. Therefore, when a load is applied perpendicular to the long axes of the crystals, both the grain boundaries and the basal planes of individual ice crystals, which are the planes of easy slip and in sea ice the planes along which the brine pockets are located, are oriented so that the specimen will fail readily. We expect, however, that in fresh ice this strength difference is primarily associated with the change in orientation of the grain boundaries since Butkovich (1955) was not able to find any change in compressive strength associated with changes in the *c*-axis

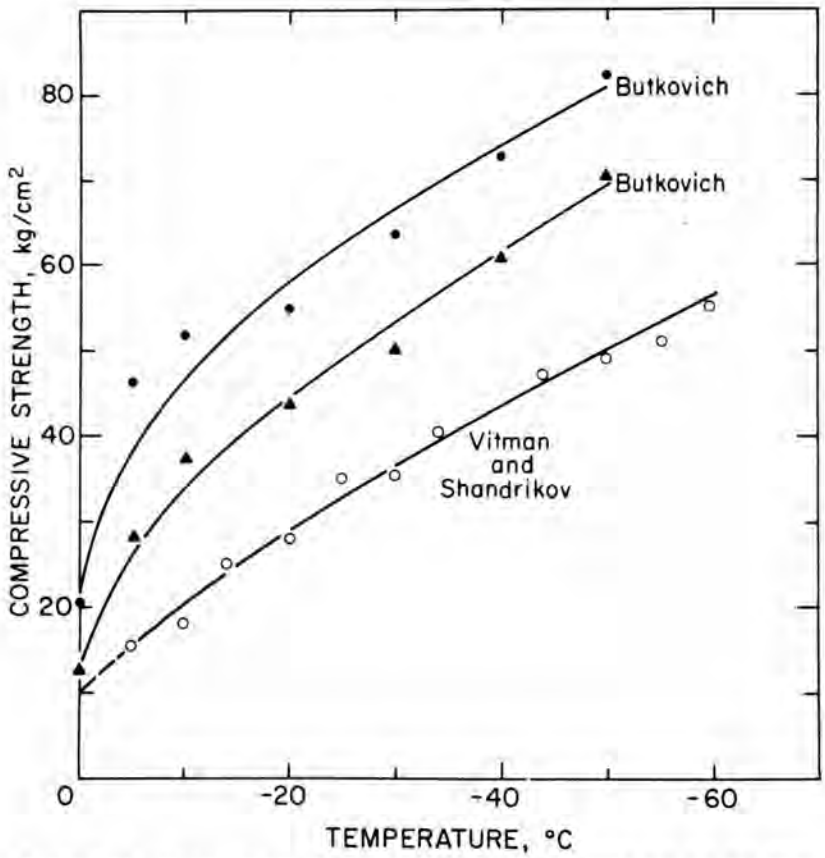

Figure 24. Unconfined compressive strength of lake ice vs ice temperature (Butkovich, 1954; Vitman and Shandrikov, 1938). In the data of Butkovich the circles indicate the load was applied parallel to the growth direction and the triangles that it was applied normal to the growth direction.

orientations in otherwise similar lake ice. Also, most compressive failures in both fresh and sea ice occur (Butkovich, 1956; Butiagin, 1966a) by the ice specimen fracturing vertically (presumably along grain or substructure boundaries) into a large number of prismatic fragments.

The effect of changes in grain size on the failure strength of fresh ice in compression has been studied by Butiagin (1966a) who found that slush ice with a random crystal orientation averaged 30% stronger than normal river ice in tests on the Ob and Yenisei. This general increase in σ_f with a decrease in mean grain diameter ($\bar{d}$) is similar to experience gained from other materials (Low, 1963). However, Butkovich (1955) has found a decrease in σ_f of between 30 and 40% when ice from Portage Lake ($\bar{d} \approx 1$ to 3 cm at the top, 2 to 5 cm at the bottom) was compared with the ice of Rice Lake and Lake Annie ($\bar{d} \approx 0.2$ to 0.5 cm at the top, 0.5 cm at the bottom). Similar results have been obtained by both Lavrov (1962) and Peschanskii (1967) who suggested that the strength decrease was produced by poorer "bonding" between crystals as a result of a higher level of trapped impurities. There is no information available on this subject for sea ice. If future studies are made of this problem, it is quite important that independent determinations be made of the amount of trapped air and chemical impurities.

The most complete set of compressive strength observations available on sea ice is reported by Peyton (1966) who ran tests on a large number of samples of different sea ice petrographic types

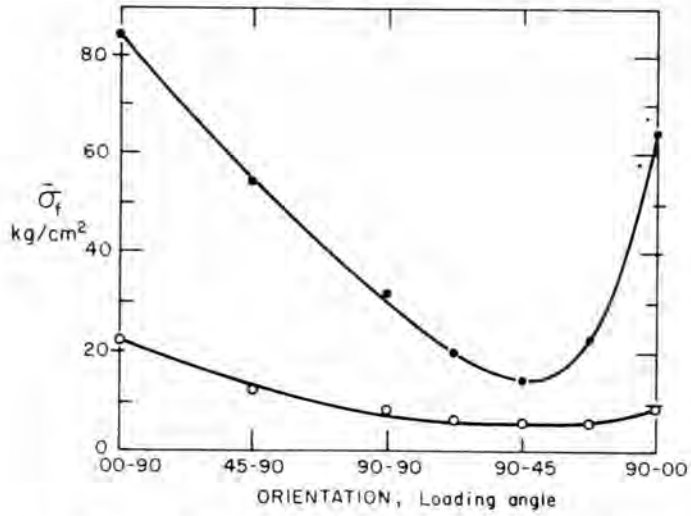

Figure 25. Average failure strength of sea ice in compression (solid circles) and in direct tension (open circles) vs sample orientation: bottom ice, -10C (Peyton, 1966). For orientation notation, see text.

at various orientations and stress rates. He found a marked dependence of compressive strength on sample orientation (Fig. 25). The ice used in these tests had a grain size larger than the dimensions of the specimens. Therefore, each sample can be considered a "single" crystal. In this type ice *c*-axis orientations in the ice sheet are always close to horizontal. The loading angle notation is as follows: the first number gives the angle between the axis of the test sample and the vertical, while the second number gives the angle between the sample and the *c*-axis of the ice crystal. Note that the ratio of the strength obtained from vertical cores to that obtained from horizontal cores is 3/1, in agreement with the results of Butkovich (1959a).

Peyton has also noted a relation between the compressive strength σ_f, and the stress rate $\dot{\sigma}$, the brine volume of the sample, and the position of the specimen in the ice sheet. He then has attempted to "remove" the effect of $\dot{\sigma}$ on σ_f by using multiple regression techniques as follows. If the regression equation is of the general form

$$\sigma_f = a\,\dot{\sigma}^b\, X_1^{y_1}\, X_2^{y_2} \cdots X_n^{y_n} \tag{37}$$

a new parameter σ_R can be defined as

$$\sigma_R = \frac{\sigma_f}{\dot{\sigma}^b} = a\, X_1^{y_1}\, X_2^{y_2} \ldots X_n^{y_n}\,. \tag{38}$$

This parameter is, of course, related to the original σ_f value, but unfortunately using Peyton's results it is difficult to interpret σ_R values in terms of actually measured compressive strengths. It would have been much simpler to correct all strength values to a common value of $\dot{\sigma}$. The range of the stress rates used was $0.06 \leq \dot{\sigma} \leq 8.2$ kg/cm² sec and the average value of b as determined by least squares was 0.22 indicating that σ_f shows a small increase with increasing $\dot{\sigma}$. If we consider σ_R as a strength index and plot it against $\sqrt{\nu_b}$ we obtain Figure 26. Peyton has interpreted the fact that ice strengths determined at temperatures below -8.7C lie above a least squares straight

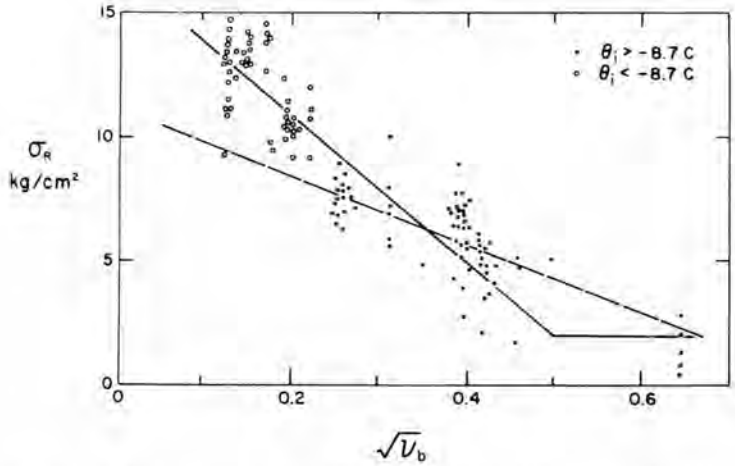

Figure 26. σ_R from compression tests on sea ice vs square root of the brine volume (Peyton, 1966). For the difference between the solid and dashed lines see discussion in text.

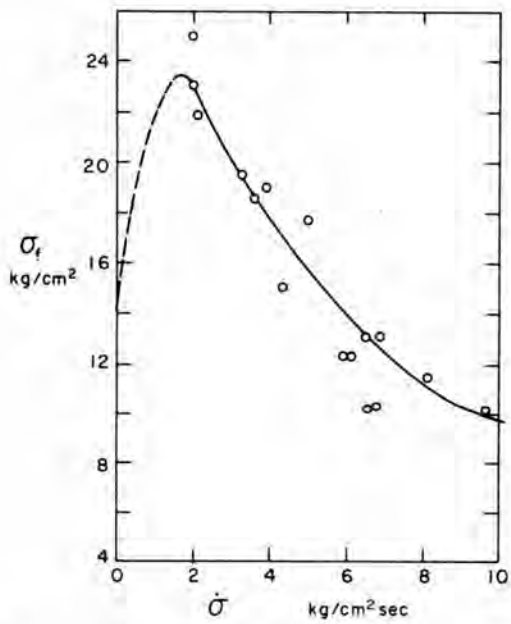

Figure 27. Relation between compressive strength σ_f of sea ice from Cook Inlet, Alaska, and stress rate $\dot{\sigma}$ (Peyton, 1966). The dashed line is conjectural based upon Arctic Ocean results.

line fitted through the strength data for temperatures above -8.7C (the dashed line) as indicating that $Na_2SO_4 \cdot 10H_2O$ precipitation is effective in strengthening the ice. This may be true. The data are, however, not conclusive inasmuch as the results of ring tensile, *in-situ* cantilever beam, and shear tests (Fig. 35, 44, 48) show a similar curvilinear relation that does not appear to be associated with the precipitation of $Na_2SO_4 \cdot 10H_2O$. Regardless of the salt reinforcement question, Figure 26 is quite important in that it indicates that compressive strength data can be analyzed

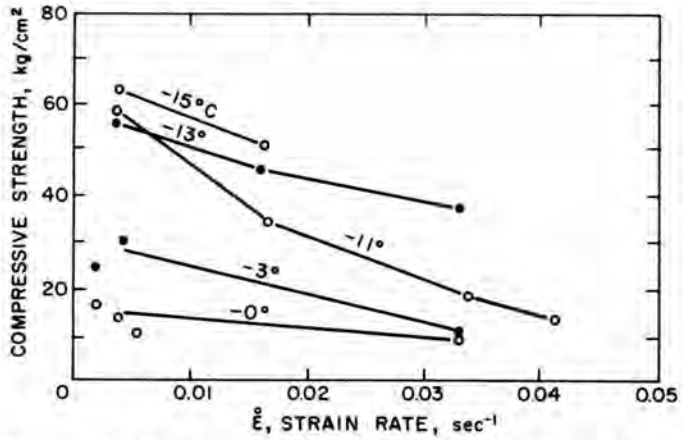

Figure 28. Compressive strength of cubes of lake ice vs strain rate. The load is applied normal to the growth direction (Korzhavin, 1962).

using eq 22 or 30. A similar conclusion can also be reached by analyzing the data on the compressive strength of sea ice as reported by Peschanskii (1967).

Peyton (1966) has also presented some results of compressive strength measurements vs σ (Fig. 27) as determined on sea ice from Cook Inlet, Alaska. These tests indicate a sharp decrease in σ_f with increasing $\dot{\sigma}$. It is interesting that this decrease occurs in the same range of $\dot{\sigma}$ values (compare Fig. 27 and 29 with Fig. 43 and 45) in which both Peyton's Point Barrow compressive data and Tabata's flexural data indicate an increase in σ_f with increasing $\dot{\sigma}$. Peyton has suggested that because the general structure of the ice at Point Barrow and Cook Inlet is different, the minimum $\dot{\sigma}$ values of the Cook Inlet tests can be interpreted to match the Barrow results (dashed line in Fig. 27) at the maximum strength value of "comparable" ice. This would then indicate a general $\sigma_f = f(\dot{\sigma})$ relation with a maximum value of σ_f at $\dot{\sigma} \approx 1$ kg/cm² sec. The experimental evidence is, at present, not sufficient for definite conclusions. Probably, the maximum $\sigma_f(\dot{\sigma})$ depends on brine volume.

For fresh ice, the effect of variations in the strain rate $\dot{\epsilon}$ on σ_f are similar to the results obtained by Peyton on the Cook Inlet ice. Korzhavin (1962) and Ptukhin (1964) have tested cubes with edge dimensions of 10 to 7 cm by applying the load normal to the long axes of the crystals and have obtained similar results. Figure 28 shows Korzhavin's test results. Korzhavin has fitted these results with the empirical relation

$$\sigma_f = \frac{a}{\sqrt[3]{\dot{\epsilon}}} \tag{39}$$

where a is a constant equal to 3.1 kg/cm² at –3C and 2.5 at 0C. He suggests this relation be used only in the $\dot{\epsilon}$ range of 0.0017 to 0.0417 sec⁻¹. Butiagin (1966a) has also noted a similar but less pronounced decrease in σ_f with an increase in $\dot{\epsilon}$. Figure 29 shows test results from lake ice that, though tested near 0C, did not show signs of spring deterioration (Korzhavin and Ptukhin, 1966). Each point is the average of 15 tests. It is interesting to note that at comparable stress rates, the values obtained by Korzhavin and Ptukhin (1966) for fresh ice are roughly four times the values obtained by Peyton (Fig. 27) for sea ice.

A pronounced relationship (Fig. 23) between the cross-sectional area of the specimen as determined normal to the axis of loading and σ_f is quite apparent for fresh ice from the test results of

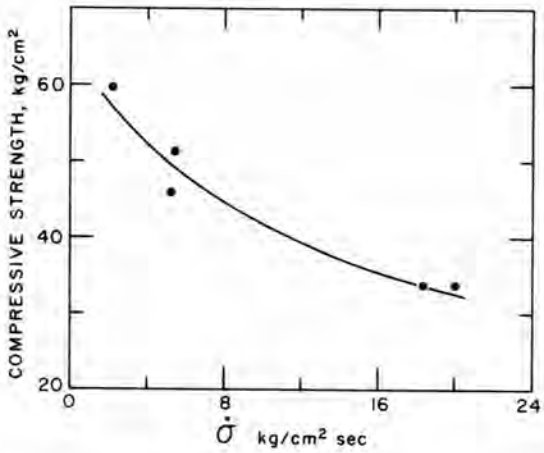

Figure 29. Compressive strength of 7-cm-diam cubes of lake ice vs stress rate. Ice temperature is near 0C but the ice has not deteriorated (Korzhavin and Ptukhin, 1966).

Butkovich (1955, 1958), Lavrov (1963) and Butiagin (1966a, b). This will be discussed in detail later in this review.

Indentation failure

The indentation failure of ice occurs, for example, when an icebreaker hits a thick ice floe or an ice field attacks a bridge pier or an offshore drilling platform. The forces developed should be higher than those determined experimentally by pure crushing because of the absence of free surfaces in the ice on either side of the indenter. For large ice fields the ice can be considered to be well confined in the lateral direction. It is not, however, confined in the vertical direction.

Experiments on this general problem have been performed by Korzhavin (1961, 1962) using clear river ice that was free of cracks, cavities, pores, and foreign inclusions. Normal freshwater ice will invariably have a lower strength. Before testing the samples were placed at 0C for 3 to 4 hours and then compression was applied perpendicular to the long axes of the crystals. The two types of loading schemes used are shown in Figure 30. The width of the indenting stamps varied between $7 \times 7 \times 20$ and $7 \times 7 \times 30$ cm. An additional number of tests were made while the ends of the samples were confined so that conditions would be similar to those experienced when an infinite sheet fails in indentation. Plastic deformation was noted for the first 1 to 2 mm of indentation. Then a series of fine cracks developed along the grain boundaries and gradually increased in number as the force increased. These cracks usually formed at an angle of 20 to 30 degrees to the vertical direction. Failure then occurred along the two main cracks in the region of the largest shear deformation. After this initial failure, spalling and extrusion of ice were observed on the upper boundaries of the sample.

The results of 199 such tests are shown in Figure 31 with the upper curve showing the results of the confined tests. Confinement obviously has a pronounced effect. The strength values are plotted against the ratio b/h where b is the width of the indenter and h is the ice thickness. In all cases the indentation strength increases as b/h decreases. Korzhavin has suggested that his results be expressed by

$$\sigma_f = \sigma_1 \sqrt[3]{B/h} \tag{40}$$

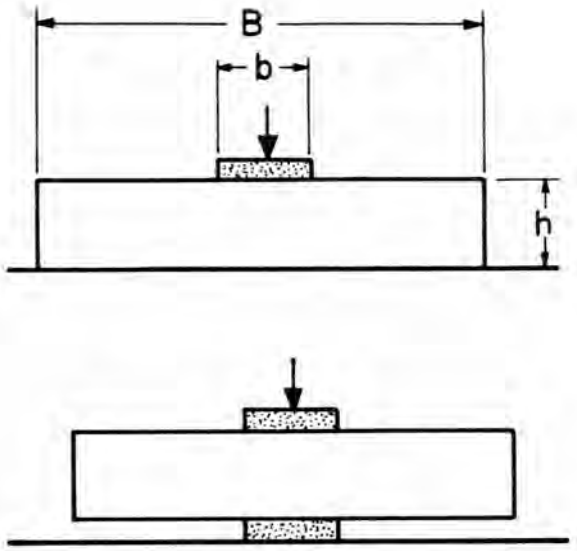

Figure 30. Types of indentation loading schemes used by Korzhavin (1962).

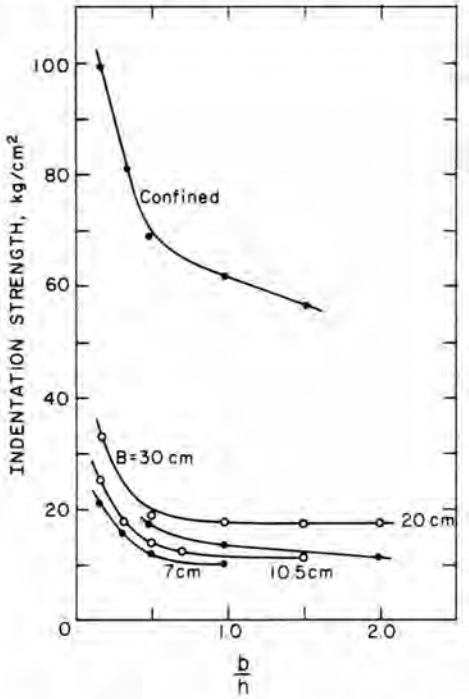

Figure 31. Indentation strength of lake ice as a function of the width of the indentor b *divided by the ice thickness* h *(Korzhavin, 1962).* B *is the width of the ice specimen.*

and

$$\sigma_1 = \sigma_0 \sqrt[3]{h/b} \tag{41}$$

where b is the length of the sample (or the width of the piece of ice moving against a pier), and σ_0 is the basic crushing reference strength determined from samples with $h/b = 1$. These empirical relations are of only limited use since they obviously violate boundary conditions. Equation 41 should give a constant value of σ_1/σ_0 for two-dimensional indentation ($b \ll h$) and another constant value for three-dimensional indentation ($h \ll b$). This latter value is the crushing strength of an infinite ice sheet that is thin in relation to the size of the indenter. Korzhavin has combined eq 40 and 41 into

$$\sigma_f = \sigma_0 \sqrt[3]{B/b} \tag{42}$$

which is a relation that is similar to equations that have been used to estimate forces produced by local crushing on concrete bridge supports. Unfortunately, eq 42 "ignores" the effect of variations in the ratio b/h and is, therefore, only workable in a range which is dependent on the limited applicability of eq 40. For very large indenters such as a large cylinder, the crushing strength should be very near to the crushing strength of an ice sheet against a flat wall. Korzhavin has comewhat arbitrarily assumed that eq 42 should be used up to $B/b = 15$ and

$$\sigma_f = \sigma_0 \sqrt[3]{15} \approx 2.5\, \sigma_0 \tag{43}$$

Table I. Fresh ice forces derived from the failure of engineering structures (Korzhavin, 1962).

Country	*Year*	*Structure*	*Damage*	*Force* (kg/cm^2)
U.S.A.	1899	Massive dam	Displacement of joint	1.7
U.S.A.	1916-17	Lock panels	Deflection	2.2
Canada	–	Massive bridge pier	Tilting of pier	7.1
U.S.A.	1920	Steel bridge	Truss removed	14.0
U.S.S.R.	1941	Crib pier	Cribs moved	2.4
China	1955	Cylindrical bridge pier	Displacement	18.5

should be used for all wider ice floes. The value of 2.5 is then incorporated into Korzhavin's final design equation which we will represent as

$$\sigma_f = l\ m\ k\ f(v)\ \sigma_0 \tag{44}$$

where l is the indentation factor for large ice fields, m is a shape factor for the indenter, k is a contact factor and $f(v)$ is a function of the velocity of the ice. Korzhavin uses different values of σ_0 depending upon whether the river flows to the south, in which case a lengthy warming precedes breakup, or to the north where the breakup of relatively undeteriorated ice is produced by increased discharge. He suggests that for test conditions with small deformation speeds $\sigma_0 = 9$ and 5 kg/cm² for north- and south-flowing rivers respectively. Because the strength of the ice depends on the speed of deformation, decreasing for high speeds, Korzhavin's final recommended value for ice which during breakup is moving with an average velocity of 1 m/sec is $\sigma_0 = 5$ to 3 kg/cm² for north- and south-flowing rivers. To obtain σ_f, these values are then multiplied by the indentation factor of 2.5 which is, as mentioned earlier, questionable.

Similar indentation tests are not available for sea ice. Peyton (1966) has, however, published a number of photographs showing the details of sea ice failure via local crushing around the cylindrical piers of offshore drilling platforms in Cook Inlet, Alaska. He also notes that the largest ice forces were observed when the ice velocity was very low.

Actual field determinations of the dynamic forces exerted by ice on structures are quite rare. Korzhavin (1962) reports surprisingly low values of 1.6 and 1.2 kg/cm² for vertical wedge type piers. This is for deteriorated river ice during spring breakup. Recent measurements on a slightly inclined bridge pier with a semicircular front in western Canada gave a maximum value of 7.2 kg/cm². Similar or even slightly higher values can apparently be obtained even on warm sea ice. Ice forces derived from the actual failure of structures may be appreciably higher (Table I). Static pressures caused by the thermal expansion of ice are not included in this table. The observation in China in 1955 appears to be the highest value reported in the literature. It should be remembered that, as a rule, pressures calculated from the failures of structures will underestimate the maximum possible ice pressure.

Ice jams or broken-up ice masses exert forces on bridge piers and similar structures under shear. Berdennikov (1967) suggests that one assume a force proportional to the product of the width of the pier times the thickness of the ice jam times a shape factor which is 1 for a straight rectangular pier, 0.9 for a semicircular pier and down to 0.6 for 45° triangular piers times the

"crushing" strength of broken ice masses. For orientation purposes this "crushing" strength can be assumed to be 0.3 to 1.5 kg/cm² for normal springtime ice jams and up to 0.6 kg/cm² for frazil ice jams which form under winter conditions provided the solid ice pieces do not exceed 15%. If more solid ice is present in a frazil ice jam the values may range from 0.6 to 2.0 kg/cm². Frazil ice with broken solid ice therefore offers more resistance than broken solid ice alone. This is in agreement with the difficulties ice breakers experience in slushy ice as compared with normal hard ice.

The effective thickness of the ice jam seems to be proportional to the increase in elevation of the water level due to the ice jam. For a particular river it was found, based on 7 years' experience, that the increase in elevation of the water level was 1.36 times the thickness of the ice jam. This factor can also be calculated from hydraulic considerations.

Tensile strength

Direct tension. Early work on the tensile strength of fresh ice has been reviewed by Butkovich (1954) and Voitkovskii (1960) The results of Pinegin (1924) and Butkovich (1954) are compared in Figure 32. The two sets of tests in which the load was applied normal to the long axes

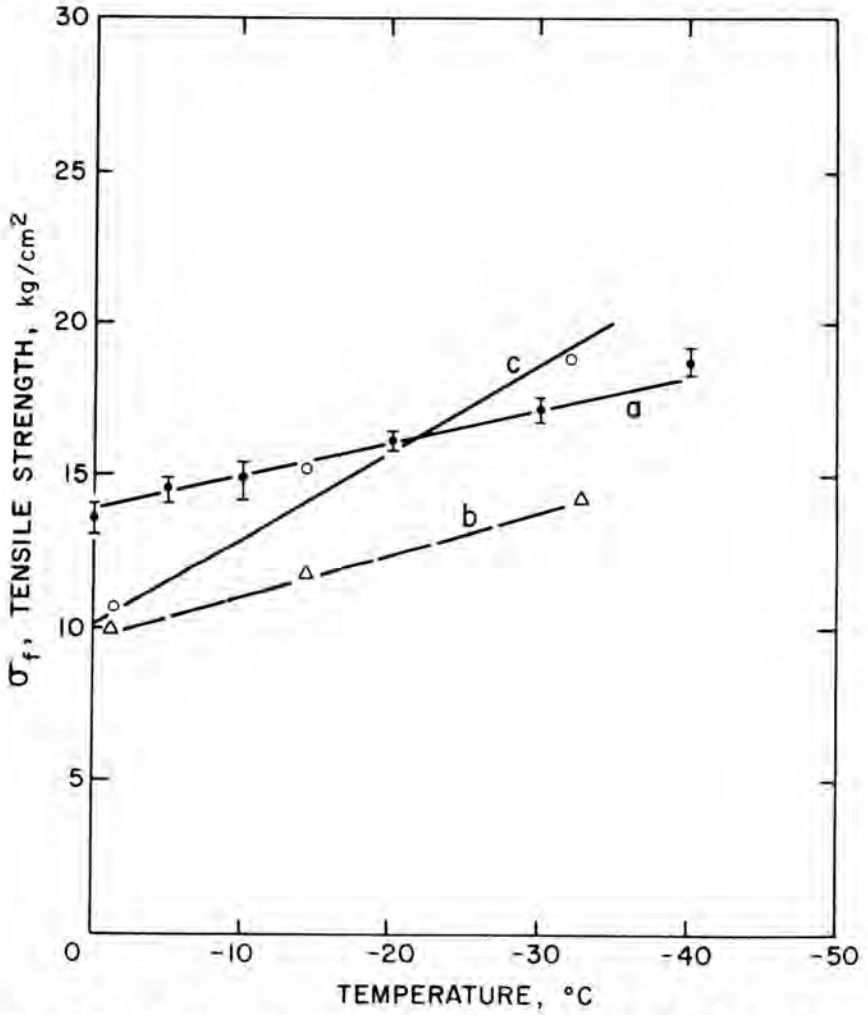

Figure 32. Tensile strength of lake ice vs ice temperature. Curve a *is artificial ice, load applied normal to the growth direction, each point is the mean of 10 tests (Butkovich, 1954); curves* b *and* c *are lake ice with the load applied normal and parallel to the growth direction respectively (Pinegin, 1924).*

of the crystals give a similar dependence of strength on temperature although the absolute values of the strengths at a given temperature differ. This difference is not, however, surprising, inasmuch as *a* is based on artificial ice while *b* is based on river ice. Curve *c*, which is based on river ice tests where the tensile axis was parallel to the long axes of the crystals, gives a more pronounced but still linear temperature dependence. Notice the small scatter in Butkovich's tests as compared to representative scatters produced by other types of testing in his experiments. In a very careful series of tests on fine-grained ice with a random crystal orientation and a density of 0.899 g/cm^3, Hawkes (personal communication) has obtained a tensile strength of 19.3 ± 1.0 kg/cm^2 at −8C. This increased strength as compared with the test results shown in Figure 32 may possibly be produced by the smaller average grain size (0.7 mm) of Hawkes' samples. An important result of Hawkes' tests is that he found that the tensile strength of his ice was essentially independent of time to failure in the time range 0.5 to 300 sec.

A similar result was obtained for sea ice by Peyton (1966) who showed that in the stress rate range 0.01 to 0.18 kg/cm^2 sec there was no pronounced variation in the value of σ_f with changes in $\dot{\sigma}$. Peyton also extended these measurements to higher values of $\dot{\sigma}$(≈ 2.6 kg/cm^2 sec) and determined the parameters a, b, $y_1, \ldots y_n$ in eq 37 by least squares in a manner similar to that used in his treatment of his compressive strength results. The average value of the coefficient b was found to be 0.05 indicating to us that σ_f is independent of $\dot{\sigma}$ in the stress rate range studied.

The most detailed series of direct tension tests on sea ice is by Dykins (1967). The reduced cross section in his tests has an area of about 13 cm^2 and the extension rate was 1.2 cm/min. The ice tested showed plate spacing values that increased from 0.35 mm near the top of the ice sheet to 0.45 mm near the bottom. A very pronounced increase in grain size from 8 grains/cm^2 at the top to 0.3 grains/cm^2 near the bottom was noted over this same vertical distance (an increase by a factor of 25 in 41 cm of ice). Because his strength profiles show no pronounced vertical variation, this can be considered as evidence that changes in grain size in sea ice have no major influence on strength. The reason for the absence of a grain size effect in sea ice is presumably that the microstructure causing failure is of the scale of the plate spacing, 0.1 to 1.0 mm (Goetze, 1965). There is, however, a consistent, roughly linear decrease in σ_f with increasing $\sqrt{\nu_b}$ (Fig. 33) with the same general form as found in the compression tests. Although the data are limited, there does not appear to be any significant change in the strength characteristics associated with the precipitation of solid salts. The orientation of the specimen relative to the direction of growth of the sea ice has a pronounced effect on tensile strength. As should be expected in this test, vertical specimens which are forced to break across the ice plates (*G*-axis in Fig. 22) show strengths similar to horizontal specimens in the "hard fail" orientation (*B*-axis) but higher strengths (2 to 3 times) than horizontal specimens in the "easy fail" orientation (*C*-axis). As a result of these differences, specimens in an arbitrary horizontal direction show an appreciably greater scatter than vertical specimens. When an equation of the form of eq 24 with $n = 1$ is fitted to these data

$$\sigma_f = 18.0 \left(1 - \sqrt{\frac{\nu_b}{0.275}}\right) \tag{45}$$

results for the upper curve in Figure 33 and

$$\sigma_f = 7.0 \left(1 - \sqrt{\frac{\nu_b}{0.275}}\right) \tag{46}$$

for the lower curve. The value of ν_0 for tension both parallel and perpendicular to the growth direction is similar. This value is also in the range of the ν_0 values determined by ring tensile tests. The estimated σ_0 value for tension parallel to the crystal axes is 18 kg/cm^2 which is similar

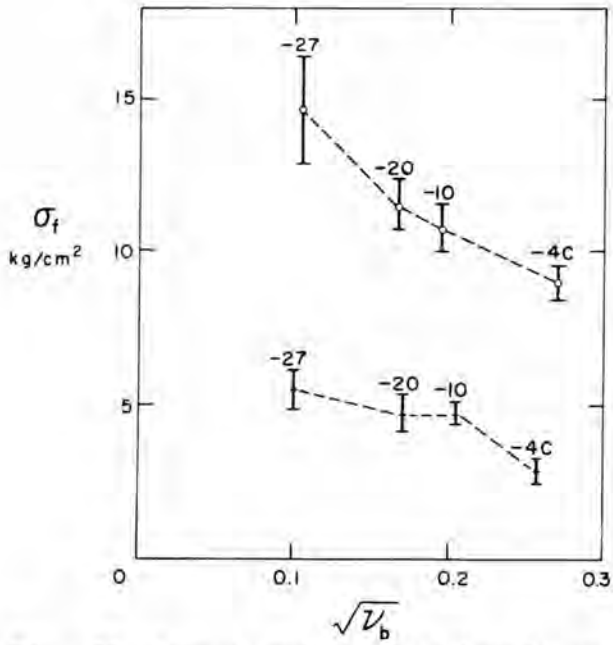

Figure 33. Average tensile strength of sea ice vs square root of the average brine volume. In the stronger samples, tension is exerted parallel to the growth direction and in the weaker samples, perpendicular. The brackets indicate the 95% confidence limits on the mean (Dykins, 1967).

to the tensile strength of pure ice at low temperatures as determined by Butkovich (1954). This σ_0 value is also roughly 2.6 times σ_0 as determined for tension normal to the crystal axes. It is conceivable that this factor of 2.6 is produced by changes in the stress concentration caused by the brine pockets when the orientation of the tensile stress changes. Referring to Figure 22 and assuming vertically interrupted circular cylinders as a model for the brine inclusions in this ice, we can use

$$K = 1 + 2\epsilon \tag{47}$$

to consider this effect (Assur, 1958). Here K is the stress concentration factor and ϵ is the ratio of the void diameter perpendicular to the stress direction to that diameter parallel to it. The ratio of the strength measured parallel to the growth direction to that measured perpendicular to it at small brine volumes should be

$$\frac{\sigma_{f(\parallel)}}{\sigma_{f(\perp)}} = \frac{1 + 2\epsilon_{(\parallel)}}{1 + 2\epsilon_{(\perp)}} \tag{48}$$

Inasmuch as we have assumed that the brine cylinders are circular in cross section, $\epsilon = 1$. To produce the observed ratio of 2.6 for $[\sigma_{f(\parallel)}/\sigma_{f(\perp)}]$, the vertical brine inclusions must, therefore, have a length 13 times their diameter.

Dykins has suggested that the results of direct tension tests can possibly be compared directly with *in-situ* flexural strength determinations on ice sheets. If this suggestion is substantiated, this type of testing will become quite important.

Ring tension. The ring tensile test has been extensively applied to studies of sea ice by American and Canadian investigators. There are several reasons for this: even in thick ice the CRREL coring auger readily produces a suitable sample and the test is simple and easy to perform. Also, the test results show pronounced changes with temperature, salinity, depth and microstructure. The test was designed to study the tensile strength of such brittle materials as concrete and rock. The theory for the test was initially developed in an article by Ripperger and Davids (1947) and has been elaborated further by Assur (1958). The test specimen consists of an ice cylinder in which a coaxial hole has been drilled. The specimen is then subjected to a compressive force normal to the axis of the cylinder. The sample fails as a result of tensile stresses that develop in a vertical plane with a maximum at the inner hole perpendicular to the direction of the load. The equation for computing the ring tensile strength contains in the numerator a stress concentration factor K_e which is a complicated function of the ratio of the inner and outer radii (r_i/r_o) of the hollow cylinder. The theory for the test predicts $K_e = 1$ for a solid cylinder without a hole. For an infinitesimally small hole $K_e = 6$ and for $r_i/r_o = 1/6$, which has commonly been used, $K_e = 7.0926$. Studies of the effect of variation of the hole size on the resulting strength have been made by several investigators. Butkovich (1959b) found no change in the values of σ_f for glacier ice when the ratio (r_i/r_o) was changed from ⅓ to ⅙. Paige and Kennedy (1967) obtained similar results for sea ice with (r_i/r_o) varying from ⅚ to ⅙. Frankenstein (1969) has also compared sea ice tests performed on specimens with a radial hole diameter of ½ in. (1.27 cm) with tests performed on solid sea ice cylinders without a predrilled hole but containing brine pockets. Assuming that the solid cylinder containing brine pockets should give the same σ_f value as the predrilled specimen, a new K_e with a value of 5.2 was computed. This is slightly less than the theoretical 6, probably because of plastic stress relief. Ice temperature and brine volume did not appear to affect this value. Because of the geometry of the ring tensile test, initial failure is restricted to a very small volume. It is difficult to estimate this volume exactly, but an approximate calculation (Goetze, 1965) suggests a region 1.5 mm × 0.3 mm × the length of the cylinder. In short, ring tensile tests force failure upon a volume that has dimensions that are much smaller than representative grain sizes for freshwater ice and are only slightly larger than the dimensions of the sea ice microstructure.

The data on the ring tensile strength of freshwater ice are rather limited. Weeks (1962) obtained σ_f values of 27.6 kg/cm² for clear freshwater ice that contained no visible flaws or air bubbles. The strength appeared to be independent of temperature in the temperature range -10 to -35C. These results are similar to σ_f values obtained by Butkovich (1959b) for glacier ice (26.0 to 30.2 kg/cm² at -5C). Frankenstein (1969), on the other hand, obtained lower values for natural lake ice (19.5 kg/cm² at -0.4C and 14.2 kg/cm² at -0.1 to -0.2C).

A detailed review of the application of ring tensile testing to sea ice is found in Weeks and Assur (1968). The first analysis of ring tensile data in terms of σ_f vs $\sqrt{\nu_b}$ plots as suggested by the formal strength models was by Assur (1958) based on his own and Butkovich's (1956, 1959a) data. Assur was able to show that at high temperatures (above -8.2C) the strength of sea ice significantly decreased with an increase in $\sqrt{\nu_b}$. He also advanced a number of hypotheses regarding the strength behavior of sea ice. Among the more interesting of these suggestions were 1) that the presence of solid $Na_2SO_4 \cdot 10H_2O$ increases σ_f by roughly one-third in the temperature range -8.2 to -22.9C and 2) that at temperatures below -22.9C, the precipitation of $NaCl \cdot 2H_2O$ causes sea ice to have strength values appreciably in excess of freshwater ice.

In an attempt to resolve a number of the questions posed by Assur's paper, Weeks (1962) ran an extensive series of tests on ice formed by freezing NaCl solutions. He found (Fig. 34) a simple linear relation between σ_f and $\sqrt{\nu_b}$ at temperatures warmer than -21C with a σ_f axis intercept $\sigma_0 = 24.7$ kg/cm² and a ν_0 value of 231‰. The value of σ_0 was slightly lower than the σ_f value determined by similar runs on freshwater ice (27.6 kg/cm²). This suggests that the ratio of stress concentration in salt ice to that in freshwater ice is in the range 1.1 to 1.5 and defeats the previous hypothesis of Anderson and Weeks (1958) who assumed that the maximum strength of sea

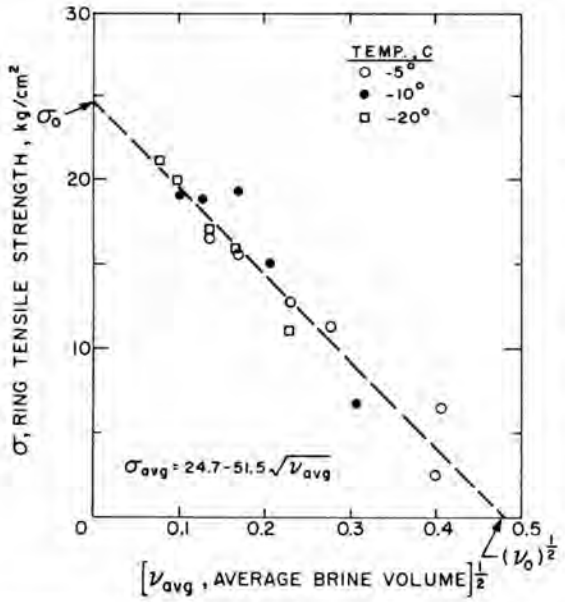

Figure 34. Average ring tensile strength vs square root of the average brine volume, NaCl ice (Weeks, 1962).

ice was one-third that of fresh ice. Similar results were obtained by Graystone and Langleben (1963) from annual ice in the Canadian Arctic. They performed their tests immediately after the sample was removed from the ice sheet and the resulting equation was

$$\sigma_f = 29.0\left(1 - \sqrt{\frac{\nu_b}{0.296}}\right) \qquad (49)$$

for samples whose ice temperature was warmer than -8.2C. This was additional strong experimental evidence in favor of the previously assumed sea ice models and was also in good agreement with the results of Weeks (1962) on NaCl ice. Note that the σ_0 value is almost identical with the ring tensile strength of pure ice as determined by Weeks. The σ_f values for samples colder than -8.2C and, therefore, containing $Na_2SO_4 \cdot 10H_2O$ fall on this same curve. This suggests that if the precipitation of $Na_2SO_4 \cdot 10H_2O$ does cause a strength increase in sea ice, the effect is very small. Similar conclusions have been reached by Weeks (1962) and Frankenstein (1969). Tests on NaCl ice colder than the eutectic temperature indicate that the strength is essentially independent of both the sample temperature and the volume of $NaCl \cdot 2H_2O$ in the sample. When the strength of the ice matrix is corrected to -10C, the strength of the $NaCl \cdot 2H_2O$ ice is 26.5 kg/cm² or slightly less than the strength of freshwater ice. There is, therefore, no indication of a pronounced strengthening effect associated with the precipitation of $NaCl \cdot 2H_2O$. It is conceptually quite possible that the precipitation of solid salts in sea ice could affect its strength and brittleness and produce microcracks as a result of volume changes in the brine pockets. With available data it is currently not possible to adequately assess any of these supposed effects. Ring tensile results from NaCl ice have also been used to demonstrate that an increase in the value of the plate spacing a_0 produced by a decrease in growth velocity causes a decrease in ν_0 (Weeks and Assur, 1963). This is further evidence in support of the assumed sea ice models. Substituting $\beta_0 = (b_0/a_0)$ in eq 22 and holding b_0 constant such an effect is predictable from theory.

Results similar to those of Graystone and Langleben have been obtained by Dykins (1963)

$$\sigma_f = 30.1\left(1 - \sqrt{\frac{\nu_b}{0.585}}\right) \qquad (50)$$

on ice cylinders in which no holes had been drilled. Dykins assumed that $K = 6$ (that brine pockets were acting as infinitesimally small holes) in making these calculations. But using the empirical K of 5.2 determined by Frankenstein (1969) we obtain a σ_0 value of 27.2 kg/cm² for Dykins' data.

Langleben and Pounder (1964) have studied 2-year-old and polar (multi-year) ice. Because of low air temperatures (-10 to -15C) and low ice salinities ($S_i < 1‰$), $\sqrt{\nu_b}$ in these tests was always less than 0.1 ($\nu_b < 10‰$). Comparing their results with the strength of annual ice with the same brine volume (eq 49), they found that biennial ice is 21% stronger than annual ice and 6% stronger than polar ice. Assur (1958) and Hendrickson and Rowland (1965) have also reported higher

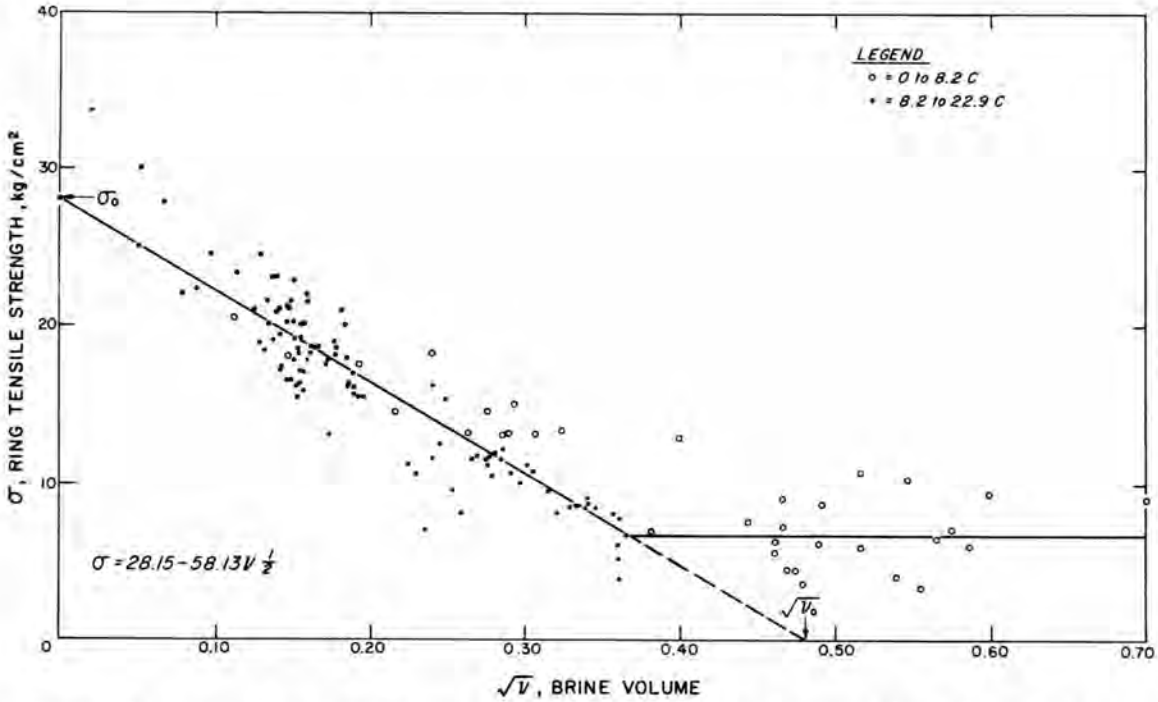

Figure 35. Average ring tensile strength vs square root of the average brine volume, sea ice (Frankenstein, 1969)

strength values for perennial ice. These differences are currently difficult to explain. Langleben and Pounder also report that a slight but apparently non-significant difference was found between σ_f values from horizontal and vertical cores: σ_f (horizontal) > σ_f (vertical) by 4%. It should be noted that the horizontal cores were not systematically placed in the "hard fail" orientation in the manner used by Butkovich (1959a) who found that horizontal cores have consistently higher values than vertical cores from annual ice. Langleben and Pounder also found that the standard deviation of the σ_f values for horizontal cores (7.6 kg/cm²) was generally greater than that of the vertical cores (4.7 kg/cm²). These differences are quite reasonable in terms of the structure of sea ice (Butkovich, 1959a).

The most extensive study of ring tensile results currently available is that of Frankenstein (1969) who reports the results of over 1400 individual tests (Fig. 35). Each point in this figure represents roughly nine tests. The least-squares equation for a straight line fit to the data when $\sqrt{\nu_b} < 0.400$ is

$$\sigma_f = 28.5\left(1 - \sqrt{\frac{\nu_b}{0.234}}\right) \tag{51}$$

Equation 51 is in good agreement with the results of Weeks (1962) and Langleben and Pounder (1964). When $\sqrt{\nu_b} > 0.400$, σ_f remains constant at approximately 6.7 kg/cm². As will be shown later, this constancy of σ_f at large values of ν_b is interesting because it also appears in the results of *in situ* cantilever beam and shear tests. Data bearing on the reasons for this behavior have recently been obtained by Paige and Kennedy (1967) who studied the variation in the ring-tensile strength of sea ice produced by changes in the crosshead speed of the testing apparatus. Figure 36 shows the results of their tests at two different temperatures on ice with a salinity of

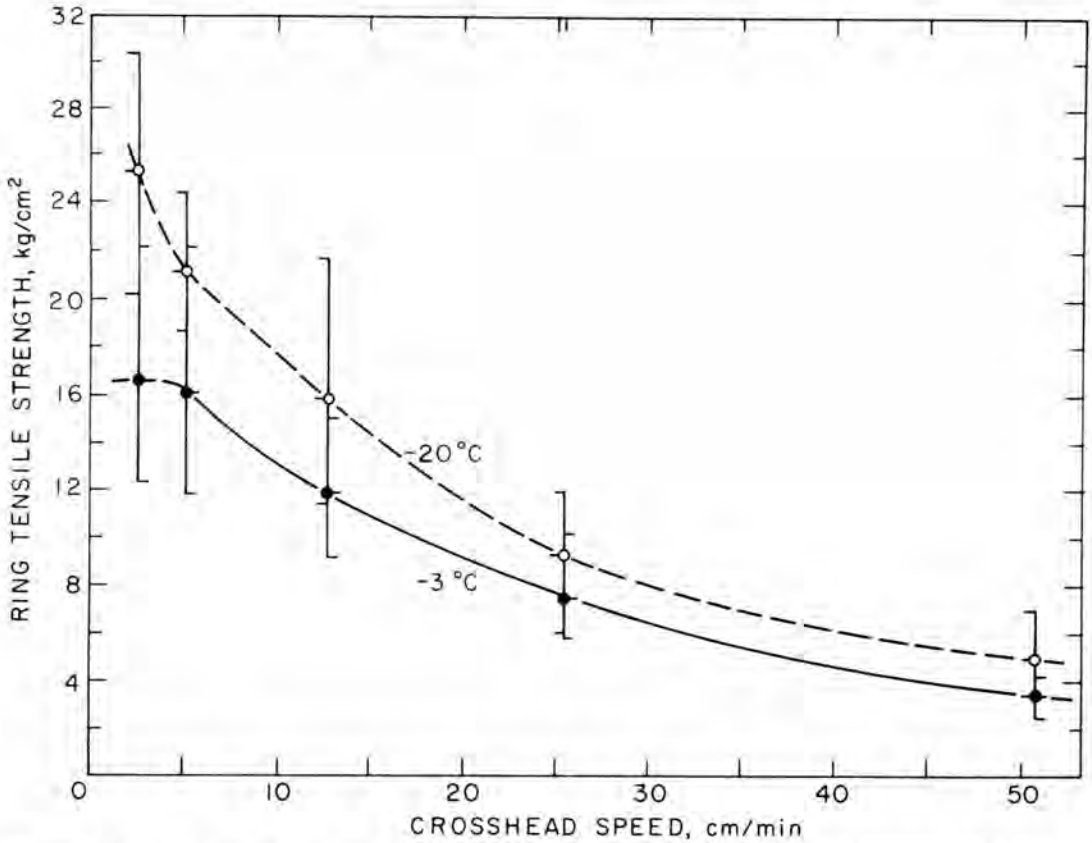

Figure 36. Ring tensile strength vs crosshead speed for sea ice with a salinity of 1.62‰ (Paige and Kennedy, 1967).

1.62‰. The pronounced decrease in strength with increasing headspeed is striking. This effect is undoubtedly caused by the plastic relief of the large stress concentrations that are presumed to exist in the ring tensile test. At the high headspeeds shown in Figure 36 the value of the stress concentration index η can be assumed as approximately 1 while at the slow headspeeds it should decrease approaching a value of 0. From eq 1 we can write

$$K_a = 1 + \eta(K_t - 1) \tag{52}$$

and express the ratio of the [theoretical failure strength assuming that the calculated stress concentration actually occurs, $\sigma_{f(t)}$], to the [actual failure strength, σ_f] as

$$\frac{\sigma_{f(t)}}{\sigma_f} = \frac{K_t}{K_a} = \frac{K_t}{1 + \eta(K_t - 1)} . \tag{53}$$

For a perfectly brittle material ($\eta = 1$), the ratio $\sigma_{f(t)}/\sigma_f$ is, of course, 1. For a perfectly plastic material ($\eta = 0$), tested using a (r_i/r_0) value of ⅙, it is approximately 7(K_t = 7.1). The average value of [σ_f (crosshead speed = 2.5 cm/min)/σ_f (crosshead speed = 50.8 cm/min)] as determined by us from the data of Paige and Kennedy (1967) is 6.03. This is in good agreement with the maximum expected value of 7.0. The observed value is slightly less than 7.0 which indicates that the extremes of perfectly brittle or perfectly plastic behavior were not obtained in these tests. Now, if

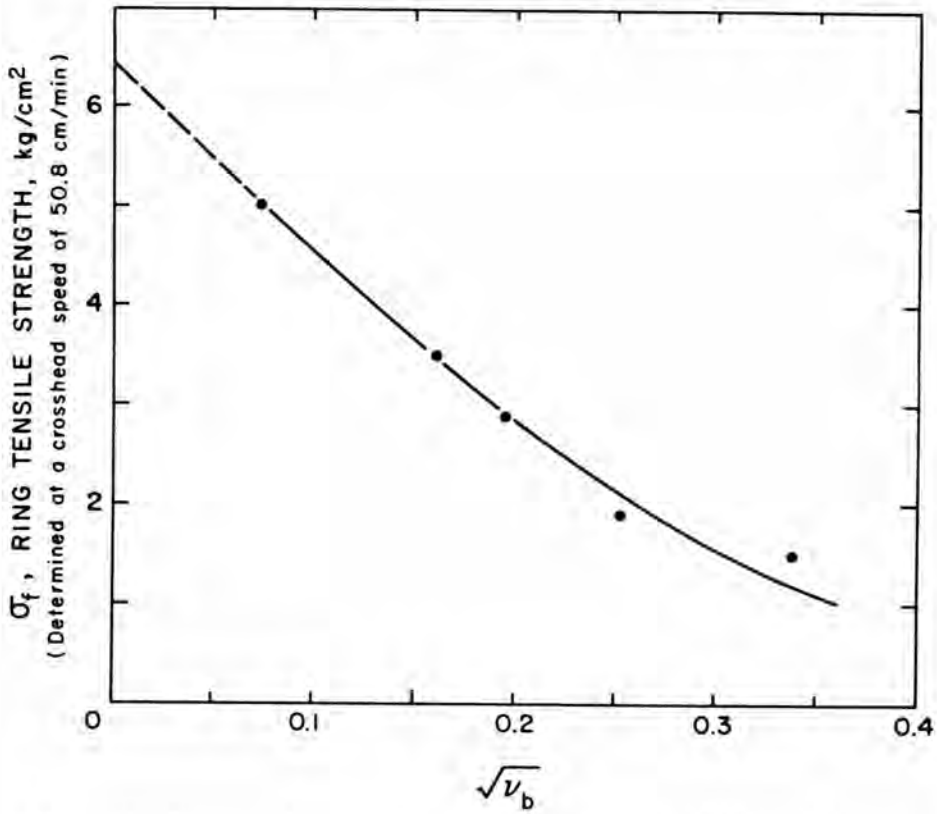

Figure 37. Ring tensile strength at a crosshead speed of 50.8 cm/min vs brine volume.

we first correct all the σ_f values of Paige and Kennedy to a headspeed of 50.8 cm/min and a random grain orientation and then plot the resulting 5 points against $\sqrt{\nu_b}$, Figure 37 results. The relation is linear throughout most of its range. It is also similar to the plots of σ_f vs $\sqrt{\nu_b}$ determined by both pure tension and *in-situ* cantilevers (Fig. 33, 44).

The details of how the internal and the external stress concentrations and the brittleness of the ice as determined by the test conditions interact to produce what is calculated to be a given type of ice strength, are only partially understood. The following discussion points out a few of the problems. Subject an ice specimen to a test in which there is an external stress concentration (K_e) associated with the geometry of the test. The ring tensile test is a fine example of this. The theory of the ring test does not admit that the material being tested possesses any structural elements that may act as internal stress concentrators. It only considers the stress concentration introduced in the specimen by the co-axial hole drilled by the experimenter. Now load the sample so rapidly that the ice behaves as an ideally brittle material (the stress concentration index $\eta = 1$). The stress concentrators locally increase the stress above the bulk stress by a factor of K_e as predicted by elastic theory. If we set the "intrinsic" strength of the material at unity, the sample fails when the local stress exceeds the "intrinsic" strength. This occurs at a measured bulk stress of $(1/K_e)$. We now compute the ring tensile strength by taking this measured bulk stress $(1/K_e)$ and multiplying it by the theoretical stress concentration factor (K_e). The calculated strength of the material is 1, which, in this case, actually equals the "intrinsic" strength of the material. Now, load an identical sample extremely slowly so that it behaves as an ideally plastic material ($\eta = 0$). Because of plastic yielding in the vicinity of the stress concentrations, there are no local increases in stress. The sample fails when the bulk stress exceeds the "intrinsic"

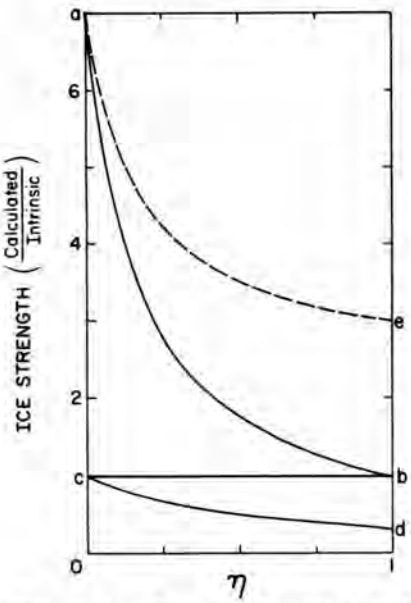

Figure 38. Ratio of the calculated ice strength to the intrinsic ice strength vs the stress concentration index η.

strength by taking the measured stress at failure, which in this case is 1 equaling the "intrinsic" strength, and multiplying it by K_e. The calculated strength is therefore fictitiously high by a factor of K_e. This type of behavior is represented by curve *ab* in Figure 38 which is calculated based on an assumed K_e of 7.

This effect may explain the relatively high values of the ring tensile strength at $\sqrt{\nu_b}$ values greater than 0.400 as shown in Figure 35. Inasmuch as most natural sea ice offers only a fairly limited salinity range, large brine volumes are usually achieved by testing at temperatures near 0C. It is, therefore, to be expected that because of the higher temperatures as well as the higher brine volumes, this ice will behave in a significantly more plastic manner ($\eta \to 0$). This would result in the calculated strengths of this high-brine-volume ice being fictitiously high relative to the other ice by some factor which depends upon the details of how the tests are performed.

Although the "intrinsic" strength of ice is of considerable interest to the physicist, for engineering purposes it would be very useful to be able to calculate the bulk tensile strength of ice from a more readily performed test such as the ring tensile. In a pure tension test there are no external stress concentrations associated with the geometry of the test. Failure strength is simply calculated by dividing the force at failure by the cross-sectional area of the assumed failure surface. The existence of internal stress concentrators is not taken into consideration in this calculation even though it is well known that they exist. Let us consider the effect of internal stress concentrations (K_i) such as the presence of solid, liquid and gaseous inclusions, or the geometry of the grain boundaries on the bulk tensile strength. As a point of discussion we will consider the stress concentrators to be isolated cylindrical voids ($K_i = 3$). If the sample is loaded slowly so that it deforms as an ideal plastic material, local plastic yielding around the internal stress concentrators will cause the local stress to be equal to the bulk stress (K_i will equal 1 instead of the theoretical 3). Therefore, the measured strength will equal the "intrinsic" strength (point *c*, Fig. 38). If the brittleness of the material is now increased by increasing the rate of loading or lowering the temperature until the direct tensile specimen fails in the brittle mode, the stress concentration affected by the internal stress concentrators increases until their theoretical elastic value is reached ($K_i = 3$). The bulk stress necessary to cause the sample to fail is then ($1/K_i = 3$). The direct tensile strength is, in this case, ⅓ of the "intrinsic" strength of ice (point *d*, Fig. 38). This points to the importance of more basic studies on the failure mechanisms and modes of deformation in both fresh and sea ice. A knowledge of the effective values of K_i for ice of different macroscopic structures would be very useful. It is also very important to know the minimum loading rate that is necessary to insure that η is effectively 1. This value will undoubtedly vary as a function of the state of the sample being tested.

If K_e, K_i and η are known, it is possible to calculate the direct tensile strength $\sigma_{f(\text{direct})}$ from the ring tensile strength $\sigma_{f(\text{ring})}$ by using eq 53

$$\sigma_{f(\text{direct})} = \frac{1 + \eta(K_e - 1)}{K_e(1 + 2\epsilon\eta)} \sigma_{f(\text{ring})} \tag{54}$$

Here ϵ is the ratio of the length of the axes of the elliptical voids normal to the direction of tensile stress relative to the length of the axes parallel to the direction of the tensile stress. Curve *ae* in

Figure 38 gives the value by which the ring tensile strength must be divided to give the direct tensile strength as a function of η assuming that $K_e = 7$ and $K_i = 3$ ($\epsilon = 1$). At the present we are not even certain of the value of K_e. As mentioned earlier, this value is calculated from elasticity theory and does not take the existence of internal defects in the material being tested into account. In a test such as the ring test, K_e definitely appears to be greater than K_i. However, because the volume of the specimen that is actually subjected to the stress concentration K_e is so small and, at least in sea ice, the size of the defects causing K_i is so large, there well may be some sort of an interaction causing a decrease in the effective value of K_e. Such interactions, if they exist, can only be revealed by careful, controlled testing. We do, however, feel that the general line of reasoning outlined in this discussion is encouraging. It suggests that when detailed studies of the mechanism of fracture are combined with carefully controlled tests utilizing different types of testing techniques, it should, in principle, be possible to make the transition from the results of rapid simple-to-perform small sample tests to the direct tensile strength of ice of any composition and temperature. That this capability be developed is important because it is difficult to perform direct tensile tests in the field.

Flexural strength

Simple beam tests. The small beam flexural strength test was one of the first tests applied to the study of fresh and sea ice (Vasenko, 1899; Makarov, 1901). The test is still used estensively in the study of fresh ice. In sea ice, however, it has, during the last 10 years, lost favor relative to the ring tensile test. The reasons for this are twofold: ring specimens are easier to prepare and the test results give better correlations with brine volume and microstructural parameters than do small sample flexural tests.

References to earlier determinations of the small beam flexural strength of freshwater ice can be found in Voitkovskii (1960). Although these results obtained from many sources vary widely, when they are grouped into 5C temperature intervals and averaged, curve a as shown in Figure 39 results. This figure also presents in curve *b* the results of Wilson and Horeth (1948), Brown (1926), and Hitch (1959); in curve *c* the results of Butiagin (1966a); and in curve *d* the results of Frankenstein (1959). Each of the plotted points represents the average of a number of tests. All four sets of data indicate a linear increase in σ_f with decreasing temperature. The general range of values as well as the temperature dependence is similar to that shown by the results of direct tensile tests. The reasons for the differences between the σ_f values as determined, for instance, by Butiagin and Frankenstein are not clear. It is not a scale effect inasmuch as their sample sizes are simple. It may quite possibly be related to structural differences in the ice that was tested.

Arnol'd-Aliab'ev (1929, 1939) was prominent in the early application of small beam flexural strength tests to sea ice. He expressed σ_f as a function of ice temperature θ_i, and interpreted deviations from this curve in terms of the salinity of the ice which he empirically related to air porosity V_a. His results can be expressed in a relation in which σ_f increases as θ_i and V_a decrease (Weeks and Assur, 1968). It is interesting to note that although Arnol'd-Aliab'ev pioneered techniques for the determination of the air content of sea ice, he correctly realized that a considerable percentage of the air porosity is the result of brine drainage prior to testing. The first set of recent small beam sea ice results accompanied by sufficient supplementary information for an analysis was provided by Butkovich (1956, 1959a). His results are shown in Figure 40. There is a large scatter and the pronounced dependence of σ_f on ν_b as shown by both compression and tension tests is absent. Quantitatively similar results have been obtained by Petrov (1954-55) and Smirnov (1961) from the Arctic Ocean, Tabata (1960) from the Okhotsk Sea, and Abele and Frankenstein (1967) from the Antarctic.

In both fresh and sea ice the small beam values are consistently lower than the ring tensile results on the same ice. Also in both types of ice the strength as determined from vertically cut

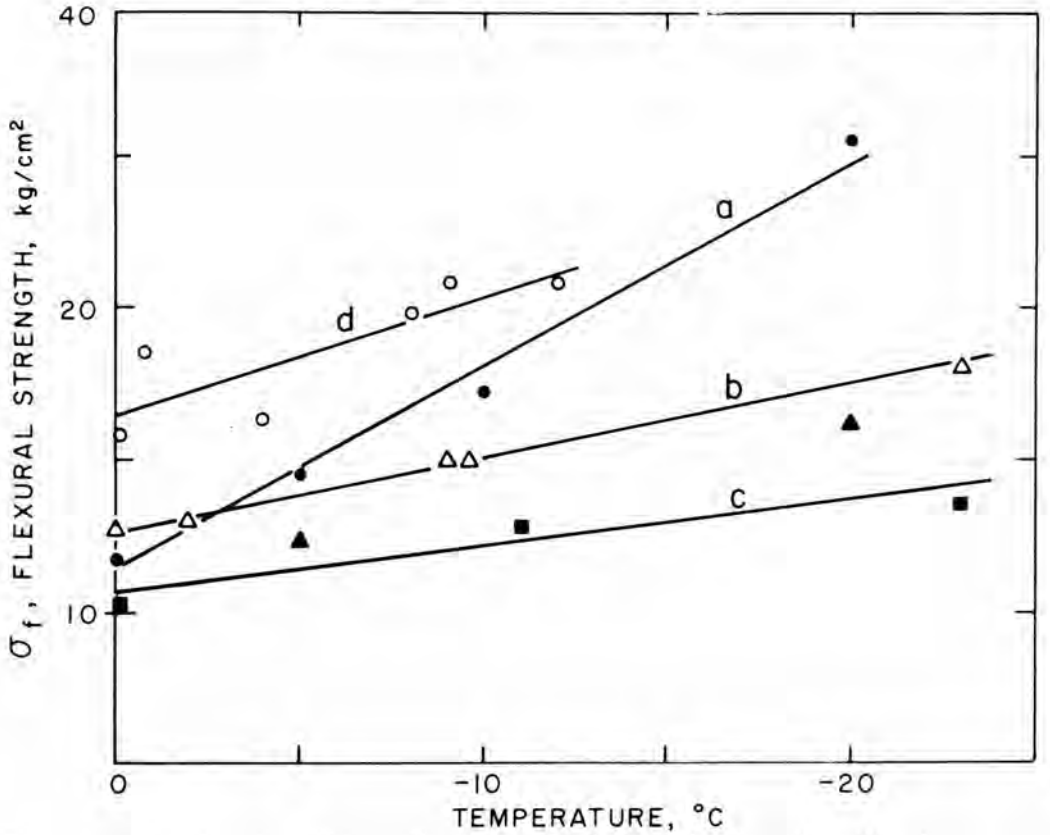

Figure 39. Results of small beam flexural strength determinations plotted vs ice temperature. For data sources see text.

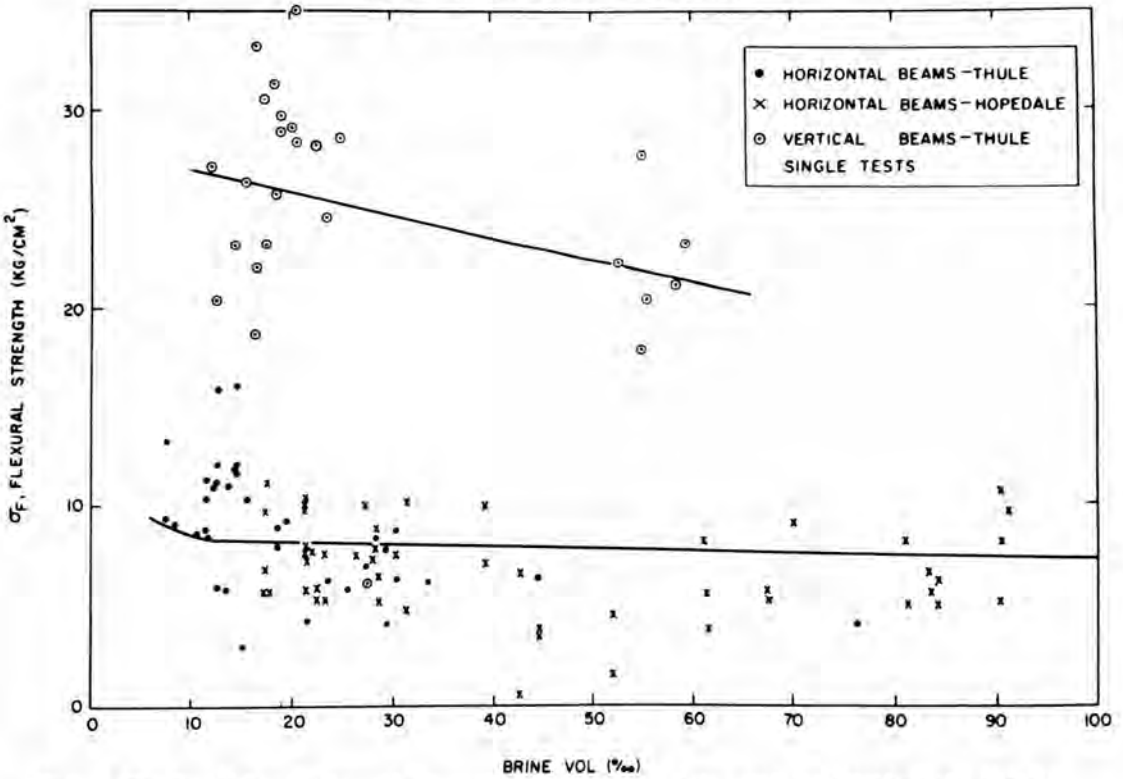

Figure 40. Small beam flexural strength of sea ice vs brine volume (Butkovich, 1959a).

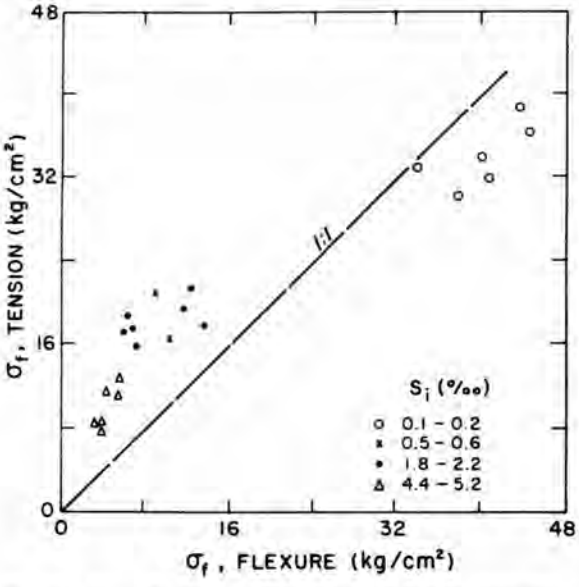

Figure 41. Average values of "roller" tensile strength vs small beam flexural strength as determined on similar sea ice samples under similar conditions (Smirnov, 1961).

beams (tension parallel to the crystal axes) is significantly higher than the strength as determined from horizontally cut beams (tension normal to the crystal axes) (Butkovich, 1956, 1959a; Butiagin, 1966a). This is quite consistent with the results from direct tension tests.

Goetze (1965) has suggested that the difference between the small beam flexural and the ring tensile values is caused by different aspects of the microstructure controlling the fracture mechanism. The fracture may be related to the dimensions of the crystals in small beams as compared to the dimensions of the brine pockets in ring tensile tests. Some justification for this suggestion may be obtained by calculating the constant in eq 34 from Butkovich's (1959b) results on the flexural strength of well annealed, uniform, isotropic glacier ice from the Tuto Tunnel. When Goetze does this he obtains an average value for $(\sigma_f \cdot d)$ of 111. Now extending this argument to the typically larger grain diameters encountered in sea and lake ice (1 to 2 cm) he obtains σ_f values of 10.5 and 7.5 kg/cm² respectively. These values are in the range of σ_f values as determined by small beam flexural tests. It should be quite simple to verify this suggestion of a grain size related fracture mechanism. All that is required is a series of small beam tests on ices with a constant brine or air volume and a range of grain sizes. It should be pointed out that Dykins' (1967) direct tension results do not appear to support the grain size argument. If the fracture mechanism was related to grain size in Dykins' tests, a pronounced vertical variation should have been observed in the failure strength. This was not the case. Because of the large cross sectional area of his tensile samples (≈ 13 cm²), the test volume does not appear to be of a size that would interfere with a grain size related fracture mechanism. Another reason for the reduced strength of larger samples is the so-called scale effect. This will be discussed in detail later.

Additional insight into the effect of the plastic reduction of stress concentration can be found in the tests of Smirnov (1961). He compared the results of a large number of small beam tests with the results of "roller" tensile tests on sea ice. The "roller" test is performed by compressing 10 × 10 × 20-cm rectangular blocks of sea ice between two cylindrical rollers. It might be expected that the ratio of the roller tensile to the flexural strength would be either 1 or at least constant. Figure 41 shows that this is not the case. For low salinities sea ice is brittle and the tensile and flexural strengths are roughly equal. For high salinities sea ice is plastic and the computed tensile strength is considerably higher than the flexural strength. We suggest that this is caused by the plastic relief of stress concentrations near ever-present small holes in the "roller" tensile samples. If so, Smirnov's data also indicate the importance of the plastic relief of stress concentrations in certain types of tests.

The effect of variations in the stress or strain rates on the value of the flexural strength of freshwater ice has not been extensively investigated. Data presented by Butiagin (1966a) suggest that in the range of loading times between 10 seconds and several minutes, there is no pronounced variation in σ_f. Wilson and Horeth (1948) and Brown (1926) have arrived at similar conclusions. This is also in agreement with the observations on the variation in the direct tensile strength of freshwater ice with loading time.

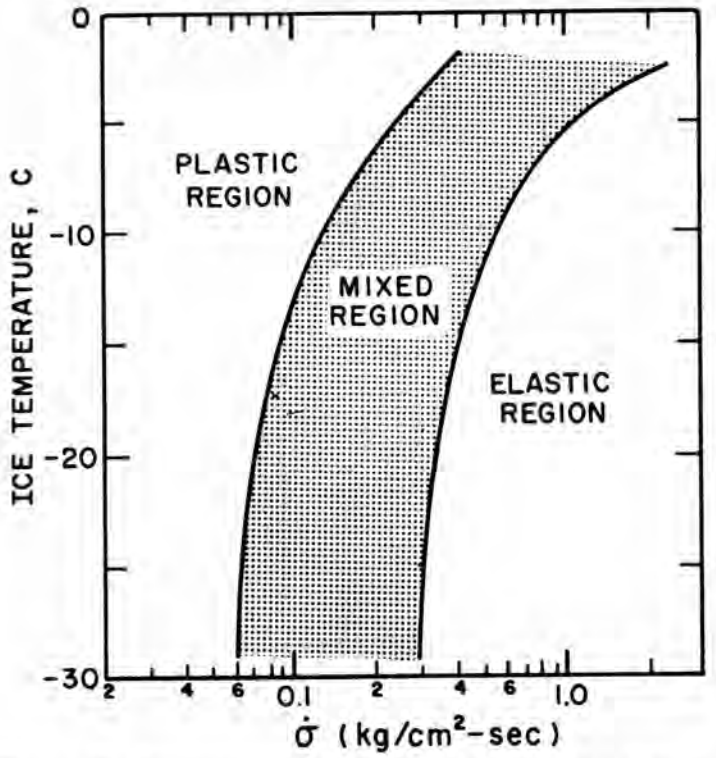

Figure 42. Approximate boundary lines between the regions of elastic, mixed, and plastic failures in relation to temperature and stress rate $\dot{\sigma}$ for sea ice. Salinities vary between 1.0 and 1.4‰ and sea ice densities between 0.86 and 0.87 g/cm³ (Tabata, 1967).

Tabata (1960, 1967) has, however, used small beam tests to study the variation of σ_f with stress rate $\dot{\sigma}$ in sea ice. During each constant deflection-rate test a plot of applied load vs time was recorded and the failure was classified as elastic or "plastic" depending upon whether or not the plot was linear. The percentage of samples that failed elastically increased from zero at low values of $\dot{\sigma}(\dot{\sigma} \leqslant 0.2$ kg/cm² sec) to 100% at high values of $\dot{\sigma}(\dot{\sigma} \geqslant 0.6$ kg/cm² sec). Between these two regions there was a mixed region in which both elastic and plastic breaks occurred (Fig. 42). The boundaries surrounding these different "failure types" are, of course, dependent on the test temperature; higher values of $\dot{\sigma}$ are required to achieve elastic failure at temperatures near the melting point. It will, in the future, be interesting to separate the effects of variations in the sample temperature from effects associated with variations in the volume of brine and air in the ice.

When constant temperature plots of σ_f vs $\dot{\sigma}$ are prepared and only specimens that failed elastically are included, σ_f appears to be independent of $\dot{\sigma}$ in the range of 0.3 to 8 kg/cm² sec. If, however, both plastic and elastic breaks are considered (Fig. 43), as $\dot{\sigma}$ increases there first occurs a slight decrease ($\approx$ 1 kg/cm²) in σ_f and then an increase. The minimum occurs in the range of the "mixed region" between plastic and elastic failures. Tabata (1960) suggests that the increase in σ_f with decreasing $\dot{\sigma}$ in the low $\dot{\sigma}$ range is due to plastic deformation of the samples before breaking. The increase in σ_f with $\dot{\sigma}$ in the high stress rate range is presumed to be related to the increase in the static Young's modulus with increasing $\dot{\sigma}$ above 3 to 5 kg/cm² sec. Because the samples used by Tabata in these studies were obtained from very warm, new sea ice (20 to 25 cm

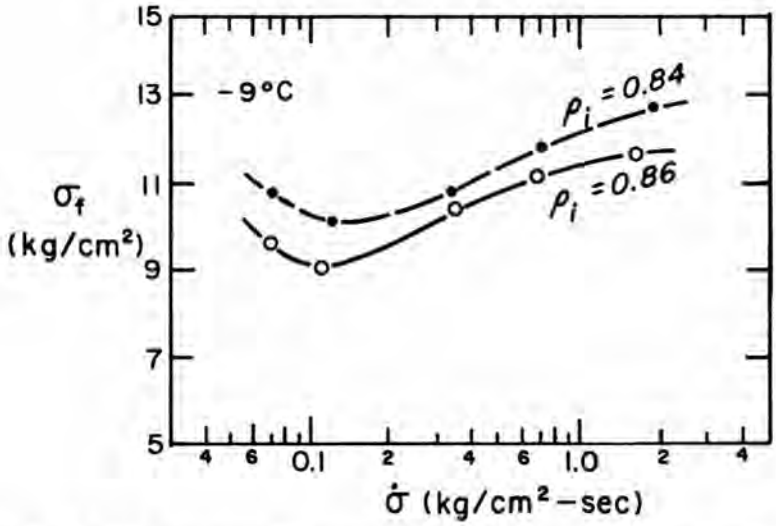

Figure 43. Relationship between small beam flexural strength σ_f for sea ice and stress rate $\dot{\sigma}$ at -9C (Tabata, 1967).

thick) and it was necessary to store the ice for appreciable periods of time, significant brine drainage occurred prior to testing. How the replacement of the initial brine by air affects the results is currently unknown. It would be desirable to repeat this careful series of tests on sea ice produced in the laboratory so that brine drainage prior to testing could be minimized.

In-situ cantilevers and simple beams. Although the results of cantilever tests have been used commonly in estimating σ_f values in bearing capacity problems, there is surprisingly little documentation in the literature. The reasons for this paucity of data are obvious to anyone who has ever performed cantilever tests or tried to analyze the results. The test is quite time consuming if the ice is thicker than about 50 cm. Therefore, at the end of a testing program one frequently does not have enough data for a good report. In addition, the analysis of cantilever tests is, as is the analysis of any test that considers the ice sheet as a whole, far from unambiguous.

The early applications of this test to fresh ice were by Troshchinsky (Weinberg *et al.*, 1940), Neronov (1946) and Shishov (1947). More recent results have been provided by Barnes (1958), Frankenstein (1959, 1961, 1968) and Butiagin (1966a). The test results range between 1.8 and 13.4 kg/cm² depending on the temperature and structure of the ice. For clear lake ice in the absence of surface melting both Frankenstein and Butiagin obtain similar results: $\sigma_f \approx 6.0$ to 7.5 kg/cm². There is no indication of a strong temperature dependence. However, the ice that was tested at 0C was commonly appreciably weaker than ice at lower temperatures. This presumably is the result of internal melting. Tests which place the bottom fiber of the beam in tension (pull-ups) commonly give higher values by at least 15% than do push-downs which exert a tensile stress on the upper fiber of the beam. This difference is undoubtedly the result of the presence of microcracks that are induced by thermal stress in the upper surfaces of the ice beams (Gold, 1963b). Frankenstein found that beams which contained an appreciable thickness of dense infiltrated snow ice gave strengths similar to those observed on clear lake ice. This casts some doubt on the common practice (Assur, 1956; Gold, 1960b) of counting only half the thickness of infiltrated snow ice when bearing capacity calculations are made.

The only extensive study utilizing the results of cantilever tests on sea ice is that of Weeks and Anderson (1958) who performed 208 tests on thin (less than 40 cm) sea ice. They demonstrated the dependence of the flexural strength on the average ice salinity and temperature but did not plot their results against brine volume. This is done in Figure 44. Figure 44 also contains the

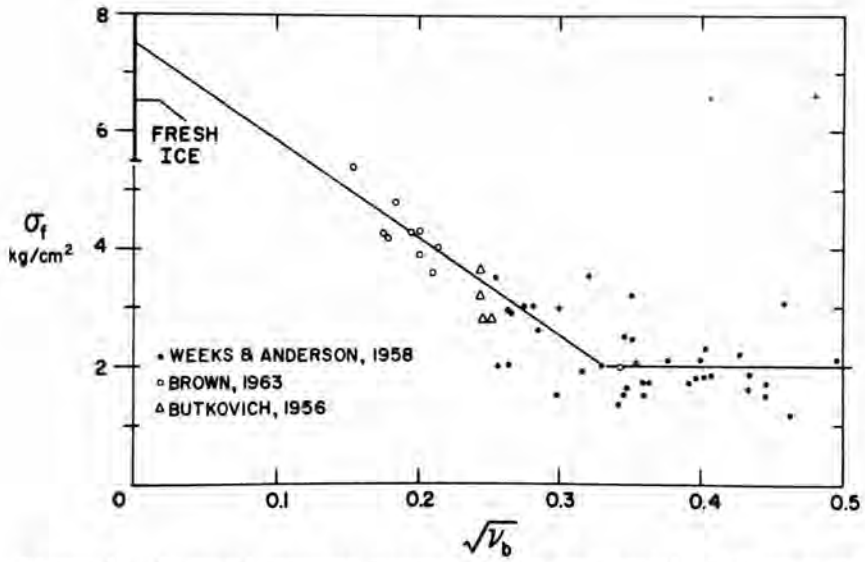

Figure 44. Flexural strength measured by in-situ *cantilever beam tests vs square root of the brine volume.*

results of Butkovich (1956) and those of Brown (1963, Fig. 11) that have not been subjected to warm temperature cycling. The equation obtained from Figure 44 is

$$\sigma_f = 7.0\left(1 - \sqrt{\frac{\nu_b}{0.202}}\right) \tag{55}$$

for $\sqrt{\nu_b} < 0.35$. When $\sqrt{\nu_b} > 0.35$ σ_f is roughly constant with a value of 2.0 kg/cm². Although additional data are badly needed, these results are quite encouraging in that the strength variation appears similar to that found by ring tensile tests. Note also that the ν_0 values are quite similar: 202‰ as compared with 234‰. In these sea ice tests little difference was noted between "pull-ups" and "push-downs." This is in contrast to results on lake ice. It is interesting to note the pronounced effect that a warm temperature cycle had on Brown's (1963) cantilever results. This is in striking contrast to the experimental results of Weeks (1962) where no change was noted in ring tensile specimens cycled and tested above the $NaCl \cdot 2H_2O$ precipitation temperature.

There has been considerable discussion regarding possible stress concentration at the sharp corner at the butt of the cantilever beam (Brown, 1963). In an attempt to resolve this question, both Frankenstein and Butiagin have performed *in-situ* tests on simply supported beams in the same series with *in-situ* cantilever tests. Both groups of tests give similar results indicating that external stress concentrations, if present, are quite small. Figure 44, however, may be interpreted as exhibiting plastic stress relief at higher brine volumes but such an argument is weak.

Tabata and his co-workers (Tabata and Fujino, 1964, 1965; Tabata, 1966; Tabata, Fujino and Aota, 1967) have also studied the effect of variations in the manually applied average stress rate $\dot{\sigma}$ on the failure strength as measured by *in-situ* cantilever beam tests on ice less than 30 cm thick. Mean ice temperatures were quite high, varying from -0.8 to -2.5C. Ice salinities varied from 4.7 to 13.6‰. Although *in-situ* tests avoid the brine drainage problem, the results are difficult to analyze because of the vertical variation in the temperature and salinity of the ice sheet. The results are, however, quite interesting. Pull-up, push-down, and pull-sideways tests gave approximately the same results. The value of $\dot{\sigma}$ varied in the range of 0.1 to 40 kg/cm² sec.

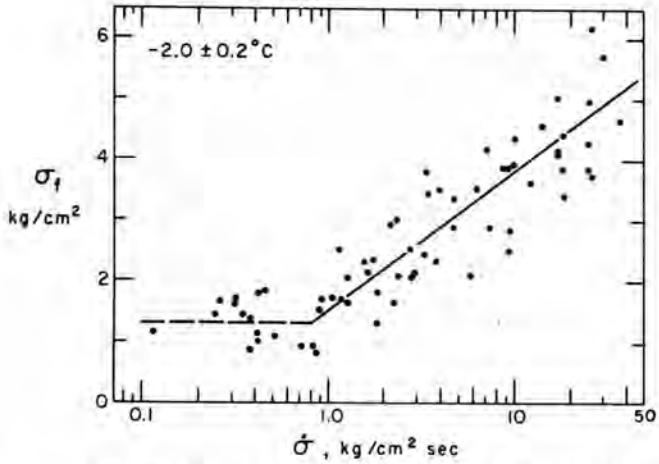

Figure 45. Relationship between in-situ *flexural strength of sea ice σ_f and the stress rate $\dot{\sigma}$ at -2C (Tabata, Fujino and Aota, 1967).*

The results of these tests (Fig. 45) show that the flexural strength σ_f is independent of $\dot{\sigma}$ at values of $\dot{\sigma} < 1.0$ kg/cm² sec. On the other hand, when $\dot{\sigma} > 1.0$ kg/cm² sec, σ_f increases as a linear function of ln $\dot{\sigma}$. Similar results have also been obtained by Ishida (1967). That the transition between these two behavorial regions coincides with the change from plastic to elastic deformation has been demonstrated by examining plots of applied force vs deflection for individual beam tests. These plots change from curved to linear at values of $\dot{\sigma} \geqslant 1$ kg/cm² sec. It is reasonable to assume that this transition to elastic behavior will occur at lower values of $\dot{\sigma}$ for lower test temperatures. The slope also appears to increase as the ice temperature is lowered.

Shear strength

The amount of information available on the shear strength of both sea and lake ice is quite limited. In addition, many of the values described as shear strengths are known to be the result of mixed-mode failures (see the discussion in Butkovich, 1954, 1956; Serikov, 1961). The lake ice data show considerable scatter as seen in the tabulation given by Kozitskii and Bybin (1967). Butkovich's (1954) data on the torsional shear strength of lake ice are presented in Figure 46. The direct shear determinations of Pinegin (1924) also show a similar temperature dependence but a slightly lower strength. At first glance the results of Wilson and Horeth (1948) also appear to agree with the results of Pinegin and Butkovich. However, because Wilson and Horeth's data include tests on both natural as well as artificial lake ice, they are difficult to interpret. On the other hand, Finlayson (1927) as well as Butiagin (1966a) have presented shear tests on lake ice that give shear strengths of 7.0 and 5.9 kg/cm² respectively and appear to be independent of temperature in the temperature range 0 to -23C. Several of these authors have found that, as might be expected, shear strengths measured normal to the long axes of the crystals give higher strengths than do values determined with the shear plane perpendicular to this direction. Butkovich's (1954) results also indicate that at -5C, σ_f is independent of $\dot{\sigma}$ for $\dot{\sigma}$ values greater than 1 kg/cm² sec.

Figure 47 shows the results of *in-situ* torsional shear strength determinations on lake ice by Kozitskii and Bybin (1967). The *in-situ* samples were vertical cylinders so that the failure plane was oriented normal to the growth direction. Their data, in contrast to the results of Butkovich (1954), indicate a linear decrease in strength right to the melting temperature. Because of limitations in the maximum applied torque that could be exerted on their specimens, Kozitskii and Bybin varied the diameters of their *in-situ* cylinders from 24 to 13.5 to 10 cm as the ice became

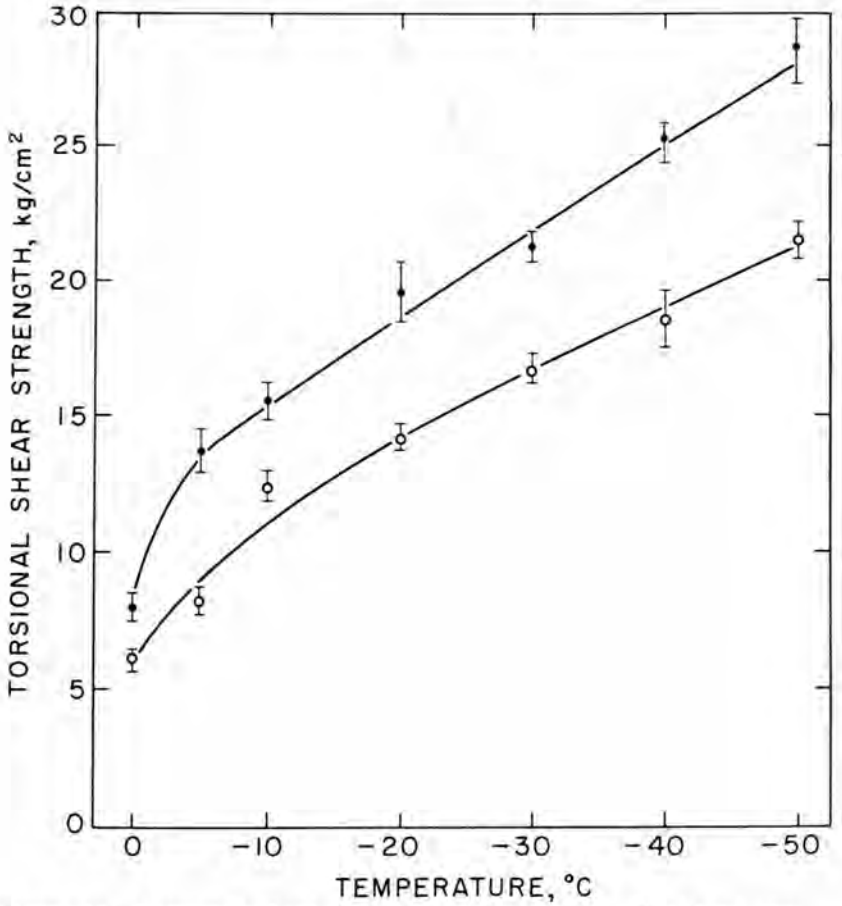

Figure 46. Torsional shear strength vs temperature: clear lake ice, Portage Lake, Michigan. In the upper curve the shear plane is normal to the growth direction; in the lower curve it is parallel (Butkovich, 1954)

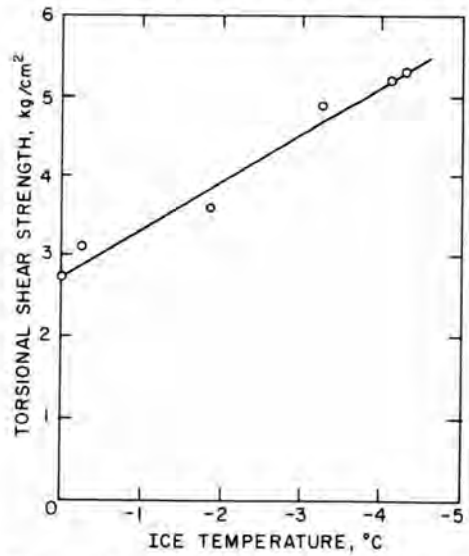

Figure 47. In-situ *torsional shear strength vs ice temperature, lake ice (Kozitskii and Bybin, 1967). Failure plane is normal to the growth direction.*

colder. Whether there is any systematic bias within their tests as a result of scale effects is not known. Butkovich's results (see Fig. 46) obtained from cylinders with a diameter of 1.95 cm are significantly higher than the results of Kozitskii and Bybin. At least a portion of this difference is undoubtedly due to a scale effect.

Kozitskii and Bybin (1967) also made an interesting attempt to measure the shear strength of deteriorating ice sheets by lowering loaded stamps from a helicopter. They obtained very low values: 0.06 to 0.07 kg/cm² from 35-cm-thick river ice determined immediately after breakup and 0.03 to 0.04 kg/cm² from dusted river ice with a thickness of 32 cm determined 8 days before breakup. Shear vane experiments on crushed ice in water under laboratory conditions discussed in the same paper gave an average of 0.021 kg/cm².

Sea ice from Hopedale, Labrador, has been studied by Butkovich (1956) by encasing the core in three close fitting metal cylinders and shearing out the central third of the core. These results, when plotted against $\sqrt{\nu_b}$, show a large scatter and indicate an average shear strength of $\approx$ 21 kg/cm² for $\sqrt{\nu_b} = 0.19$. There is no obvious correlation between σ_f and $\sqrt{\nu_b}$. The data do suggest a slight increase in σ_f with decreasing test temperature. These shear strengths are considerably higher than the tensile strengths reported by Butkovich on vertical cores. Shear failures are forced to occur across the columnar grains in this case and, therefore, the break occurs across the ice platelets.

Serikov (1961) has reported the results of 11 shear or punch tests in which the failure mode is questionable. His average shear stress is 8.6 kg/cm² with a maximum (11.2 kg/cm²) near the center of the ice sheet. The only supplementary information provided is that the air temperature varied between -0.9 and -4.1C during the tests. Petrov (1954-55) has also reported the results of a large number of shear tests on arctic pack ice. Unfortunately, his results have not, at present, been analyzed in terms of either ν_b or ν_a. His average values of σ_f are 7.0 and 3.9 kg/cm² for cold 1-year-old and perennial sea ice respectively.

The best set of shear tests available is by Paige and Lee (1967) from McMurdo Sound. Their results (Fig. 48), determined on 7.6-cm-diam cores, were obtained by using specially designed shearing heads which moved at 20 cm/min during the application of the failure load. Note that their shear strengths are consistently lower than their ring tensile values and that the shear strength decreases as $\sqrt{\nu_b}$ increases in the same general manner as in the ring tensile and *in-situ* cantilever results.

The fact that sea ice shear values determined by Butkovich as well as by Paige and Lee are significantly higher than values reported for lake ice can be explained in several possible ways. If the lake ice tested has its *c*-axes oriented vertically, then the glide planes of the ice crystals would be oriented in the easy-fail direction, producing lower strengths. Also, the composite fibrous nature of sea ice may simply result in a higher shear strength than lake ice. It is also conceivable that these differences are only related to differences in testing procedures and do not reflect differences in the intrinsic properties of the material being tested. Support for this latter suggestion can be found in the pronounced differences between the results of Petrov and those of Butkovich and Paige and Lee.

Impact strength

Only very limited information is available on impact testing of ice. Itagaki and Sabourin (in prep.) have determined the Charpy impact values for commercial ice using both notched and unnotched specimens. For unnotched specimens they obtained

$$C = 0.386(1 - 1.638 \times 10^{-3}\,\theta_i) \tag{56}$$

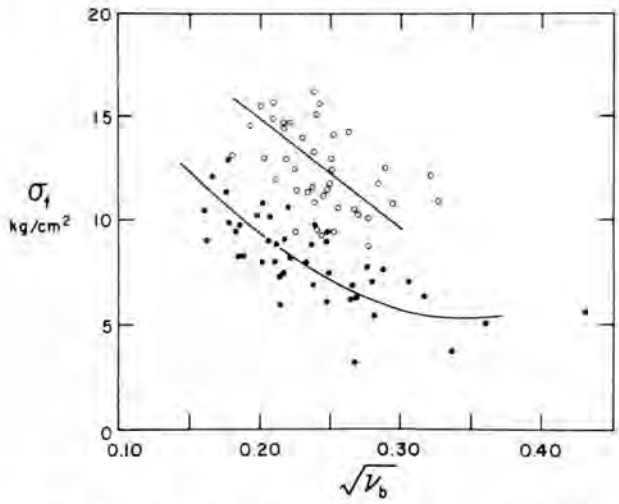

Figure 48. Shear strength (solid circles) and ring tensile strength (open circles) vs square root of the brine volume (Paige and Lee, 1967).

where θ_i is the specimen temperature (°C) and C is the Charpy value in kg-cm for a 1-cm² cross section. The temperature was varied between -2 to -190C. For notched commercial ice they obtained 0.342 kg-cm at -10C. The only Charpy values available for sea ice were measured by Petrov (1954-55) who obtained average values of 1.7 and 1.6 kg/cm for one year ice and 4.0 and 3.9 kg/cm for perennial ice when the fracture surfaces were respectively normal and parallel to the ice/air interface. Petrov's values were determined using ice bars with a 5 × 5-cm cross section and are expressed in work per unit area of cross section (kg cm/cm²). The units of kg/cm² listed in Petrov's data tables must be in error. Inasmuch as Itagaki and Sabourin's fresh ice values were determined on beams with a cross section of 1 cm², it should be possible to directly compare Itagaki and Sabourin's results with Petrov's. If such a comparison is valid, then the fact that sea ice gives Charpy values between 4 and 10 times those of fresh ice would be rather surprising. The explanation, of course, is that the impact work is not strictly proportional to area as commonly assumed. The height of the sample is more effective than the width.

The only other impact tests with which we are acquainted are from a study of the penetration and fracture of sea ice as a result of impact loading (Ross, 1967). In these tests several different shapes of penetrators were dropped down guide rails and it was noted whether or not the ice sheet was partially or completely perforated. The results were initially analyzed by Ross in terms of available potential energy vs a characteristic geometric quantity ($\pi D h^2/2$, where D is the diameter of the penetrator and h is the ice thickness). Quite a good separation was obtained between partial and complete penetration on this type of plot. Shear yield stresses based on the threshold values for penetration can also be calculated from these results. The values obtained range from 0.9 to 2.0 kg/cm². Even considering the large amount of brine in the ice tested, these values are appreciably lower than the shear strengths measured directly by Paige and Lee (1967). This difference may be caused, in part, by the higher strain rates achieved during impact testing.

One must be aware that Ross effectively assumes that most of the work is absorbed during the process of moving an ice plug through the sheet after initial failure. Initial failure should, however, be proportional to h, not h^2. In Figure 49 we have reanalyzed Ross' data assuming a simple cylindrical shear surface. A good separation between partial and complete penetration is also achieved but the plotted linear relation does not have a zero intercept which is difficult to explain.

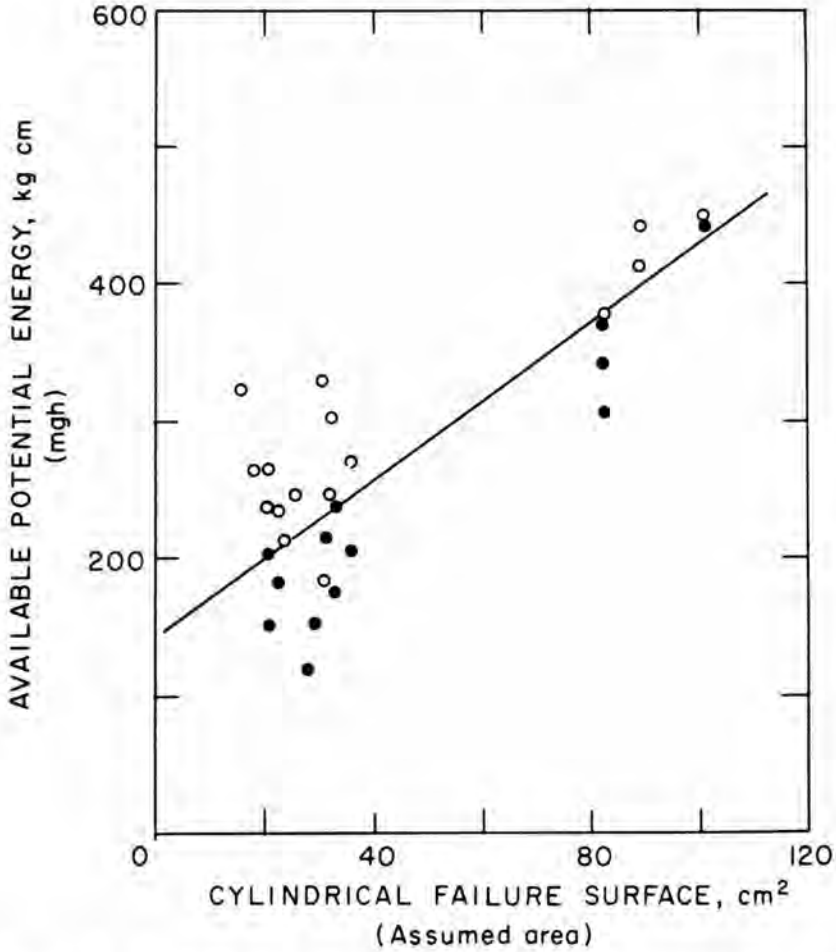

Figure 49. Available potential energy vs the area of an assumed cylindrical failure surface. The solid circles indicate partial penetration while the open circles indicate complete penetration. Data from Ross (1967).

If a conical 45° failure surface is assumed, a similar analysis gives a non-zero intercept on the abscissa. This is in agreement with Ross' observations which suggest that in many cases the actual failure surface is of a combined cylindrical-conical shape.

Scale effects

It has been known for some time that the measured strength of ice is some function of the size of the sample. Small samples give high strength values relative to values determined on larger samples. Finally, the failure of large ice masses under loads can be explained only by assuming still lower strength values. An adequate understanding of these scale effects is important in order that proper design values can be used in problems involving the strength of ice.

One of the first attempts to apply scale effect ideas to sea or lake ice was by Butkovich (1958, 1959a). He attempted to explain the observation that the failure strength of identical ice specimens decreases in the sequence σ_f (ring tensile) > σ_f (small beam) > σ_f (*in-situ* cantil ver). This suggestion was based on the earlier obsérvations of Butkovich (1955) and Jellinek (1958) who found that the compressive strength of lake ice and the tensile strength of snow ice both decrease as the volume of the specimen increases. If it is assumed, following Jellinek (1958), that

ice contains a distribution of defects and that each of these defects can withstand stresses up to a certain size, then it follows that the probability of the "weakest" imperfection occurring in this volume is proportional to the volume size. Therefore, tests that force failure on a small volume (ring tensile) should presumably yield higher strength values. This volume effect is very pronounced in material such as coal and glass where the defect distribution shows a wide scatter. On the other hand, in polycrystalline materials, where the defects are related to the microstructure, the variation in well annealed samples is commonly much less. It is not at all surprising that an appreciable volume effect should exist in natural ice specimens. In sea ice, for instance, we have on the smallest scale the molecular defects that are present within the individual platelets of pure ice. Then as the spacing between the defects increases, there are the intracrystalline flaws such as the brine pockets and the small angle grain boundaries between the platelets, then the intercrystalline defects associated with the grain boundaries, then the presence of large brine drainage channels (Bennington, 1963a) and finally the presence of cracks with different spacings. The probability of the more obvious "large" defects being effective in initiating fracture in a small sample test is very small. Indeed, such a sample would invariably be rejected as unsuitable for testing. However, the "larger" defects would commonly be present in the large ice masses that fail in most engineering applications of interest. The scale effect in ice has also been studied by Lavrov (1958, 1962, 1965). He assumes that the strength of ice is determined by the strength of the molecular bonds which are independent of sample size. The scale effect is believed to result because the larger the sample the smaller the relative elongation at which failure is presumed to occur and the smaller the ultimate strength. Lavrov's interpretation of the scale effect has not been widely accepted (Bartenev and Tsepkov, 1960).

Butkovich's suggestion partially explains the difference in the observed failure strengths inasmuch as the volumes within the samples subjected to stress increase in the sequence: ring tensile < small beam < *in-situ* cantilever. There are, however, problems in extending this argument in a quantitative sense because it is difficult in a test such as the ring tensile to estimate the exact volume of the ice that is subjected to the increased stress. There are also the additional interpretive problems associated with the differences in the degree of stress concentration between different test types.

A simple approach to the scale effect problem could be the following: consider the ratio (σ_S/σ_L) between the measured strength of a small sample σ_S and that of a larger sample σ_L. The classical assumption would be that $(\sigma_S/\sigma_L) = 1$. We know that the ratio is actually higher $(\sigma_S/\sigma_L) = (1 + E)$ and we expect that the excess E will prove to be a function of the size of the failure surface. Let us assume that the failure surface is a square with the side a. Then as a general statement we may say

$$\frac{\sigma_S}{\sigma_L} = 1 + f(a). \tag{57}$$

For a rectangular failure we may use $L = \sqrt{ab}$ where b is the width of the failure surface or, in general $L = \sqrt{F}$ where F is the area of the failure surface. In order to keep eq 57 dimensionally homogeneous we should divide a by a length l_0 which in some unknown way is associated with typical distances between effective defects.

$$\frac{\sigma_S}{\sigma_L} = 1 + f\left(\frac{L}{l_0}\right). \tag{58}$$

If for the function $f(L/l_0)$ we make the simple assumption of linearity and combine the constant with $l_0(L_0 \equiv l_0/\text{const})$ then

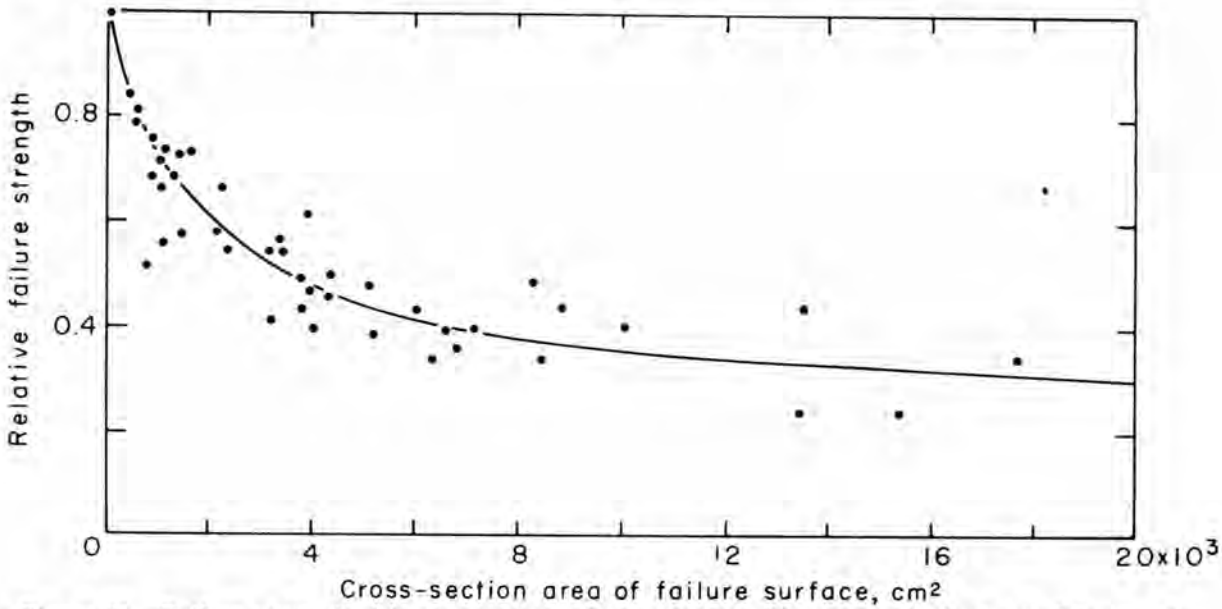

Figure 50. Failure strength of freshwater ice relative to the failure strength of a control beam of the same ice with a 70-cm² cross section vs the cross-sectional area of the failure surface. Tests are simply supported beams (Butiagin, 1966a).

$$\frac{\sigma_S}{\sigma_L} = 1 + \frac{L}{L_0} . \tag{59}$$

The usefulness of such a relation can only be assessed by using actual test results. Fortunately, Butiagin (1966a, b) has, over a 13-year period, performed on lake and river ice a large number of different types of tests in which the size of the specimen was varied over a wide range. A representative plot of some of these tests is shown in Figure 50. The effect of sample size is quite noticeable. In this figure, Butiagin has chosen to plot the relative failure strength (σ_L/σ_S) where σ_S is taken as the strength of a series of control beams, here beams with a 70-cm² cross section. Ideally measurements of control beams should be performed simultaneously with each set of measurements involving beams with larger cross sections. In most cases Butiagin followed this procedure. In our treatment of Butiagin's data we will in three cases use strength values derived from the strength of the complete ice sheet. In these cases we have followed Butiagin's suggestion and assumed that the critical cross section was $7h$ where h is the ice thickness. In the beams utilized, the width ranged up to 200 cm and the height up to 100 cm. A total of 516 flexural tests were used and were grouped and averaged according to decreasing L without weighting according to the number of tests in each group. The result of our analysis according to eq 59 is shown in Figure 51. Note that in this figure the line must by definition go through $(\sigma_S/\sigma_L) = 1$ and $L = \sqrt{70} = 8.37$. A similar data analysis not shown here where the width is held constant and the height allowed to vary also gives a linear relationship but with a different slope. The flexural strength appears to be more sensitive to variations in the thickness of the beams than in the widths. Figure 52 shows our analysis of groups of Butiagin's data with similar thicknesses and variable widths plotted as (σ_f^{-1}) vs L. Each group of data gives a linear relation but with different intercepts and slopes. Assuming that the effects of width variations are completely accounted for in the variation of L, we found that the intercepts of the lines in Figure 52 expressed in strength can be meaningfully related to temperature as shown in Figure 53 varying from 5.3 kg/cm² at 0C to roughly twice that value at -25C. The slopes, however, exhibit the opposite tendency (Fig. 54), producing a

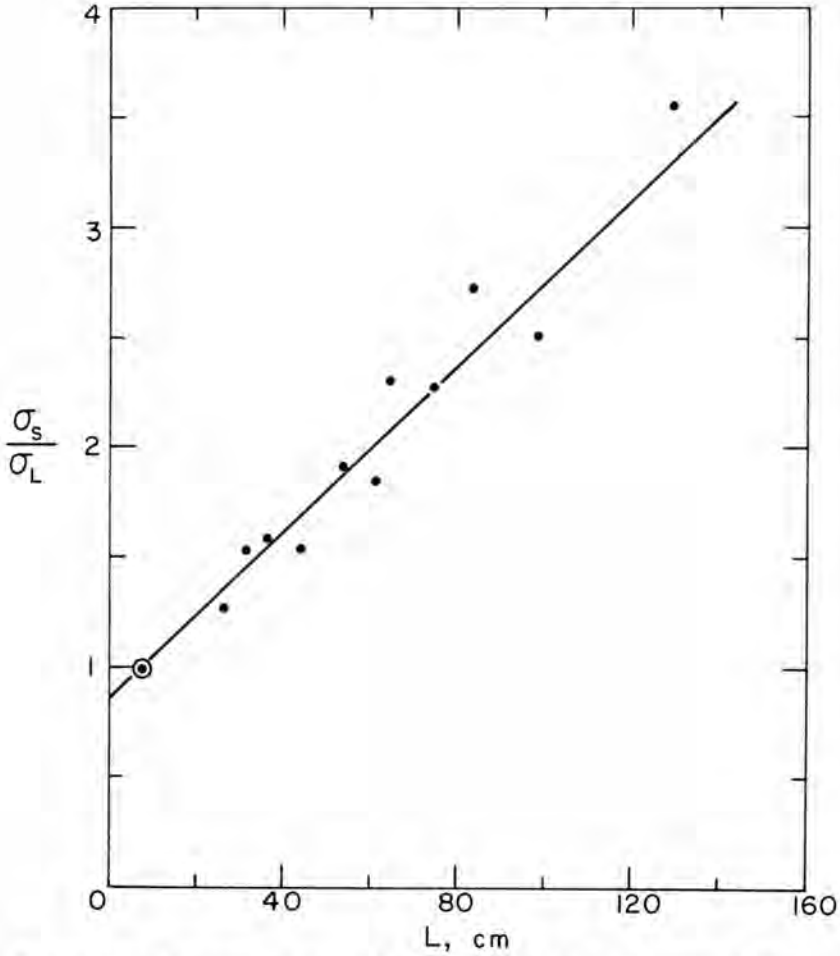

Figure 51. The ratio σ_S/σ_L where σ_S is the flexural strength of a control beam with a 70-cm² cross section and σ_L is the flexural strength of a beam of identical ice that is tested under similar conditions vs L, the square root of the cross-sectional area.

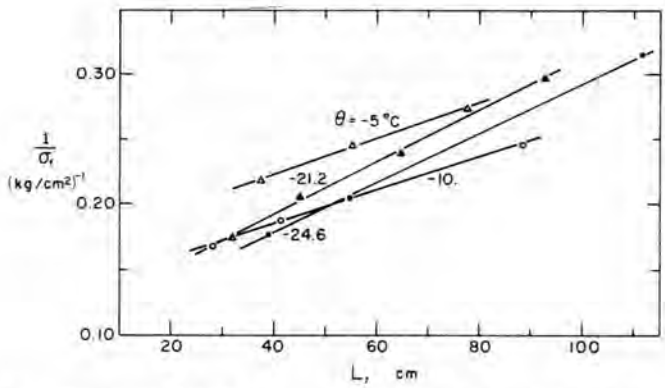

Figure 52. σ_f^{-1} for groups of test beams with similar thicknesses and variable widths vs L, the square root of the cross-sectional area.

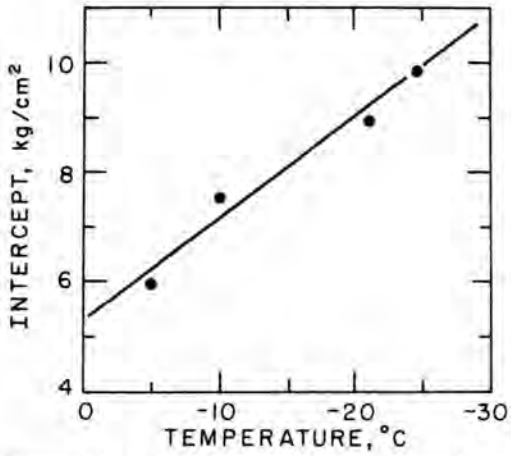

Figure 53. The intercepts from Figure 52 expressed in terms of σ_f vs ice temperature.

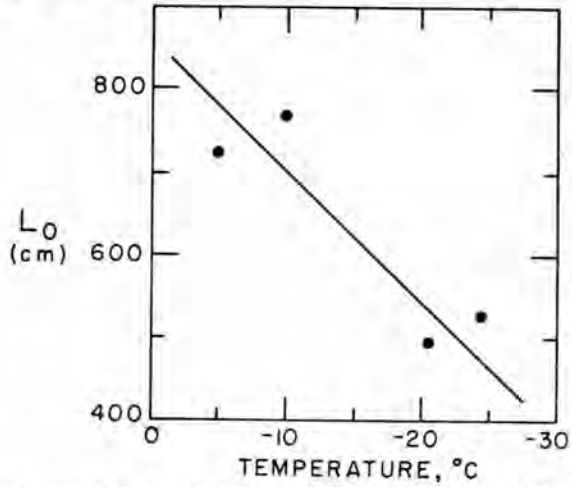

Figure 54. L_0 based on the slopes of the different lines drawn in Figure 52 vs ice temperature.

complex relation between flexural strength and temperature. Since L_0 in our thinking is related to the spacing of effective flaws and cracks in the ice sheet, Figure 54 simply means increased brittleness at lower ice temperatures. This may meaningfully relate to the Canadian experience reported by Gold (1960b) whereby more fresh ice breakthrough accidents occur at low air temperatures.

Butiagin (1966a) also presents data indicating a similar decrease in failure strength with increasing sample cross section for cubic compression specimens. It is important to note that even considering the large number of tests performed by Butiagin, the number available is still just marginally sufficient for an adequate analysis. The collection of even more extensive sets of data designed to investigate the scale effect problem should be undertaken as soon as possible. We feel that an understanding of the scale effect in ice testing is essential before a thorough scientific basis can be developed for the utilization of small scale testing in engineering design problems.

Since Figure 54 indicates that the parameter L_0 decreases with decreasing θ_i and, therefore, could be related to brittleness, we suspect that for sea ice L_0 should be considerably larger than for fresh ice. Unfortunately, presently available data do not allow this suggestion to be evaluated. It is not even adequate for sea ice to repeat the testing methodology used by Butiagin (1966a) on fresh ice, because in sea ice strength is highly dependent upon both the salinity as well as the temperature profile. As remarked earlier (Fig. 11, 12) thick ice sheets have consistently different salinity profiles than thin ice sheets. Therefore, even if the experimenter could arbitrarily control the temperature profile in a natural ice sheet, it would be difficult to produce a thick ice sheet which could be tested and compared directly with thinner ice sheets or separate layers of a thick ice sheet. One may be able to circumvent this difficulty by calculating reference values of flexural strength based upon temperature and salinity values using the computational techniques discussed earlier (Weeks and Assur, 1968, eg. 5.25 and 5.26).

Strength deterioration in the spring

The strength of a given ice cover changes systematically with the seasons of the year. The most dramatic portion of this change occurs during the spring deterioration and breakup. This rapid decrease in strength with time is strikingly shown in Figure 55 (Butiagin, 1966a) which is based on measurements from both a lake and a river in Russia. There are a number of factors which contribute to the rapid deterioration of strength: a decrease in the overall thickness of the ice sheet (Bilello, 1961), an increase in the temperature causing a decrease in the strength of the

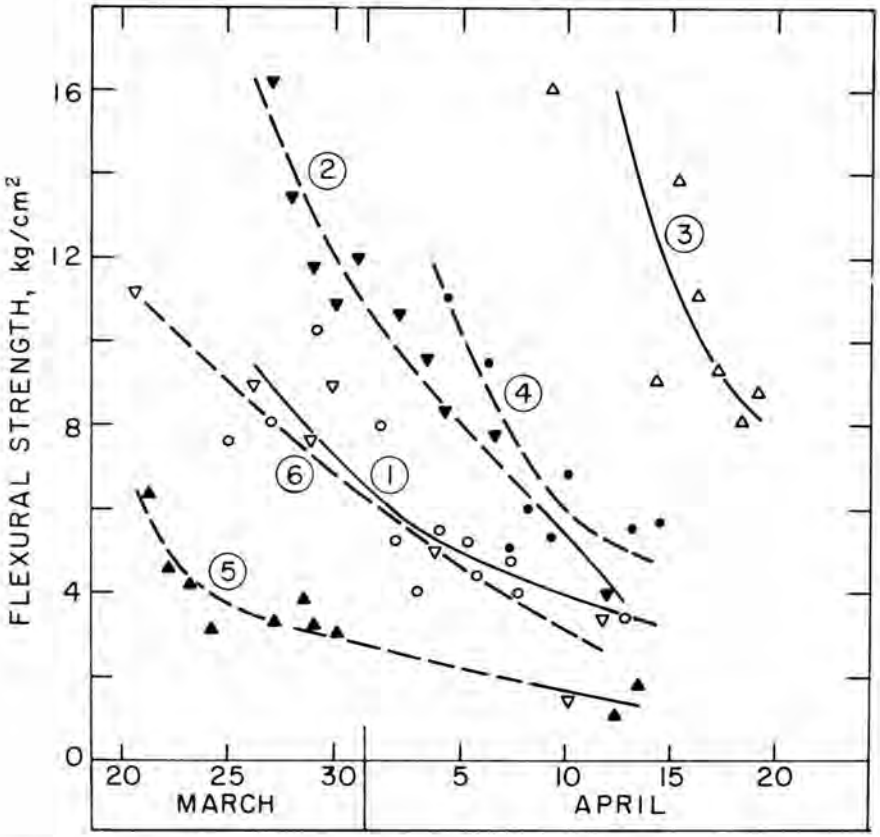

Figure 55. Deterioration of ice strength with time in the spring as measured on simple beams with 8 × 8-cm cross sections. The portions of the curves shown as dashed lines indicate time periods when the average daily air temperature was below freezing. Data from Shumikha Village on the Yenisei River, 1) 1961 and 2) 1962; and from the Novosibirsk Reservoir, 3) 1958, 4) 1959, 5) 1962 and 6) 1963 (Butiagin, 1966a).

ice itself, and an increase in the amount of liquid present within the ice causing substantial weakening.

The spring deterioration of freshwater ice has received considerable attention. Deteriorated ice produces the flooding and structural damage commonly associated with ice jams and debacles. In the spring as air temperatures and the amount of incoming solar radiation increase, ice temperatures rise rapidly. Once the ice is at a temperature near zero, the selective absorption of radiant energy along grain boundaries causes localized grain boundary melting. Two phases, ice and water, now coexist. Because freshwater ice is essentially pure water and pressure variations can be neglected, the phase rule indicates that this coexistence can occur only at a fixed temperature, 0C. Therefore, once a fresh ice sheet becomes isothermal at 0C, its strength becomes effectively "undefined" because the transition from 100% ice to 100% water occurs at constant temperature. Because of the localized nature of the melting process, the relative intercrystalline porosity increases rapidly with an associated decrease in strength. The decrease in the *in-situ* torsional shear strength vs the total absorbed solar radiation in cal/cm^3 at the level of the shear failure has been studied by Kozitskii and Bybin (1967). Their results are shown in Figure 56. Time zero was arbitrarily taken as the date when the mean annual air temperature became positive. Figure 47 shows that the ice in Figure 56 presumably reaches 0C when its strength is 2.7 kg/cm^2. Just how rapidly pronounced strength changes may occur in a sheet of lake ice during the spring is shown by

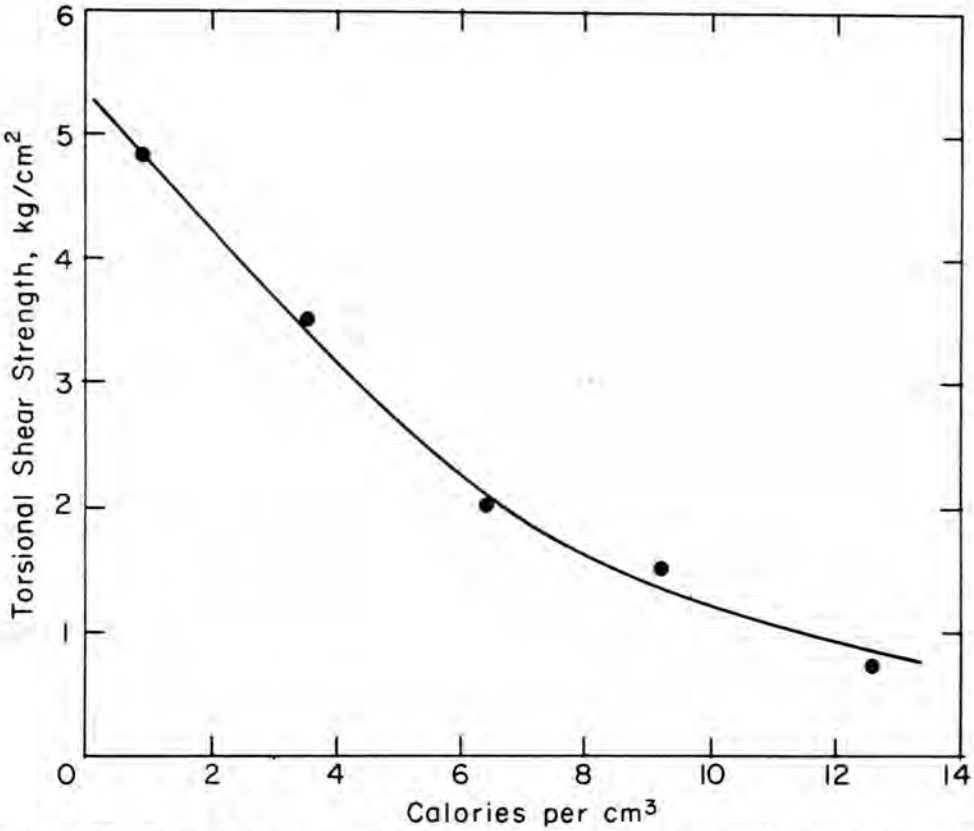

Figure 56. Dependence of in-situ *shear strength of lake ice on the total solar radiation absorbed in the layer at 15- to 20-cm depth in the ice sheet (Kozitskii and Bybin, 1967).*

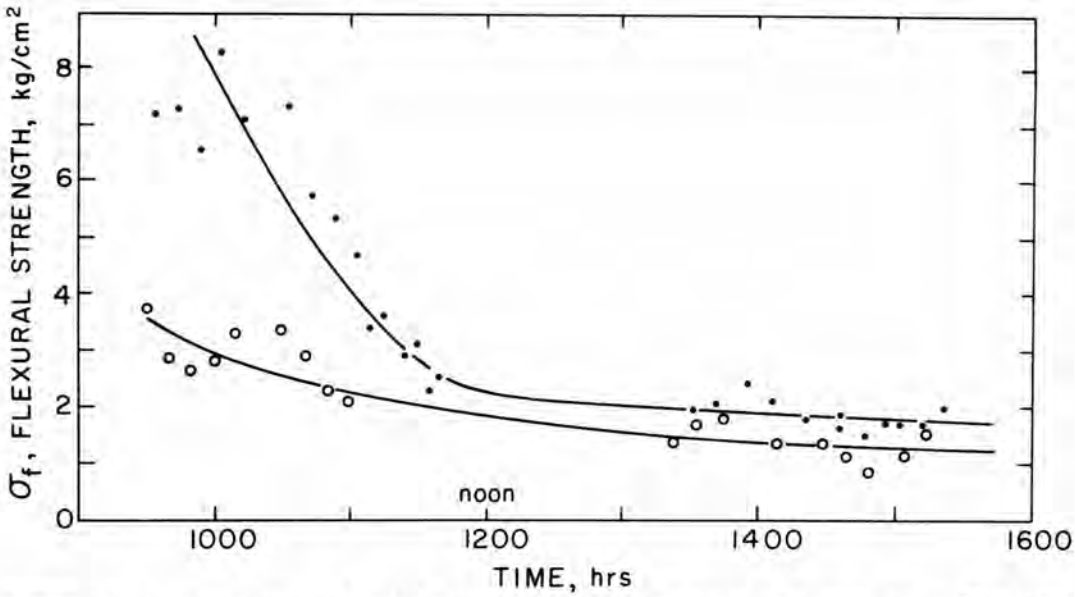

Figure 57. Flexural strength vs time, push-down simply supported beam tests. The solid circles indicate tests where failure occurred with the upper surface of the ice sheet in tension. In the tests represented by open circles, the lower surface of the ice sheet was in tension (Frankenstein, 1961).

a series of tests performed by Frankenstein (1961) on 1 April 1958 at Keweenaw Bay near Houghton, Michigan. It was a bright sunny day and at the start of the test series (0930) the ice surface and air temperatures were -0.9C and -1.0C respectively. At 1315 the air temperature was +2.5C. The results are shown in Figure 57. The rapid decrease in the flexural strength of the ice with tension at the ice/air interface is striking.

The final deterioration of lake ice occurs when the ice sheet separates into a weak mass of individual "candles." A detailed description of the deterioration of ice on a perennially frozen lake in northern Greenland is given in Taylor and Lyons (1959) and Barnes (1960). It is interesting to note that lake ice with its *c*-axes oriented vertically deteriorates significantly slower than ice with its *c*-axes oriented horizontally. This difference is produced by changes in the effective albedo of the ice (Fig. 4). The structural reasons for this albedo change are not fully understood (Knight, 1962). For a general description of the deterioration of lake ice see Williams (1968).

During the deterioration process the average strength not only decreases, but the ratio of the strength measured parallel to the growth direction to the strength measured normal to it $(\sigma_{f(||)}/\sigma_{f(\perp)})$ also changes. Korzhavin (1962) has observed an increase in the value of the ratio $(\sigma_{f(||)}/\sigma_{f(\perp)})$ from roughly 1.25 to as much as 4 for compressive strengths and Butiagin (1966a) has noted a similar variation in flexural strengths. This ratio is important in the analysis of forces on structures.

The deterioration process in sea ice, although inadequately described, appears to differ from that of freshwater ice. Because of the salt in seawater, there is an equilibrium amount of brine that will coexist with ice at near "melting" temperatures. Therefore, provided the bulk ice salinity and temperature can be adequately measured, it is possible to determine the amount of liquid present in the ice from the phase relations. In sea ice, grain boundary melting with its resulting "candling" does not appear to dominate the deterioration process. Instead, extensive brine drainage features develop and the ice becomes very porous. The overall change in the strength profile of a sheet of perennial sea ice as a function of the season of the year has been studied by Peschanskii (1967, Fig. 23b). Peschanskii indicates that during the early summer the upper portion (≈ 30 cm) of the ice sheet becomes essentially strengthless and the strength of the underlying ice decreases to approximately ¼ of the average winter strength. The only data on the change in the ratio $(\sigma_{f(||)}/\sigma_{f(\perp)})$ during the deterioration process is by Bruns and Deriugin (Zubov, 1945). They found that $(\sigma_{f(||)}/\sigma_{f(\perp)})$ as measured in compression decreased from roughly 2 (Butkovich (1959a) obtained values as high as 4) and approached unity for deteriorated summer ice. The difference in the deterioration of strength between sea and lake ice is undoubtedly caused by "structural" differences produced during the deterioration process. The boundaries between the elements of pure ice contain the impurities. These boundaries are intercrystalline in the case of fresh ice and intracrystalline in the case of salt ice. Therefore, "candles" are found in the first case and overall internal deterioration is experienced in the second case. Because of the practical importance of the problem, it is hoped that well conceived field observations will soon become available.

RECOMMENDED RESEARCH

Ice has many desirable features which make it an attractive material to use in studying fracture at or near melting temperatures. These temperatures are convenient for experimentation and the melt is non-corrosive. In addition, both the liquid and solid phases are transparent so that simple optical techniques utilizing transmitted light can be used. Also, due to its low birefringence, ice is optically very sensitive to slight stresses. That this can be used quite effectively in the study of fracture in ice has recently been shown by Wakahama (1967) and Hawkes (personal communication). It is also possible to readily achieve a wide range of grain sizes.

In spite of these advantages, it is only recently that the mechanical properties of ice have been systematically investigated. Most of this work has been directed toward improving our understanding of glacier flow and has focused on the properties of randomly oriented polycrystalline ice and of single crystals of ice. The basic study of fracture in lake and sea ice, although a more important problem from an engineering point of view, has received appreciably less attention. The reason for this is quite simple: most glaciologists are interested in glaciers.

In the present review we have attempted to point out areas where additional work could profitably be undertaken as we discussed specific aspects of the fracture of lake and sea ice. In this closing section we will briefly mention only problems which we feel are particularly important. The study of dislocations in ice by X-ray topography and the microscopic determination of initial crack formation and propagation in both fresh and sea ice appear to be profitable. Gold's studies of crack formation in artificial fresh ice have only provided us with the beginnings of an experimental basis for interpreting fracture in more heterogeneous natural lake and river ice. In sea ice our studies of the failure mechanisms have been mainly limited to speculations based on conceptual models of the microstructure as augmented by the information from a few "rubbings" and photomicrographs. Although the gross details of these ideas undoubtedly correspond to reality, it is highly desirable that statistical information be obtained regarding systematic variations in all aspects of the sea ice substructure as well as their relation to initial crack nucleation and propagation. If possible, any systematic structural variations should first be related to growth conditions and finally to the meteorological and oceanographic parameters that control the growth (Assur and Weeks, 1963). It is only by making these types of transitions that it will prove possible to adequately predict the strength of ice sheets.

Because it is quite probable that the mechanical properties of fresh ice vary with grain size, it would be useful to investigate to what degree the conditions during the initial nucleation and formation of an ice skim specify the grain-size characteristics of the resulting ice sheet. This problem is also of importance in the use of ice in model testing since by controlling the variation of the grain size as well as the amount of air incorporated in the ice one can manipulate the properties of artificial ice sheets.

Certain small sample testing methodologies should be standardized so that investigators with different groups can compate the "state" of their specimens by using one or two simple test methods. Considerable care should be taken in designating procedures to minimize problems such as brine drainage and thermal shock. Rapid methods should also be developed to obtain the subsidiary information (i.e. grain size, brine and air volume, crystal orientation, etc.) necessary to adequately describe a specimen. The time has passed whereby significant contributions can be made by field expeditions which merely repeat a battery of tests that have been performed previously. Test series should be designed to examine certain hypotheses such as "Is $Na_2SO_4 \cdot 10H_2O$ reinforcement a significant factor in determining the strength of sea ice?"

Although in the past the strength of sea ice has been largely treated as a function of brine volume, we are not at all certain that this is an adequate assumption. When test results are initially grouped according to the salinity of the ice and then analyzed in terms of brine volume, some unusual effects have been noted in the results from both low salinity and perennial ice. This also emphasizes the almost complete lack of information regarding the structure and properties of brackish water ice.

The variation of such parameters as stress rate, strain rate, or crosshead speed can now be definitely shown to have a pronounced effect on the failure strength of both fresh and sea ice as determined by certain types of tests. However, in some cases the results of different investigators appear to contradict each other. Before recommendations can be made regarding a standardized testing methodology, these problems must be resolved. It is also desirable that a better understanding of the interrelations between the results of different types of tests be developed. An interesting aspect of this problem is the effectiveness of possible internal and external stress concentrators as a function of the plasticity of the specimen as determined by the test conditions.

There is, at present, no general relation which expresses the failure strength in terms of either the area of the failure surface or the volume subjected to stress. Additional sets of experimental observations that are designed to study this problem are needed inasmuch as the available data are still somewhat contradictory. Because it is currently impossible to predict ice forces on engineering structures from small scale tests, there is a distinct need for the large scale determination of these forces in a few well designed tests. In the past, because such tests are extremely expensive, they have usually been performed by private commercial interests. Unfortunately the results have not been readily obtainable. Tests should also be devised to study the shear resistance of broken ice masses and frazil ice as a function of effective confining pressure. Such information would be helpful in the development of a rational mechanics for ice jams and in the design of icebreakers and bridge piers.

We feel quite certain that it will eventually be possible to effectively compute the forces exerted by large ice masses from small scale test data. Indeed, it is imperative that such methods be developed because of the prohibitive costs and time requirements of large scale testing.

SUMMARY

In the cold regions of the earth there are a number of geophysical and engineering problems in which the fracture of lake and sea ice plays an important roll. Nevertheless, only recently have systematic efforts been made to develop a basic body of knowledge on this subject. This paper attempts to assist the reader in developing a basic understanding of the subject as well as summarizing the main results from the world literature. Only the most common types of ice that form on naturally occurring water bodies are discussed: namely sea ice covering saline water bodies and lake ice covering quiet freshwater bodies.

Except for a thin upper layer of snow and slush ice, the main body of an ice sheet grows in a columnar form with vertical ice crystals which gradually increase in size with depth. Strength results depend strongly upon the direction of stresses relative to the growth direction. In addition, the orientation of the crystallographic *c*-axis of the ice crystal is important: for sea ice, and frequently for lake ice, the orientation is perpendicular to the growth axis but otherwise random. Impurities are partially rejected during the growth of the ice and incorporated on the grain boundaries between crystals and in parallel striations within the ice crystals. In particular the microstructure of sea ice is determined by parallel planes of brine pockets which are arranged perpendicular to the *c*-axes of the enclosing ice crystals. The distribution of impurities has a profound effect on the mechanical properties of the ice. Fortunately, the relative amount of brine in sea ice can conveniently be calculated from the phase relations.

Work on the direct observation of dislocations in ice is just beginning. The initial results are extremely promising. Microcracking occurs in ice samples long prior to failure. Recent studies of this phenomenon have contributed to our understanding of the basic fracture mechanisms in ice. Ice can behave in either a brittle or a plastic manner depending upon the temperature, brine volume and strain rate. This causes difficulties in the interpretation of test results but also provides the opportunity of developing new approaches toward the analysis of the behavior of a material near its melting point. A distinction is made between internal stress concentrators which are a property of the material and external stress concentrators which are due to the shape of the specimen. Both are affected by the characteristic behavior of the material which ranges from plastic to brittle.

The distinctive microstructure of sea ice allows the development of structural models for its physical property variation. Several petrographic parameters such as the spacing of platelets which depend upon growth velocity, the spacing and shape of brine pockets, air pockets, etc. can be utilized in a coherent system of models which enable the investigator to explain the properties of sea ice on a rational basis.

Large discrepancies in compressive strength results are due to differences in the size and shape of samples, the orientation of stresses and the degree of bonding between crystals. Although the stress rate appears to have a pronounced effect, available results are not consistent. Very high compressive strengths are obtained for vertical sea ice samples illustrating the importance of the ice structure. Indentation failure has attracted some interest due to practical considerations. Results indicate that the ratio of the ice thickness to the width of the indenting structure is important. Large scale failures of engineering structures give typical crushing strength values which are appreciably below laboratory results.

Direct tension tests show a slight dependence on temperature for fresh ice and a distinct dependence on brine volume for sea ice. The orientation of the tensile stress to the *c*-crystallographic axis profoundly affects the results in sea ice. These results can be explained by differences in stress concentration as well as the geometry of the brine pockets. Tests on cylindrical or ring samples cut from ice cores have been utilized extensively. In a simple sea ice model the "basic strength" for zero brine volume compares well with similar tests for fresh ice. The ring tensile strength decreases proportional to the square root of the brine volume. The nominal zero strength intercept on the brine volume axis gives consistent results which compare well with similar relations determined for other mechanical properties. A recent extension of the structural model explains the behavior of warm sea ice at high brine volumes. At low temperatures a considerable portion of the salts precipitate. Reinforcement by solid salt inclusions has still not been demonstrated conclusively and is likely to be less significant than previously assumed. The high theoretical stress concentration in ring tensile samples leads to a discussion of the effect of plasticity and brittleness on test results. The derivation of correct tensile strength values is still a major difficulty.

A time-honored but time-consuming procedure for determining the flexural strength is the testing of small beams cut from the ice sheet. The values are consistently lower than ring tensile results and depend strongly upon the orientation of the beam to the growth direction. The results of flexural tests on beams cut *in-situ* from the full ice sheet are of major conceptual importance because they can be directly related to problems of bearing capacity and forces exerted on sloping engineering structures. The results for sea ice can be meaningfully related to brine volume. Stress rate has a pronounced effect on the flexural strength which is not easily explained.

Shear strength values are not only meager but contradictory. An interesting recent development is *in-situ* values which can be related to absorbed radiation under conditions of deterioration. Only limited information is available on impact strength.

One of the most important problems concerned with the gap between science and application in ice engineering is the scale effect in test results. Small ice volumes show considerably higher strengths than the large ice volumes involved in applications. This could lead to unjustified optimism in the use of ice sheets for traffic or unjustified pessimism in the design of structures to withstand ice forces. The scale effect has been known for many years but only recently have exhaustive test results become available so that attempts can be made to develop a coherent picture. For large volumes of ice the basic physical strength properties become less important than the effective distances between major defects such as cracks. This distance is governed by brittleness which is high for cold fresh ice and low for warm ice or normal sea ice. The strength of small samples increases with lower temperature but the scale effect produces the opposite result when large ice volumes are involved in failure.

Ice deteriorates rapidly under springtime conditions. This must be considered when ice sheets are used for traffic or when the effect on engineering structures after breakup is being calculated. Numerical results indicate a pronounced decrease in strength after the onset of above-freezing air temperatures as well as a distinct decrease in the ratio of crushing strength perpendicular to growth to strength values parallel to growth.

The attempt to present a coherent system of the failure of lake and sea ice has only partially succeeded because of unresolved contradictions in the available data. On the other hand, it has opened several avenues in which further investigation would lead to fruitful results.

SELECTED BIBLIOGRAPHY

Titles of Japanese and Russian papers are given in English. The letters (J) and (R) following the titles indicate the original language. The abbreviations CRREL and SIPRE stand for the U.S. Army Cold Regions Research and Engineering Laboratory and the U.S. Army Snow Ice and Permafrost Research Establishment.

Abele, G. and Frankenstein, G. (1967) Snow and ice properties as related to roads and runways in Antarctica. CRREL Technical Report 176, 37 p. (AD665386).

Anantha, N.G. and Chalmers, B. (1967) Electrical phenomenon occurring during freezing of dilute aqueous solutions. *Journal of Applied Physics*, vol. 38, no. 11, p. 4416-4420.

Anderson, D.L. (1958) A model for determining sea ice properties. In *Arctic sea ice*. U.S. National Academy of Sciences, National Research Council, Publication 598, p. 148-152.

_____ (1960) The physical constants of sea ice. *Research*, vol. 13, p. 310-318.

_____ and Weeks, W.F. (1958) A theoretical analysis of sea ice strength. *Transactions of the American Geophysical Union*, vol. 39, p. 632-640.

Andrews, J.T. (1962) Variability of lake ice growth and quality in the Schefferville region, central Labrador-Ungava. *Journal of Glaciology*, vol. 4, p. 337-347.

Arakawa, K. (1955) The growth of ice crystals in water. *Journal of Glaciology*, vol. 2, p. 463-467.

Arnol'd-Aliab'ev, V.I. (1925) Methodology of ice study from ice breakers in the Gulf of Finland (R). *Zhurnal Geofiziki i Meteorologii*, vol. 2, p. 79-88.

_____ (1929) Investigation of ice strength of the Finnish Gulf in 1923, 1927, and 1928 (R). *Izvestiia Glavnoi Geofizicheskoi Observatorii, Leningrad*, vol. 2, p. 15-28.

_____ (1934) Determination of density and porosity of ice under field conditions (R). *Trudy Komissii Po Izucheniu Vechnoi Merzloty, Akademy Nauk SSSR*, vol. 3, p. 127-150.

_____ (1939) Strength of the ice in the Barents and Kara Seas (R). *Problemy Arktiki*, vol. 6, p. 21-30.

Assur, A. (1956) Airfields on floating ice for routine and emergency operations. SIPRE Report 36, p. 1-20 (AD 99688).

_____ (1958) Composition of sea ice and its tensile strength. In *Arctic sea ice*. U.S. National Academy of Sciences, National Research Council, Publication 598, p. 106-138. Also SIPRE Research Report 44, 1960 (AD 276604).

_____ and Weeks, W.F. (1963) Growth, structure, and strength of sea ice. International Union of Geodesy and Geophysics (Comm. Snow and Ice, Berkeley) Publication 61, p. 95-108. Also CRREL Research Report 135, 1964 (AD 450186).

Ballard, G.E.H. and Feldt, E.D. (1966) A theoretical consideration of the strength of snow. *Journal of Glaciology*, vol. 6, p. 159-170. Also CRREL Research Report 184, 1965 (AD 631000).

Ballard, G.E.H. and McGaw, R.W. (1966) A theory of snow failure. *International Symposium on Scientific Aspects of Snow and Ice Avalanches*, Davos, Commission on Snow and Ice, International Union of Geodesy and Geophysics Publication 69, p. 160-169. Also CRREL Research Report 137 (AD XL 624198).

Barnes, D.F. (1958) Preliminary measurements of the strength of melting lake ice. *Transactions of the Engineering Institute of Canada*, vol. 2, 108-111.

Barnes, D.F. (1960) An investigation of a perennially frozen lake. Geophysical Research Directorate, Air Force Cambridge Research Laboratories, *Surveys in Geophysics*, no. 129, p. 1-134.

Bartenev, G.M. and Tsepkov, L.P. (1960) On the nature of the size effect in ice (R). *Zavodskaia Laboratoriia*, vol. 26, p. 330-331.

Bennington, K.O. (1963a) Some crystal growth features of sea ice. *Journal of Glaciology*, vol. 4, p. 669-688.

_____ (1963b) Some chemical composition studies of arctic sea ice. In *Ice and snow – processes, properties, and applications* (W.D. Kingery, ed.), p. 248-257. Cambridge, Mass.: MIT Press.

Berdennikov, V.P. (1967) Calculation of ice pressure from frazil and normal ice jams on structures (R). Gosudarstvennyi Gidrologicheskii Institut, Leningrad, Tr. 48, p. 3-28.

Bilello, M.A. (1961) Formation, growth and decay of sea-ice in the Canadian Arctic Archipelago. *Arctic*, vol. 14, p. 3-24. Also SIPRE Research Report 65, 1960 (AD 653137).

Brill, R. (1962) The structure of ice. *Angewandte Chemie, International Edition*, vol. 1, p. 563-567.

Brown, E. (1926) Experiments on the strength of ice. *Report of the Joint Board of Engineering, St. Lawrence Waterway Project*, p. 423-453.

Brown, J.H. (1963) Elasticity and strength of sea ice. In *Ice and snow – processes, properties, and applications* (W.D. Kingery, ed.), Cambridge, Mass.: MIT Press, p. 79-106.

Bryant, G.W. and Mason, B.J. (1960) Etch pits and dislocations in ice crystals. *Philosophical Magazine*, vol. 5, p. 1221-1227.

Bullough, R. (1964) The cracked dislocation under tension. *Philosophical Magazine*, vol. 9, p. 917-925.

Butiagin, I.P. (1966a) Strength of ice and ice cover (R). Izdatel'stvo "Nauka" Sibirskoe Otdelenie, Novosibirsk, p. 1-154.

_____ (1966b) Scale factor in evaluation of ice strength (R). Materialy VIII Vsesoiuz. mezhduvedomstvennogo soveshchaniia po geokriologii (merzlotovedeniiu), vol. 5, p. 73-78.

Butkovich, T.R. (1954) Ultimate strength of ice. SIPRE Research Report 11, p. 1-12 (AD 50514).

_____ (1955) Crushing strength of ice. SIPRE Research Report 15, p. 1-5 (AD 75249).

_____ (1956) Strength studies of sea ice. SIPRE Research Report 20, p. 1-15 (AD 125593).

_____ (1958) Recommended standards for small-scale ice strength tests. *Transactions of the Engineering Institute of Canada*, vol. 2, p. 112-115. Also SIPRE Technical Report 57, 1958 (AD 211569).

_____ (1959a) On the mechanical properties of sea ice, Thule, Greenland, 1957. SIPRE Research Report 54, p. 1-11 (AD 235872).

_____ (1959b) Some physical properties of ice from the TUTO tunnel and ramp, Thule, Greenland. SIPRE Research Report 47, p. 1-17 (AD 225569).

Chalmers, B. and Williamson, R.B. (1965) Crystal multiplication without nucleation. *Science*, vol. 148, p. 1717-1718.

Devik, O. (1949) Freezing water and supercooling. *Journal of Glaciology*, vol. 1, p. 307-309.

Dykins, J.E. (1963) Construction of sea ice platforms. In *Ice and snow – processes, properties and applications* (W.D. Kingery, ed.). Cambridge, Mass.: MIT Press, p. 289-301.

Dykins, J.E. (1967) Tensile properties of sea ice grown in a confined system. In *Physics of snow and ice*, Institute of Low Temperature Science, Hokkaido University, vol. I, no. 1, p. 523-537.

Elbaum, C. (1959) Substructures in crystals grown from the melt. *Progress in Metal Physics*, vol. 8, p. 203-253.

Finlayson, J.N. (1927) Tests on the shearing strength of ice. *Canadian Engineer*, vol. 52, p. 101-103.

Frankenstein, G. (1959) Strength data on lake ice. SIPRE Technical Report 59, p. 1-6 (AD236204).

_____ (1961) Strength data on lake ice, Part II. SIPRE Technical Report 80, p. 1-18.

_____ (1968) Strength of ice sheets. In *Proceedings, Conference on Forces that Ice can Exert Against Structures*, Laval University, National Research Council, Canada, Associate Commission on Geotechnical Research, Technical Memo no. 92, p. 79-88.

_____ (1969) Ring tensile strength studies of ice. CRREL Technical Report 172, p. 1-36 (AD 665386).

_____ and Garner, R. (1967) Equations for determining the brine volume of sea ice from -0.5° to -22.9°C. *Journal of Glaciology*, vol. 6, p. 943-944.

Fujino, K. and Suzuki, Y. (1959) Observations on the process of the ice rind formation on the surface of still water (J). *Low Temperature Science*, vol. A18, p. 149-155.

Glen, J.W. (1968) The effect of hydrogen disorder on dislocation movement and plastic deformation of ice. *Phys. kondens. Materie*, vol. 7, p. 43-51.

Goetze, C.G. (1965) A study of brittle fracture as applied to ice. CRREL Technical Note (unpublished).

Gold, L.W. (1960a) The cracking activity in ice during creep. *Canadian Journal of Physics*, vol. 38, p. 1137-1148.

_____ (1960b) Field study on the load bearing capacity of ice covers. *Woodlands Review*, vol. 61, p. 11-15.

_____ (1963a) Deformation mechanisms in ice. In *Ice and snow – processes, properties, and applications* (W.D. Kingery, ed.). Cambridge, Mass.: MIT Press, p. 8-27.

_____ (1963b) Crack formation in ice plates by thermal shock. *Canadian Journal of Physics*, vol. 41, p. 1712-1728.

_____ (1965) The initial creep of columnar-grained ice. Part I: Observed behavior. *Canadian Journal of Physics*, vol. 43, p. 1414-1422.

_____ (1966) Dependence of crack formation on crystallographic orientation for ice. *Canadian Journal of Physics*, vol. 44, p. 2757-2764.

_____ (1967) Time to formation of first cracks in ice. In *Physics of Snow and Ice*, Institute of Low Temperature Science, Hokkaido University, vol. 1, no. 1, p. 360-370.

Graystone, P. and Langleben, M.P. (1963) Ring tensile strength of sea ice. In *Ice and snow – processes, properties, and applications* (W.D. Kingery, ed.), Cambridge, Mass.: MIT Press, p. 114-123.

Hallett, J. (1960) Crystal growth and the formation of spikes in the surface of supercooled water. *Journal of Glaciology*, vol. 3, p. 698-702.

Harrison, J.D. and Tiller, W.A. (1963) Controlled freezing of water. In *Ice and snow – processes, properties and applications* (W.D. Kingery, ed.). Cambridge, Mass.: MIT Press, p. 215-225.

Hendrickson, G. and Rowland, R. (1965) Strength studies on antarctic sea ice. CRREL Technical Report 157, p. 1-20.

Higashi, A.; Koinuma, S.; and Mae, S. (1964) Plastic yielding in ice single crystals. *Japanese Journal of Applied Physics*, vol. 3, p. 610-616.

Hitch, R.D. (1959) The flexural strength of clear lake ice. SIPRE Technical Report 65, p. 1-8 (AD 227121).

Ishida, T. (1967) Rupture and vibrations of sea ice sheets. In *Physics of Snow and Ice*, Institute of Low Temperature Science, Hokkaido University, vol. 1, no. 1, p. 551-556.

Itagaki, K. and Sabourin, R. (in prep.) Fracture behavior of ice in Charpy impact testing.

Jellinek, H.H.G. (1958) The influence of imperfections on the strength of ice. *Proceedings of the Physical Society, London*, vol. 71, p. 797-814.

Kamb, W.B. (1961) The glide direction in ice. *Journal of Glaciology*, vol. 3, p. 1097-1106.

Ketcham, W.M. and Hobbs, P.V. (1967) The preferred orientation in the growth of ice from the melt. *Journal of Crystal Growth*, vol. 1, p. 263-270.

Kingery, W.D. and French, D.N. (1963) Stress-rupture behavior of sea ice. In *Ice and snow – processes, properties, and applications* (W.D. Kingery, ed.). Cambridge, Mass.: MIT Press, p. 124-129.

Knight, C.A. (1962a) Studies of arctic lake ice. *Journal of Glaciology*, vol. 4, p. 319-335.

_____ (1962b) Curved growth of ice on surfaces. *Journal of Applied Physics*, vol. 33, p. 1808-1815.

_____ (1962c) Polygonization of aged sea ice. *Journal of Geology*, vol. 70, p. 240-246.

_____ (1966) Grain boundary migration and other processes in the formation of ice sheets on water. *Journal of Applied Physics*, vol. 37, p. 568-574.

Korzhavin, K.N. (1961) The effect of local crushing on the mechanical properties of river ice (R). *Tr. Transportno-Energeticheskogo Institut*, vol. 11, p. 13-23.

_____ (1962) Action of ice on engineering structures (R). Izdatel'*stvo "Nauka" Sibirskoe Otdelenie*, Novosibirsk, p. 1-220.

_____ and Ptukhin, F.I. (1966) Evaluating the compressive strength of ice under short-term rapidly increasing loads (R). *Matérialy VIII Vsesoiuz. mezhduvedomstvennogo soveshchaniia po geokriologii (merzlotovedeniiu)*, Yakutsk, vol. 5, p. 61-72.

Kozitskii, I.E. and Bybin, E.A. (1967) Experimental determination of the strength of an ice sheet during various stages of its deterioration (R). *Gosudarstvennyi Gidrologicheskii Institut Tr.*, vol. 148, p. 45-63.

Kudriavtsev, V.A. (1957) Study of the mechanical and physical properties of ice (R). *Izdatel'stvo Akad. Nauk SSSR*, Moscow, p. 1-63.

Kumai, M. and Itagaki, K. (1953) Cinematographic study of ice crystal formation in water. *Journal of the Faculty of Science, Hokkaido University (Hokkaido Daigaku, Sapporo, Japan Rigakubu)*, vol. II4, p. 235-246.

Kuroiwa, D. and Hamilton, W.L. (1963) Studies of ice etching and dislocation etch pits. In *Ice and snow – processes, properties, and applications* (W.D. Kingery, ed.). Cambridge, Mass.: MIT Press, p. 34-55.

Kusunoki, K. (1958) Measurement of gas bubble content in sea ice (J). *Low Temperature Science*, vol. 17, p. 123-134.

Lang, A.R. (1958) Direct observation of individual dislocations by X-ray diffraction. *Journal of Applied Physics*, vol. 29, p. 597-598.

_____ (1959) Studies of individual dislocations in crystals by X-ray diffraction microradiography. *Journal of Applied Physics*, vol. 30, p. 1748-1755.

Langleben, M.P. (1959) Some physical properties of sea ice, II. *Canadian Journal of Physics*, vol. 37, p. 1438-1454.

_____ and Pounder, E.R. (1964) Arctic sea ice of various ages I. Ultimate strength. *Journal of Glaciology*, vol. 5, p. 93-98.

Lavrov, V.V. (1958) The nature of the scale effect in ice and the strength of an ice cover (R). *Doklady Akademiia Nauk SSSR*, vol. 122, p. 570-573.

Lavrov, V.V. (1962) Questions of the physics and mechanics of ice (R). *Tr. Arkticheskogo i Antarkticheskogo Nauchno-Issledovatel'skogo Institut*, vol. 247, p. 1-118.

_____ (1963) Supplementary basis for the hypothesis of constancy of absolute extension values in the breaking of ice (R). *Problemy Arktiki i Antarktiki*, vol. 14.

_____ (1965) On the problem of mechanical properties of ice. *Problemy Arktiki i Antarktiki*, vol. 21, p. 60-65.

Levi, L.; de Achaval, E.M.; and Suraski, E. (1965) Experimental study of non-basal dislocations in ice crystals. *Journal of Glaciology*, vol. 5, p. 691-699.

Lofgren, G. and Weeks, W.F. (1969) Effect of growth parameters on substructure spacing in NaCl ice crystals. *Journal of Glaciology*, vol. 8, p. 153-163. Also CRREL Research Report 195, 1969 (AD 687280).

Lonsdale, K. (1958) The structure of ice. *Proceedings of the Royal Society (London)*, vol. 247, p. 424-434.

Low, J.R. (1963) The fracture of metals. *Progress in Materials Science*, vol. 12, no. 1, p. 1-96.

Makarov, S.O. (1901) Notes on ice science (R). In *Ermak vo L'dakh*, p. 388-417. St. Petersburg.

Malmgren, F. (1927) On the properties of sea ice. *Scientific Results, Norwegian North Pole Expedition with the "Maud", 1918-1925*, vol. 1, no. 5, p. 1-67.

Michel, B. (1967a) Morphology of frazil ice. In *Physics of Snow and Ice*, Institute of Low Temperature Science, Hokkaido University, vol. 1, no. 1, p. 119-128.

_____ (1967b) From the nucleation of ice crystals in clouds to the formation of frazil ice in rivers. In *Physics of Snow and Ice*, Institute of Low Temperature Science, Hokkaido University, vol. 1, no. 1, p. 129-136.

_____ (1968) Ice covers in rivers. In *Proceedings of the Conference on Forces that Ice can Exert Against Structures*, Laval University, National Research Council Canada, Associate Commission of Geotechnical Research, Technical Memo no. 92, p. 231-247.

Muguruma, J. and Higashi, A. (1963) Observations of etch channels on the (0001) plane of ice crystal produced by non-basal glide. *Journal of Physical Society of Japan*, vol. 18, p. 1261-1269.

Muguruma, J. and Kikuchi, K. (1963) Lake ice investigation at Peters Lake, Alaska. *Journal of Glaciology*, vol. 4, p. 689-708.

Nagle, J.F. (1966) Lattice statistics of hydrogen bonded crystals. I. The residual entropy of ice. *Journal of Mathematics and Physics*, vol. 7, p. 1484-1491.

Neronov, I.N. (1946) The problem of the value of temporary resistance to bending of thawing spring ice (R). *Tr. Nauchno-Issledovatel'skikh Uchrezhdenii*, Ser. V, no. 20, p. 50-57.

Owston, P.G. (1958) The structure of ice I, as determined by X-ray and neutron diffraction analysis. *Advances in Physics*, vol. 7, 171-188.

Paige, R.A. and Kennedy, R.A. (1967) Strength studies of sea ice – effect of load rate on ring tensile strength. Naval Civil Engineering Laboratory Technical Report R545, p. 1-25.

Paige, R.A. and Lee, C.W. (1967) Preliminary studies on sea ice in McMurdo Sound, Antarctica, during "Deep Freeze 65." *Journal of Glaciology*, vol. 6, p. 515-528.

Pauling, L. (1935) Structure and entropy of ice and of other crystals with randomness of atomic arrangements. *Journal of the American Chemical Society*, vol. 57, p. 2608-2684.

Perey, F.G.J. and Pounder, E.R. (1958) Crystal orientation in ice sheets. *Canadian Journal of Physics*, vol. 36, p. 494-502.

Peschanskii, I.S. (1967) Ice science and ice technology (R). *Gidrometeorologicheskoe Izdatel'stvo*, Leningrad, p. 1-461.

Peterson, S.W. and Levy, H.A. (1957) A single-crystal neutron diffraction study of heavy ice. *Acta Crystallographica*, vol. 10, p. 70-76.

Petrov, I.G. (1954-55) Physical and mechanical properties and thickness of ice cover (R). In *Materialy nablyudeniy nauchno-issledovatel'skoy dreyfuyushchey stantsii 1950-51 goda* (M.M. Somov, ed.), Arkticheskiy Nauchno-Issledovatel'skiy Institut 2, Leningrad, p. 103-165.

Peyton, H.R. (1966) Sea ice strength. Geophysical Institute, University of Alaska, Report no. NR 307 - 247/7-6-55, p. 1-273.

Pinegin, V.N. (1924) Preliminary information concerning research on the strength of river ice in connection with temperature variations (R). Vestnik Sibirskikh Inzhenerov IV, Tomsk.

Pounder, E.R. and Little, E.M. (1959) Some physical properties of sea ice I. *Canadian Journal of Physics*, vol. 37, p. 443-473.

Ptukhin, F.I. (1964) Concerning the influence of the speed of deformation on the strength limit of river ice (R). In *Thermal situation of the ice on the rivers of Siberia and its variation during the building of the hydroelectric station.* Tr. Transportno-Ekonomicheskogo Institut Severnogo Otdeleniya Akademy Nauk SSSR, Novosibirsk, vol. 15.

Ragle, R.H. (1963) An investigation of the formation of lake ice in a temperate climate. CRREL Research Report 107, p. 1-22 (AD 433794).

Ramseier, R.O. (1968) Origin of preferred orientation in columnar ice. *Journal of Crystal Growth*, vol. 3-4, p. 621-624.

Ripperger, E.A. and Davids, N. (1947) Critical stresses in a circular ring. *Proceedings of the American Society of Civil Engineers*, vol. 12, p. 619-635.

Rohatgi, P.K. and Adams, C.M. (1967a) Ice-brine dendritic aggregate formed on freezing of aqueous solutions. *Journal of Glaciology*, vol. 6, p. 663-679.

_____ (1967b) Freezing rate distributions during unidirectional solidification of solutions. *Transactions of the Metallurgical Society of the American Institute of Mechanical Engineers*, vol. 239, p. 850-857.

_____ (1967c) Effect of freezing rates on dendritic solidification of ice from aqueous solutions. *Transactions of the Metallurgical Society of the American Institute of Mechanical Engineers*, vol. 239, p. 1729-1736.

Ross, B. (1967) Penetration and fracture of sea ice due to impact loading. In *Physics of snow and ice*, Institute of Low Temperature Science, Hokkaido University, vol. 1, no. 1, p. 499-521.

Rutter, J.W. and Chalmers, B. (1953) A prismatic substructure formed during solidification of metals. *Canadian Journal of Physics*, vol. 31, p. 15-39.

Sala, I. (1961) Experimental studies on the stress concentration index of ice. Commission on Snow and Ice, International Union of Geodesy and Geophysics Publication 54, Helsinki, p. 15-19.

Savel'ev, B.A. (1958) Study of ice in the region of the drift of station NP-4 during melting and break-up in 1955 (R). *Problemy Severa*, vol. 2, p. 47-79.

_____ (1963) Structure, composition and properties of the ice cover of sea and fresh waters (R). *Izdatel'stvo Moskovskogo University of Moscow*, p. 1-541.

Serikov, M.I. (1961) Mechanical properties of Antarctic sea ice. *Informatsionnyi Biulletin' Antarkticheskoi Ekspeditsii*, vol. 3, p. 181-185.

Shishov, N.D. (1947) Concerning the strength of ice (R). *Meteorologiia i Gidrologiia*, vol. 2.

Shumskii, P.A. (1955) A study of ice in the Arctic Ocean (R). *Vestnik Akademii Nauk SSSR*, vol. 25, no. 2, p. 33-38.

_____ (1964) *Principles of structural glaciology.* New York: Dover Pub., p. 1-487.

Smirnov, V.I. (1961) Quantitative characteristics of ice as a material (R). *Trudy Arkticheskogo i Antarkticheskogo Nauchno - Issledovatel'skogo Instituta*, vol. 256, p. 40-46.

Smith, D.D. (1964) Ice lithologies and structure of ice island Arlis II. *Journal of Glaciology*, vol. 5, p. 17-38.

Stroh, A.N. (1954) The formation of cracks as a result of plastic flow. *Proceedings of the Royal Society (London)*, vol. A233, p. 404-414.

_____ (1957) A theory of the fracture of metals. *Advances in Physics*, vol. 6, p. 418-465.

Suzuki, Y. (1967) On disorder entropy of ice. In *Physics of snow and ice*, Institute of Low Temperature Science, Hokkaido University, vol. 1, no. 1, p. 21-41.

Swinzow, G.K. (1966) Ice cover of an arctic proglacial lake. CRREL Research Report 155, p. 1-43 (AD 632987).

Tabata, T. (1958) Studies on the mechanical properties of sea ice II. Measurement of elastic modulus by lateral vibration method (J). *Low Temperature Science*, vol. A17, p. 147-166.

_____ (1960) Studies on the mechanical properties of sea ice V. Measurement of flexural strength (J). *Low Temperature Science*, vol. A19, p. 187-201.

_____ (1966) Studies on the mechanical properties of sea ice IX. Measurement of the flexural strength *in situ* (J). *Low Temperature Science*, vol. A24, p. 259-268.

_____ (1967) The flexural strength of small sea ice beams. In *Physics of snow and ice*, Institute of Low Temperature Science, Hokkaido University, vol. 1, no. 1, p. 481-497.

_____ and Fujino, K. (1964) Studies on the mechanical properties of sea ice VII. Measurement of the flexural strength *in situ* (J). *Low Temperature Science*, vol. A22, p. 147-154.

_____ (1965) Studies of the mechanical properties of sea ice VIII. Measurement of the flexural strength *in situ* (J). *Low Temperature Science*, vol. A23, p. 157-166.

_____ and Aota, M. (1967) The flexural strength of sea ice *in situ*. In *Physics of snow and ice*, Institute of Low Temperature Science, Hokkaido University, vol. 1, no. 1, p. 539-550.

Tabata, T. and Ono, N. (1957) On the structure of sea ice (J). *Low Temperature Science*, vol. A16, p. 197-210.

_____ (1962) On the crystallographic study of several kinds of ices (J). *Low Temperature Science*, vol. A20, p. 199-214.

Taylor, L.D. and Lyons, J.B. (1959) Ice structures, Angiussaq Lake, Northwest Greenland. AF Cambridge Research Center, Geophysical Research Directorate, TN-59-461, p. 1-33.

Tegart, W.J. McG. (1966) *Elements of mechanical metallurgy*. New York: MacMillan Co., p. 1-251.

Tiller, W.A. (1963) Principles of solidification. In *The art and science of growing crystals*. New York: Wiley and Sons, p. 276-312.

_____; Jackson, K.A.; Rutter, J.W.; and Chalmers, B. (1953) The redistribution of solute atoms during the solidification of metals. *Acta Metallurgica*, vol. 1, p. 428-437.

Treshnikov, A.F. (1963) Features of the ice regime of the southern ocean (R). *Trudy Sovetskoy Antarkticheskoy Ekspeditsii*, vol. 21, p. 1-237.

Tsurikov, V.L. (1940) The problem of ice strength (R). *Severnyi Morskoi Put'*, vol. 16, p. 45-74.

_____ (1947a) The problem of the influence of the cavities of ice on its strength (R). Gos. Okeanograficheskii Institut, Tr., vol. 2, no. 14, p. 66-88.

Tsurikov, V.L. (1947b) The influence of the salinity of sea ice on its strength. Gos. Okeanograficheskii Institut, Tr., vol. 2, no. 14, p. 89-108.

_____ (1965) Formation of the ionic composition and salinity of sea ice. *Oceanology*, vol. 5, p. 59-66.

Untersteiner, N. (1967) Natural desalination and equilibrium salinity profiles of old sea ice. In *Physics of snow and ice*, Institute of Low Temperature Science, Hokkaido University, vol. 1, no. 1, p. 569-577.

Vasenko, B.P. (1899) *Ice Handbook of the Institute of Engineers Itinerary Information* (R). Siberia, Issue 1.

Vitman, F.F. and Shandrikov, N.P. (1938) Some investigations of the mechanical strength of ice (R). *Tr. Arkticheskogo Instituta*, vol. 110, Leningrad, p. 83-100.

Voitkovskii, K.F. (1960) The mechanical properties of ice (R). Izdatel'stvo Adademii Nauk SSSR, 100 p.

Wakahama, G. (1964) On the plastic deformation of ice V. Plastic deformation of polycrystalline ice. *Low Temperature Science*, vol. A22, p. 1-24.

_____ (1967) Plastic deformation and internal fractures of ice crystal. In *Physics of snow and ice*, Institute of Low Temperature Science, Hokkaido University, vol. 1, no. 1, p. 357.

Walton, D. and Chalmers, B. (1959) The origin of the preferred orientation in the columnar zone of ingots. *Transactions of the Metallurgical Society of the American Institute of Mechanical Engineers*, vol. 215, p. 447-457.

Webb, W.W. and Hayes, C.E. (1967) Dislocations and plastic deformation of ice. *Philosophical Magazine*, vol. 16, p. 909-926.

Weeks, W.F. (1962) Tensile strength of NaCl ice. *Journal of Glaciology*, vol. 4, p. 25-52.

_____ and Anderson, D.L. (1958) An experimental study of strength of young sea ice. *Transactions of the American Geophysical Union*, vol. 39, p. 641-647.

Weeks, W.F. and Assur, A. (1963) Structural control of the vertical variation of the strength of sea and salt ice. In *Ice and snow – processes, properties and applications (W.D.* Kingery, ed.). Cambridge, Mass.: MIT Press, p. 258-276. Also CRREL Research Report 113, 1964 (AD 602458).

_____ (1968) The mechanical properties of sea ice. In *Proceedings of the Conference on Forces that Ice can Exert Against Structures*, Laval University. National Research Council Canada, Associate Commission on Geotechnical Research, Technical Memo no. 92, p. 25-78. Also CRREL Monograph IIC3 (AD 662716).

Weeks, W.F. and Hamilton, W.L. (1962) Petrographic characteristics of young sea ice, Point Barrow, Alaska. *American Minerologist*, vol. 47, p. 945-961. Also CRREL Research Report 101, 1962 (AD 294162).

Weeks, W.F. and Lee, O.S. (1958) Observations on the physical properties of sea ice at Hopedale, Labrador. *Arctic*, vol. 11, p. 134-155.

Weeks, W.F. and Lofgren, G. (1967) The effective solute distribution coefficient during the freezing of NaCl solutions. In *Physics of snow and ice*, Institute of Low Temperature Science, Hokkaido University, vol. 1, no. 1, p. 579-597.

Weinberg, B.P.; Al'tberg, V.Ia.; Arnol'd-Aliab'ev, V.I.; and Golovkov, M.P. (1940) Ice, its properties, appearance and disappearance (R). Gos. Izdatel'stvo Tekhniko-Teoreticheskoi Literatury, p. 1-524.

Williams, G.P. (1959) Frazil ice, a review of its properties with a selected bibliography. *The Engineering Journal*, vol. 42, no. 11, p. 55-60.

_____ (1968) Freeze-up and break-up of fresh water lakes. In *Proceedings of the Conference on Forces that Ice can Exert Against Structures*, Laval University. National Research Council Canada, Associate Commission on Geotechnical Research, Technical Memo no. 92, 203-215.

Wilson, J.T. and Horeth, J.M. (1948) Bending and shear tests on lake ice. *Transactions of the Geophysical Union*, vol. 29, p. 209-212.

Wilson, J.T. Zumberge, J.H.; and Marshall, E.W. (1954) A study of ice on an inland lake. SIPRE Report 5, p. 1-78 (AD 43143).

Yoshida, Z. and Wakahama, G. (1962) Models of dislocations in ice crystal. *Low Temperature Science*, vol. A20, p. 29-56.

Zubov, N.N. (1945) Arctic ice (R). Izdatel'stvo Glavsevmorputi, Moscow, p. 1-360. Translation, U.S. Naval Electronics Laboratory (1963).

DOCUMENT CONTROL DATA - R & D

(Security classification of title, body of abstract and indexing annotation must be entered when the overall report is classified)

1. ORIGINATING ACTIVITY *(Corporate author)* U. S. Army Cold Regions Research and Engineering Laboratory Hanover, New Hampshire 03755	2a. REPORT SECURITY CLASSIFICATION Unclassified 2b. GROUP

3. REPORT TITLE

FRACTURE OF LAKE AND SEA ICE

4. DESCRIPTIVE NOTES *(Type of report and inclusive dates)*

Research

5. AUTHOR(S) *(First name, middle initial, last name)*

W. F. Weeks and A. Assur

6. REPORT DATE September 1969	7a. TOTAL NO. OF PAGES 86	7b. NO. OF REFS 175
8a. CONTRACT OR GRANT NO. b. PROJECT NO. c. d.	9a. ORIGINATOR'S REPORT NUMBER(S) Research Report 269 9b. OTHER REPORT NO(S) *(Any other numbers that may be assigned this report)*	

10. DISTRIBUTION STATEMENT

This document has been approved for public release and sale; its distribution is unlimited.

11. SUPPLEMENTARY NOTES	12. SPONSORING MILITARY ACTIVITY Department of the Navy Office of Naval Research Washington, D. C. 20360

13. ABSTRACT

The increased activity in cold regions has made a thorough understanding of fracture in lake and sea ice quite desirable, inasmuch as this information has application to a number of problems of geophysical as well as engineering importance. This survey starts with a discussion of the structure of ice I and the macro- and microstructure of sea and lake ice as well as their chemistry and phase relations. Recent work on the direct observation of dislocations as well as the formation of cracks in ice is summarized. Formal ice-brine-air models for analyzing variations in ice strength are also reviewed. The results of the different types of tests are discussed and compared (compressive, indentation, direct and ring-tension, small beam flexure and in situ cantilevers and simple beams, shear, and impact). Scale effects are considered as well as the rapid strength deterioration experienced by ice sheets in the spring. Finally, a number of recommendations are made concerning future research in this field.

14. KEY WORDS

Ice breakers	Ice navigation	Fracture properties	Sea ice
Ice breakup	Ice openings	Lakes	
Ice disintegration	Floating ice	Pack ice	

DD FORM 1 NOV 65 1473 REPLACES DD FORM 1473, 1 JAN 64, WHICH IS OBSOLETE FOR ARMY USE.